TARGETED INACTIVATION OF *SALMONELLA ENTERICA* SEROVAR TYPHIMURIUM IN FRESH CANTALOUPE FLESH (*CUCUMIS MELO* L.) USING ELECTRON BEAM IRRADIATION

A Dissertation

by

EZEKIEL MASWE CHIMBOMBI

Submitted to the Office of Graduate Studies of
Texas A&M University
in partial fulfillment of the requirements for the degree of

DOCTOR OF PHILOSOPHY

May 2010

Major Subject: Biological and Agricultural Engineering

TARGETED INACTIVATION OF *SALMONELLA ENTERICA* SEROVAR TYPHIMURIUM IN FRESH CANTALOUPE FLESH (*CUCUMIS MELO* L.) USING ELECTRON BEAM IRRADIATION

A Dissertation

by

EZEKIEL MASWE CHIMBOMBI

Submitted to the Office of Graduate Studies of
Texas A&M University
in partial fulfillment of the requirements for the degree of

DOCTOR OF PHILOSOPHY

Approved by:

Chair of Committee,	M. Elena Castell-Perez
Committee Members,	Rosana G. Moreira
	Leslie A. Braby
	Luis Cisneros-Zevallos
	Marcos X. Sanchez-Plata
Head of Department,	Gerald Riskowski

May 2010

Major Subject: Biological and Agricultural Engineering

ABSTRACT

Targeted Inactivation of *Salmonella enterica* Serovar Typhimurium in Fresh Cantaloupe Flesh (*Cucumis melo* L.) Using Electron Beam Irradiation.

(May 2010)

Ezekiel Maswe Chimbombi, B.S.; M.B.A., University of Botswana;

M.S., Texas A&M University

Chair of Advisory Committee: Dr. Elena Castell-Perez

Food irradiation is costly in terms of the energy utilized and the time spent, therefore, it is imperative to optimize it in order to avoid sub lethal dose or an overdose both of which have detrimental effects on the quality of fresh produce such as cantaloupe. The bacterial load in fresh cut cantaloupe flesh was quantified on the basis of growth and mobility over time, and used as the basis for targeted irradiation simulation. The bacterial growth was predicted using the Gompertz model, while a power law function was used for predicting the bacterial mobility. The microbiological structure of cantaloupe flesh was assessed using Transmission Electron, Scanning Electron, and Light Microscopy as a basis for understanding the mobility of the bacteria into the internal mesocarp tissues. A plate assay was also undertaken to determine the possibility of *S. typhimurium* producing cell wall degrading enzymes such as polygalacturonase to gain access into intact fresh cantaloupe tissues.

S. typhimurium in fresh cut cantaloupe flesh has a lag phase duration of 7.76 hours and can reach a maximum population of 7.98 logs CFU/g in 30 hours. Cantaloupe

flesh has a vast network of intracellular spaces through which the bacteria can move into the internal mesocarp tissues, particularly because *S. typhimurium* (LT2) does not produce any enzymes such as polygalacturonase which could be breaking down the cell wall binding structures as a mechanism for internalization into intact internal tissues. A theoretical bacterial inactivation dose estimate based on the experimentally determined D_{10}-value and the bacterial population was used to simulate irradiation treatment of the cantaloupe flesh samples using a 10MeV electron beam irradiator (LINAC) to establish the best treatment. The optimal 10 MeV electron beam irradiation treatment for *S. typhimurium* internalized in fresh cut cantaloupe samples for 30 hours was determined to be a double beam with 0.5 cm attenuation of Lucite® at the top and 3.3 cm at the bottom.

DEDICATION

To God

To my late father, I. P. “Tata” Chimbombi

To my late brother, Buna Aptiro Chimbombi

To my late friend, Victor Virgo Ranko Ghanie

ACKNOWLEDGEMENTS

Special thanks to my advisor, Dr. Elena Castell-Perez for guiding me through this long journey of graduate studies. Dr. Castell's immense support and leadership made me appreciate and enjoy doing research. I am thankful to Dr. Rosana Moreira for the expert guidance in my research, particularly regarding food irradiation. Thank you Dr. Marcos X. Sanchez-Plata for guiding me very professionally and patiently through the microbiological work. Dr. Leslie A. Braby was always there whenever I needed technical assistance in the area of radiation dosimetry, and I am greatly thankful for that. Thank you Dr. Luis Cisneros-Zevallos for always asking those critical questions, which motivated and guided me to research further.

I am thankful to the Fulbright program for funding the first two years of my studies. I am indebted to my employer and sponsor, the Botswana College of Agriculture for granting me study leave, and financially supporting me and the research. I would like to express my gratitude to all my colleagues, who have helped me one way or the other. They are: Dr. Jongsoon Kim, Xiaolei Xun, Carmen Gomes, Paulo Cesar Fortes da Silva, Taehoon Kim, Sean Tolle, Raghavendra Jana, Dipankar Dwivedi, Akhilesh Pandey, Philomene Balihe, Joseph Mbaiwa, Leo Mpofu, Dumisani Sayi, Llulu Sayi, Kgomotso Magosi, Tswelelo Magosi and Bao Mosinyi**.** Last but not least, thanks to my family, particularly my parents, Mami Chimbombi and Galentloge Motswagole as well as my two sons, Tshwetso and Kaiko. My dear wife, Omphemetse, thank you for being my anchor.

NOMENCLATURE

β_0	Constant
β_1	Constant
C	Charge of an Electron
D	Dose, kGy
d	Sample Depth, (mm)
D-Value	D-Value in Thermal Processing of Foods is the Decimal Reduction Time, or the Time Required to Destroy 90 % of the Organisms, (Seconds, Minutes, or Hours)
D_{10}-Value	D_{10}-Value in Irradiation of Foods is the Dose Required to Destroy 90 % of the Organisms (kGy per 1 Log_{10} Cycle)
e	Napier's Constant
Gy	Gray, the SI Derived Unit of Absorbed Dose
GT	Generation Time
LET	Linear Energy Transfer (keV/μm)
LPD	Lag Phase Duration (hours)
BM	Log Count of Bacteria [Log_{10}(CFU/g)] at Time t
MPD	Maximum Population Density (Log_{10}(CFU/g))
N	Bacterial Population (Log_{10}(CFU/g))

TABLE OF CONTENTS

CHAPTER Page

CHAPTER Page

CHAPTER Page

LIST OF FIGURES

FIGURE Page

FIGURE Page

LIST OF TABLES

TABLE Page

CHAPTER I

INTRODUCTION

Cantaloupes (*Cucumis melo*) and other melons have been associated with numerous outbreaks of food-borne illnesses in recent years, the causative organisms being *Salmonella* spp. including Chester and Poona (Ukuku, 2004). *Salmonella* is a bacterium that is widespread in the intestines of birds, reptiles and mammals, and can spread to humans via a variety of different foods of animal origin causing salmonellosis, which typically includes fever, diarrhea and abdominal cramps (CDC, 2009). Cantaloupes grow on the ground and therefore are in constant contact with the soil and other natural contaminants, with the meshwork of raised tissue covering the cantaloupe surface providing protection for the microorganisms (Parnell, et al., 2005). Subsequent to contamination of mesocarp tissues of cantaloupe fruit after surface integrity is compromised by disease, bruising, cutting or peeling *Salmonella* spp. such as *S. poona* have been recovered at depths of 3 – 4 cm from the rind surface within 7 days (Richards & Beuchat, 2005a). Watermelon, cantaloupe and tomato are some of the fruit crops which have occurrence of hollowing resulting in creation of intercellular spaces which can be the route for bacterial internalization (Kano, 1993).

This dissertation follows the style of the *Journal of Food Engineering*.

A plate assay (McKay, 1988) was also done to determine whether *S. typhimurium* produces some cell wall degrading enzymes such as polygalacturonase as an aid to internalization into fresh cantaloupe. Subject to practical limitations of using an actual pathogen in the Microscopy and Imaging Center at Texas A&M University, as well as in the irradiation facilities, a non-pathogenic surrogate bacteria *S. typhimurium* LT2 was used for microscopy and irradiation tests.

Irradiation, also referred to as cold pasteurization, is an appropriate and increasingly popular control measure for the management of hazards of the food chain. It is a safe technology and has been recognized as such by the FAO/WHO Codex Alimentarius Commission (Molins, et al., 2001). Gomes and others (2008) noted that the main assets of the irradiation technology include its high lethality, low quality detrimental effects, unmatched penetration into the product core, cold application, capabilities to be applied in a conveyor belt, and tested safety of the intervention technology.

However, the irradiation process has to be well administered in terms of dosimetry and the actual process of irradiating. Applied irradiation dose varies significantly according to the effect required, i.e. sprout inhibition doses are usually below 0.15 kGy whereas disinfection doses range up to 0.75 kGy, and spice sanitization doses sometimes surpass 10 kGy. Many food products have a well defined maximum tolerance to radiation, and there are also legislative restrictions on maximum doses, therefore the radiation equipment must ensure a good dose uniformity, i.e. it must be able to deliver the maximum effective dose while at the same time not exceeding regulatory

limits or product tolerance doses (Kunstadt, et al., 1993). A prediction of the inactivation dose was developed for the 50 mm depth of a cylindrical cantaloupe flesh sample.

The main goal of this research was to predict bacterial growth and mobility in fresh cut cantaloupe flesh, to subsequently simulate a targeted bacterial inactivation scheme.

The specific objectives were:

1. To quantify the accumulation (growth and mobility) of *S. typhimurium* in fresh cut cantaloupe.
2. To develop a correlative basis for internalization of *S. typhimurium* into the internal mesocarp tissues of fresh and intact cantaloupe flesh.
3. To determine the best scheme for inactivation of internalized *S. typhimurium* in fresh cantaloupe samples using electron beam irradiation.

CHAPTER II

LITERATURE REVIEW

2.1 FOODBORNE ILLNESSES

The last 25 years have seen recognition of pathogens such as *Campylobacter jejuni, Escherichia coli* O157:H7, *Listeria monocytogenes,* Noroviruses, *Salmonella* Enteritidis, *Shigella* species, *Toxoplasma gondii, Vibrio vulnificus, Vibrio parahaemolyticus,* and *Yersinia enterocolitica* as predominantly being foodborne (Hillers, et al., 2003). These pathogens share some or all of the following characteristics: (i) they can spread to humans from an animal reservoir, (ii) they may contaminate food early in the production process rather than just before consumption, (iii) foods contaminated with them often look, smell, and taste normal, and/or (iv) some of them may survive traditional preparation techniques (Tauxe, 1997).

Fresh produce is an important part of a healthy diet, and during the period 1973 - 1977, the number of outbreaks caused by foodborne pathogens associated with fresh produce consumption reported to the Centers for Disease Control and Prevention (CDC) increased with a total of 190 produce-associated outbreaks being reported, associated with 16,058 illnesses, 598 hospitalizations, and 8 deaths. The food items most frequently implicated included salad, lettuce, juice, melon, sprouts, and berries. Among 103 (54%) produce-associated outbreaks with a known pathogen, 62 (60%) were caused by bacterial pathogens, of which 30 (48%) were caused by *Salmonella* (Sivapalasingam, et al., 2004).

New hazards are emerging from both familiar pathogens such as *Salmonella* and previously unrecognized microbial threats, due to increasing internationalization of the food supply chain with the importation of foods from all parts of the globe (Blaser, 1996;

Tauxe, 2002). For instance, in the 1980s, a few strains of *Salmonella* Enteritidis swept through the egg laying and broiler flocks of much of the world, making it the most common *Salmonella* serotype worldwide (Tauxe, 2002).

2.2 BACTERIAL GROWTH MODELING

The increased demand by consumers for minimally processed foods, combined with the ready availability of micro and minicomputers has stimulated an interest in the development of predictive microbiology techniques that can be applied to food systems. The traditional approach to establishing food safety through challenge tests using the pathogen of concern are expensive, slow, demanding on facilities and microbial skills. Models enable a full understanding of the response of the microbes of concern to the key controlling factors in the food environment, with capabilities to build a cumulative store of knowledge, and to develop the means to interpolate calculated microbial responses (Baranyi & Roberts, 1995). A predictive food microbiology model is a mathematical expression that describes the growth, survival, inactivation or metabolic activity of foodborne microorganisms of interest.

According to Buchanan and Whiting (1997) models can be mechanistic or empirical, whereby mechanistic models are based on an underlying mechanism within the cells that control its metabolism, for example, the Monad-type models relating substrate concentration to growth rate, while empirical models are more statistical in nature. The Monod's growth model differs from classical growth models such as the Gompertz because it introduces the concept of a limiting nutrient, which has a casual relationship between its exhaustion and the end of growth (Lobry, et al., 1992). Empirical models acquire sufficient experimental data relating bacterial growth or survival to an

environmental variable, and fit the data to an appropriate mathematical relationship with no attempt to infer a mechanistic rationale.

Whiting and Buchanan (1993) classified microbial models as primary, secondary, or tertiary according to the following criteria:

(i) **Primary Models** measure the response of the microorganism with time to a single set of conditions. The response can either be direct measurement of microbial population density (e.g plate count, microscopy, etc), indirect measures (e.g. absorbance, impedence, etc) or products of microbial metabolism (e.g. acid production, toxin synthesis, etc). Each population-time curve can be described by a set of specific values for each of the parameters in the models. Examples of primary models include the Gompertz model (Huang, 2008; Lu, et al., 2007), the Growth-Decline model of Whiting and Cygnarowicz, D-values of thermal inactivation, Survival-Inactivation models, Growth Rate values and even subjective estimation lag time or times to turbidity or toxin formation.

(ii) **Secondary Models** describe the response of one or more parameters of a primary model to changes in one or more of the cultural conditions. The response surface model (Buchanan & Phillips, 1990) calculates the changes in primary model parameters such as growth rate and Gompertz M (time at which the absolute growth rate is maximal) values, with respect to changes in temperature, pH, water activity, and other factors.

(iii) **Tertiary Models** are applications of one or more secondary models to generate systems for providing predictions to non-modelers, such as user friendly or applications software and expert systems. The level includes algorithms to

calculate changing conditions, such as transient temperature after 5 days of storage, compare microbial behavior under different conditions such as two salt levels, or graph the growth of several microorganisms simultaneously.

2.2.1 Mechanistic Primary Models

Baranyi and Roberts (1994) proposed a simple deterministic version of modeling bacterial growth which assumes that the kinetics of a homogenous bacterial cell population can be characterized by the extracellular, physicochemical environment (temperature, atmosphere, substrate, etc) and the intracellular conditions. The mathematical model so developed shall have built in variables divided into the three classes of:

(1) Extracellular conditions assumed to be unaffected, or negligibly affected by the growth of the cells that characterize the growth independent environment which may change with time.

(2) Extracellular conditions which are changed by the growing culture. These will be the growth dependant environmental quantities, and they include the concentration of various chemicals such as growth substrates and metabolic products surrounding the cells.

(3) Intracellular concentrations of certain substrates, like DNA and RNA which will change during growth and characterize the physiological state of the cells.

The model proposed by Baranyi and Roberts (1994) after the above listed considerations is in the form of:

$$\frac{dx}{dt} = \mu_{max} \propto (t)u(x)x \qquad (0 \leq t < \infty;\ 0 < x) \qquad (2.1)$$

where x(t) denotes the cell concentration of a bacterial population at the time t [Log_{10} CFU/g), the initial value x(0) = x_0 and x_o > 0; the derivative of x(t) gives the (absolute) growth rate μ(x), which is the specific growth rate.

If μ(x) = μ_{max} ≡constant, then EQ. 2.1 describes the pure exponential growth. The factor α(t) is an adjustment function derived from the variable q(t) representing the physiological state of the cells, which refers to whether cells are metabolically active with biosynthesis taking place. Typically, metabolically active cells are described to be on the logarithmic growthl phase while cells in the stationary phase are not active (Nagy, et al., 1968). From q(t) by a simple transformation in EQ. 2.2 the value of the adjustment function α(t) can be calculated as:

$$\propto (t) = \frac{q(t)}{1+q(t)} \tag{2.2}$$

The adjustment function α(t) can be considered as a capacity-type quantity expressing the proportion of the potential specific growth rate (which is determined by the actual environment) that is utilized by the cells, and it is characterized by the gradual increase of α(t) from a low value towards 1. The function u(x) is called the inhibition function because it ensures the transition of the growth curve to the stationary phase. Its values are between 0 and 1 and it decreases as x increases from 0 to x_{max}.

Monod's deterministic growth model introduces a concept of a limiting nutrient where there is a causal relationship between its exhaustion and the end of growth (Lobry, et al., 1992):

$$\frac{dx}{dt} = x\mu_m \frac{s}{K_s+s} \tag{2.3}$$

where x is the microbial concentration (shortly the biomass) at time t, *s* is the limiting nutrient (or substrate) concentration at time t, μ_m is the maximum specific growth rate,

and K_s is the substrate concentration which supports half the maximum specific growth rate. The model (EQ. 2.3) treats the units of biomass and substrate in various kinds, depending on the way growth is measured, and the important feature of the model is that the growth rate is zero when there is no substrate and tends to an upper limit when the substrate is in great excess, the link in these two extreme conditions being described by a rectangular hyperbola (Fig. 2.1). The growth rate of biomass increases up to a certain limit with the increase of substrate concentration. The biomass concentration remains constant at the maximum limit while the substrate concentration continues to decrease and finally gets exhausted.

2.2.2 Empirical Primary Models

The promising approach used to develop predictive equations that describe the effects of various cultural factors on the growth of selected foodborne pathogens is the response surface regression analysis of data generated using the Gompertz function to describe growth kinetics (Buchanan & Phillips, 1990). A curve fitting of $\log_{10}$ counts of the number of bacteria is modeled as a function of time by either the Logistic or Gompertz curve, which are chosen because they both consist of the four phases which may be compared with the four stages of microbial growth curves (Fig. 2.2), namely an initial lag phase where no change occurs, followed by a period of accelerating change, a period of decelerating change and finally a stationary phase (Buchanan & Phillips, 1990; Gibson, et al., 1987).

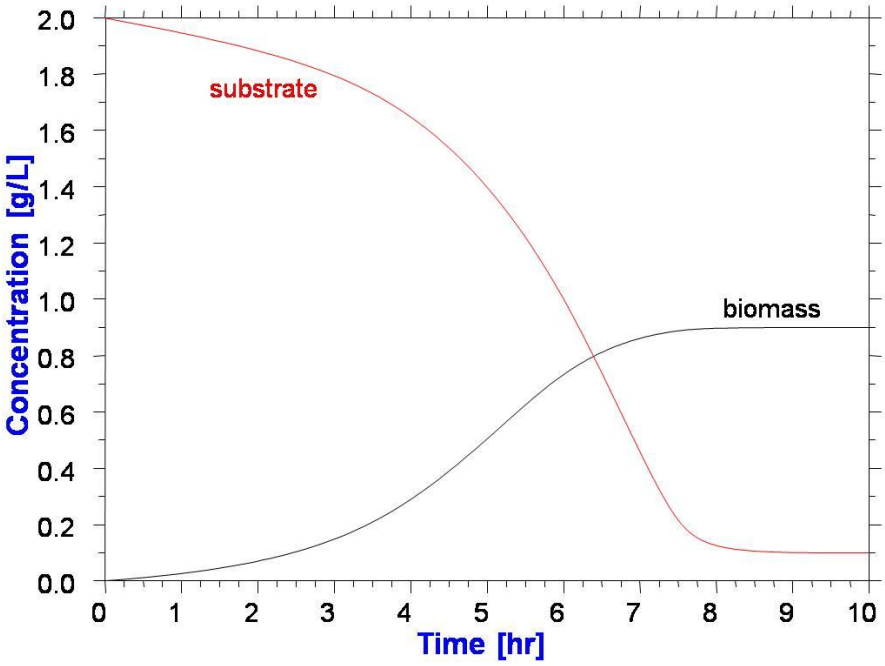

Fig. 2.1 Schematic of Monod's Deterministic Growth Model Showing Biomass Accumulation in Response to Concentration of the Limiting Nutrient Substrate. Adapted from Lobry et al. (1992).

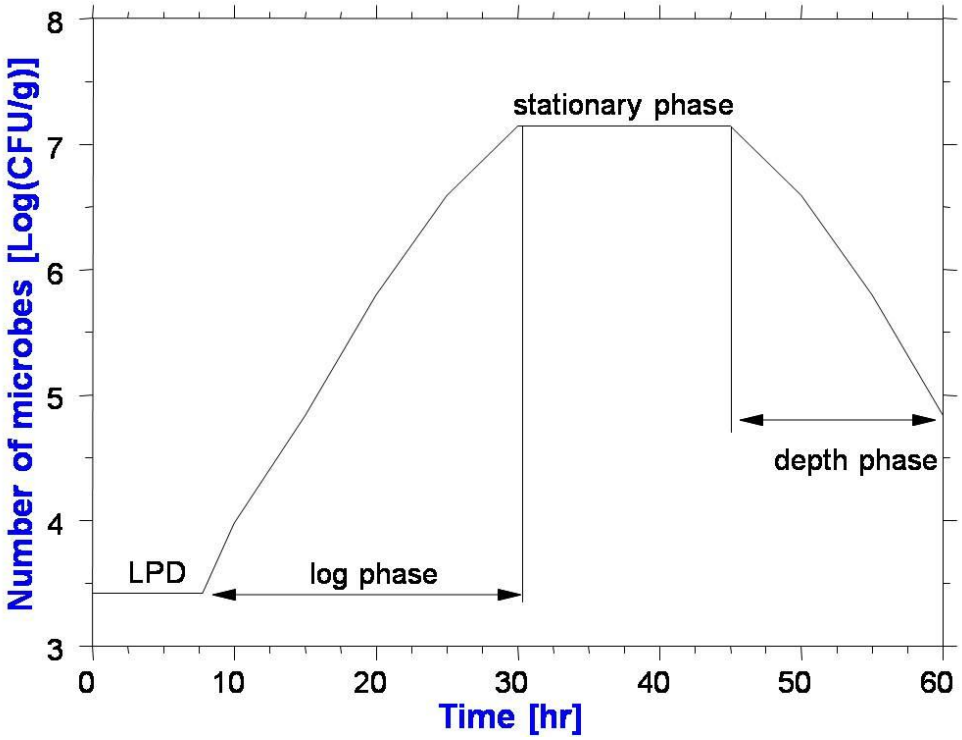

Fig. 2.2 Schematic of the Bacterial Growth Curve. Adapted from Buchanan and Whiting; (1997) and Lu et al. (2007). LPD Stands for Lag Phase Duration.

The logistic curve is of the form:

$$L_{(t)} = \frac{A+C}{1+e^{(-B(t-M))}} \quad (2.4)$$

and the Gompertz curve is of the form:

$$L_{(t)} = A + Ce^{-e^{(-B(t-M))}} \quad (2.5)$$

where for both curves, $L_{(t)}$, [Log (CFU/g)] is the log count of the number of bacteria at time t, *A*, [Log (CFU/g)] is the asymptotic log count as t decreases indefinitely, *C*, [Log (CFU/g)] is the asymptotic amount of growth that occurs as t increases indefinitely, and *B* [(Log (CFU/g))/h] is the relative growth rate at M, where *M* [h] is the time at which the absolute growth rate is a maximum. The difference between the two models is that the Logistic curve (EQ. 2.4) is symmetric about M, whereas the Gompertz curve (EQ. 2.5) is not. Growth kinetics for the Logistic curve are:

$$\text{Growth rate (GR)} = \frac{BC}{4} \quad (2.6)$$

$$\text{Lag Phase Duration (LPD)} = M - \frac{2}{B} \quad (2.7)$$

$$\text{Generation time (GT)} = \frac{96\ log_{10}(2)}{B\ x\ C} \quad (2.8)$$

while the growth kinetics for the Gompertz curve are:

$$\text{Growth rate (GR)} = \frac{BC}{e} \quad (2.9)$$

$$\text{Lag Phase Duration (LPD)} = M - \frac{1}{B} \quad (2.10)$$

$$\text{Generation time (GT)} = \frac{24\ log_{10}(2)e}{BC} \quad (2.11)$$

where e is the Napier's Constant and is equal to 2.72.

2.3 THE DIMENSION OF SPACE IN BACTERIAL GROWTH MODELS

Dens and Van Impe (2001) postulated that considering space in a model means that in addition to the evolution of biomass, *N* (Number of cells per unit of inoculums mass or volume (CFU/g)) at each location in the food, transfer of biomass through the food must also be taken into account. The basis of this postulation is that in a real structured food in which there is no perfect mixing of biomass, yet exchange of biomass in the food is possible. Then, the accumulation of biomass is composed of two parts namely, (i) biotransformation (growth) of cells at that location as a function of the environmental conditions, and (ii) transport of cells between neighboring locations. The authors chose to model the transfer of biomass by the diffusion law, diminishing the diffusion coefficient to simulate the mechanical hindrance the biomass goes through. The corresponding partial differential equation for the complete spatially extended model for a single species in which transport is included is:

$$\frac{dN(x,y,t)}{dt} = \mu(x,y,t).N(x,y,t) + Ds.\nabla^2 N(x,y,t) \quad (2.12)$$

where *N* is the number of cells per unit of volume, representing the cell densities of the microorganism species, *x* and *y* are the continuous spatial coordinates, *t* is time, μ(x,y,t).N(x,y,t) is the biotransformation term and $D.\nabla^2 N(x,y,t)$ is the transport term. ∇^2 is the diffusive operator which is the second partial derivative with respect to space:

$$\nabla^2 N(x,y,t) = \frac{d^2N(x,y,t)}{dx^2} + \frac{d^2N(x,y,t)}{dy^2} \quad (2.13)$$

where Ds is the surface unit per time, a measure of the firmness of the food. This parameter approaches infinity if the food is very liquid, and is zero if no movement of microorganisms is possible (Dens & Van Impe, 2001). The relevance of the dimension of space in bacterial growth modeling is that there is possibility of bacterial internalization

which can be in terms of space, as biomass is transported by bacterial mobility over distance. This is consistent with the findings by Richards and Beutchat (2005a) that *S. poona* was recovered from cantaloupe tissues at a depth of 3-4 cm within 7 days after inoculation on the wound.

2.4 ASSOCIATION OF *SALMONELLA SPP* WITH CANTALOUPE

Among the different fruits and vegetables associated with foodborne illnesses, cantaloupes (*Cucumis melo*) have been consistently linked to outbreaks of *Salmonella* infection in the United States (US) and Canada. A large multistate outbreak in the US in 1990 had 25 000 cases of *Salmonella* serotype Chester reported, and the infection was traced to the consumption of cantaloupes. Salmonella along with many other microorganisms capable of causing human diseases can survive in soil for protracted durations. *Listeria monocytogenes* is capable of surviving 8 weeks while Salmonella and *E. coli* 0157:H7 can survive up to 23 weeks, and viruses for 3 weeks (Bowen, et al., 2006).

Melons grow on the ground and are exposed to microorganisms, giving them the potential to become contaminated with pathogens. Cantaloupe surface is composed of a meshwork of tissue commonly referred to as the net, and the raised net tissue gives the surface of the cantaloupe an inherent roughness which favors microbial attachment and hinder microbial detachment (Ukuku & Fett, 2002). The study further determined that although *E. coli* strains comparatively exhibited the largest initial numbers of attached bacteria on the melon surface, Salmonella had the strongest bacterial attachment to the melon surface making it more difficult for the washing treatments to detach the pathogen from the melon surface with water. The transmission of pathogens to the interior of the

cantaloupe was reported to have occurred while cutting the unwashed melons (Castillo, et al., 2004). Subsequent association of foodborne illnesses with salad bars and fruit salads suggests that *Salmonella* may have been introduced into the fruit from the rind by the physical act of cutting the melon, or contact by cut pieces of melon with contaminated rinds (Golden, et al., 1993).

2.5 HANDLING, PACKAGING AND PRESERVATION OF CANTALOUPES AND QUALITY RETENTION

In the United States, cantaloupes are handled and packed differently in each state. Georgia grown cantaloupes are brought to sheds, washed and packed whereas California grown cantaloupes are field packed (Akins, et al., 2008). Cantaloupes (*Cucumis melo*) have been identified as a vehicle for *Salmonella* infection implicated in foodborne Salmonellossis in the USA and Canada. This has resulted in the Federal Drug Administration (FDA) issuing guidelines for keeping the fruit fresh and safe for processors and consumers, outlining safe handling processes for fresh produce, including a thorough washing of the rind with cold tap water before cutting.

Storage of untreated inoculated cantaloupes at room temperature (19 ± 1 ^{o}C) for 24 to 72 hours post-inoculation caused a significant ($p<0.05$) increase in *Salmonella* Poona and *Escherichia coli* populations compared with storage at 4 ^{o}C. This indicates that cantaloupes should be refrigerated as soon as possible following harvest to suppress the growth of any contaminant on the rind (Annous, et al., 2004). The research further showed that surface pasteurization of cantaloupes stored at 4^{o}C for 2 to 3 minutes at 76^{o}C reduced the residual microbial population from 6.18 log CFU/cm^2 to 3.88 log CFU/cm^2. This confirms that surface pasteurization process is a viable option for maintaining the

firmness quality and increase the shelf life of cantaloupes. Firmness expressed as force newtons (N) of the whole intact fruit devoid of rind was evaluated in terms of resistance of the mesocarp tissue to puncture with a 4.5 cm long and 30 mm diameter tip using a Chatillon Force Gauge (Lundy Electric, Glen Head, NY, 11545) assembly (Lester & Bruton, 1986).

The desire of processors, distributors and retailers of fresh fruits and vegetables is to keep pre-cut fruits and vegetables looking and tasting like the unprocessed raw fruits and vegetables. Cantaloupe melon is used more than any other fruit in fresh cut processing (Lamikanra, et al., 2002). However, cutting induces degradative changes associated with plant tissue senescence and a consequent decrease in shelf life relative to the unprocessed produce. The most common method of preservation is cold storage, which retards many biochemical processes in foods. However, reactions related to psychrotrophic enzymes and microorganism growth continues at low temperatures, and in case of tropical and subtropical produce, chilling injury occurs when storage temperatures are <12^{o}C (O'Connor, et al., 1994).

Lamikanra et. al. (2000) determined that the average pH, total acidity and ^{o}Brix for the fresh cut cantaloupe fruit were 6.5, 0.225 g/100 mL, and 8.8 respectively and this values did not change significantly over a period of two weeks at 4 ^{o}C. The study further observed a 17 % reduction in soluble solid content and a 2–fold increase in total acidity after 2 days of storage at 20^{o}C. It is for these reasons that fresh cut cantaloupe is commonly displayed on ice in retail supermarkets. O'Connor et. al. (1994) determined that the shelf life of fresh cut cantaloupe pieces stored at 4^{o}C was 4 days, after which a reduction of flavor, lower bitterness levels and increased level of paleness were observed.

A comparative evaluation of three different Modified Atmospheric Packaging (MAP) systems whereby (1) the package was allowed to naturally form a modified atmosphere (nMAP), (2) the internal atmosphere of the package was flushed with a gas mixture of 4 kPa O_2 plus 10 kPa CO_2 (fMAP), and (3) the film was perforated with a needle to have 10 1.5 mm holes (PFP) was undertaken. At 5^oC temperature storage the PFP maintained the shelf life of the fresh cut cantaloupe for 5 to 7 days, while the nMAP and fMAP maintained it for 9 to 12 days (Bai, et al., 2001).

2.6 STRATEGIES FOR THE TREATMENT OF CANTALOUPES CONTAMINATED WITH BACTERIA

2.6.1 Surface Treatments

2.6.1.1 Water, Ethanol and Hydrogen Peroxide Washes

Washing treatments of submerging melons in sterile water and agitating for 5 minutes with a glove covered hand to assure complete coverage with water did not significantly ($p>0.05$) reduce the population of *Salmonella* compared to the controls where there was no wash treatment (Ukuku, 2004). It only reduced the aerobic plate counts for cantaloupe rind from 6.48 to 6.09 log CFU/cm^2 while it reduced the aerobic plate counts on the fresh cut samples from 3.50 to 3.32 log CFU/cm^2. Surface treatment of cantaloupes with 70 % ethanol for 1 minute caused 1.34 and 1.45 $\log_{10}$CFU/cm^2 reduction of surface mesophilic aerobes enumerated on Plate Count Agar media incubated at 25^oC and 35^oC respectively (Ukuku, et al., 2001).

However, washing *Salmonella* inoculated cantaloupes with 2.5 % and 5 % hydrogen peroxide for 5 minutes caused a significant ($p>0.05$) reduction of *Salmonella* population by 2.56 and 2.29 log CFU/cm^2 respectively (Ukuku, 2004). In a different

study, exposure of whole melon surfaces to 97^{o}C water and 5 % hydrogen peroxide (70 ^{o}C) for 1 minute caused a 3.6 to 3.8 log reduction for *Salmonella*. The desirability of the hot water treatment was complimented by the fact that cantaloupes treated with 80^{o}C water for 2 minutes showed no evidence of visual damage or decay, and only minimal weight loss of about 2% during storage at 4^{o}C for 4 weeks. The weight loss was attributed to the disruption of natural waxes in the melon rind during exposure to 80^{o}C water, thereby increasing the water vapor permeability of the rind (Ukuku, et al., 2004).

2.6.1.2 Chlorine Washes

Soaking cantaloupes for 60 seconds in 200 ppm total chlorine concentration resulted in a 1.8 $\log_{10}$CFU/sample *S. typhimurium* population reduction, while scrubbing with a brush for 60 seconds in 200 ppm total chlorine improved removal by an additional 1 $\log_{10}$ CFU/sample (Parnell, et al., 2005). The presence of chlorine more importantly limited the cross contamination from the sites inoculated with the bacteria to the non-inoculated sites. Parnell et. al. (2005) further hypothesized that a surfactant would improve contact of chlorine with the bacteria, but surfactants often caused sensory problems and in some cases may increase decay or spoilage by increasing the water soaking of intercellular spaces. Ukuku and Sapers (2001) observed that washing of laboratory inoculated whole cantaloupes in chlorinated (1,000 ppm) water for 5 minutes within 24 hours after inoculation reduced the population of attached *Salmonella* Stanley on the cantaloupe surface by 3.4 $\log_{10}$ CFU/cm^2, and also reduced the possibility of cross contamination during fresh cut preparation.

2.6.1.3 Vacuum Steam Vacuum Treatment (VSV)

A Vacuum Steam Vacuum treatment is a surface intervention process which uses a brief exposure to vacuum to remove surface air and water to expose the bacteria. An initial vacuum is applied for 0.1 s followed by a short treatment with 138^{o}C saturated steam (0.1 s), a second vacuum treatment (0.5 s) evaporatively cools the surface, resulting in the destruction of bacteria with little or no thermal damage, and the cycle can be repeated two or more times. VSV treatments of two or three cycles resulted in a significant reduction of aerobic mesophilic bacteria (~ 1 log CFU/cm^2), yeasts and molds ((~ 2 log CFU/cm^2), and Pseudomonas spp. (~ 1 log CFU/cm^2) on cantaloupe surfaces (Ukuku, et al., 2006). The cantaloupes treated with VSV showed no evidence of visual damage, decay, or weight loss during storage at 5^{o}C for 9 days.

2.6.1.4 Nisin, EDTA (Ethylenediaminetetraacetic Acid), Sodium Lactate and Potassium Sorbate as Sanitizers

Nisin (50 µg/ml), EDTA (0.02 M, disodium salt), Sodium Lactate (NAL, 2 %) and Potassium Sorbate (KS, 0.02 %) when tested individually did not cause a significant ($p>0.05$) reduction in populations of a five strain cocktail of *Salmonella* in Tryptic Soy broth (TSB), whole melon surfaces and fresh cut pieces. However, when used in combination the population of bacteria obtained before storage was reduced by 3 log units in fresh cantaloupe surfaces, and the nisin-NAL-KS combination which was deemed most effective resulted in a 1.4 log CFU/g reduction in fresh cut cantaloupe pieces (Ukuku & Fett, 2004). All the compounds tested in this study are GRAS (Generally Regarded as Safe) and are commonly used in foods as antimicrobials.

2.6.1.5 Chlorine Dioxide (3 and 5 ppm), Ozone (3 ppm), Chlorinated Trisodium Phosphate (100 – 200 ppm Chlorine) and Peroxyacetic Acid (80 ppm)

Chlorine dioxide gas which has 2.5 times the oxidation capacity of chlorine is generally more effective than chlorine for inactivating surface microorganisms on fresh produce, with reductions of 3 to 4 logs reported using concentrations of 3 to 10 ppm in water. Additionally, chlorine dioxide is broadly bactericidal with a variable activity reported against bacterial spores, *Cryptosporidium* oocysts, and hepatitis A virus. Produce inoculation studies by Rodgers et. al. (2004) on apples, lettuce, strawberries and cantaloupe found that chlorine dioxide (5 ppm) reduced populations of mesophilic bacteria by ~4 logs, Ozone (3 ppm) reduced it by ~4 to 5 logs after 5 minutes exposure. Chlorinated Trisodium Phosphate (200 ppm chlorine) reduced the populations of *E. coli* 0157:H7 and *L. monocytogenes* by 4.8 to 5.1 logs, while peroxyacetic acid (80 ppm) yielded maximum reductions of 4.3 to 4.5 log for *L. monocytogenes* and *E. coli* 0157:H7 after 5 minutes.

2.6.2 Food Irradiation

Radiation refers to a physical phenomenon in which energy travels through space or matter. Food irradiation is the process of applying this energy to a food material to sterilize or preserve it by destroying microorganisms, parasites, insects, or other pests (Radomyski, et al., 1994). When food is preserved by ionizing radiation under processing conditions proposed for commercial production, nutrient destruction is no greater than that which occurs when food is preserved by more conventional means (Josephson, et al., 1978).

Food irradiation uses ionizing radiation which is generally characterized by its ability to excite and ionize atoms of matter with which they interact. Energy of the order of 4 – 25 eV is needed to cause a valence electron to escape an atom, and radiations must carry kinetic or quantum energies in excess of this to be called ionizing (Attix, 1986). Three principal types of radiation sources can be used in food irradiation according to the Codex Alimentarius General Standard (FAO, 1983), and these are gamma rays, x-rays and electron beams.

2.6.2.1 Gamma (γ) Radiation from Radionuclides such as ^{60}Co or ^{137}Cs[8]

The radioactive decay of ^{60}Co or ^{137}Cs results in a daughter cell formed in an excited and unstable state, which results in the release of a gamma-ray during the transition from the excited state to the ground energy level (Prasad, 1995). Gamma rays and X –rays occupy the same region within the electromagnetic spectrum and are distinguished only by their origin, as gamma-rays result from nuclear transition while X-rays result from interactions of electrons outside the nucleus.

Educating primary producers in good agri- and aqua-culture practices and consumers in safe food handling is an essential control measure in ensuring food safety and preventing foodborne illnesses, but this alone is not sufficient. The efficacy of such measures would be greatly enhanced if irradiation were introduced in the food chain as an additional control measure which can decontaminate many solid raw foods of animal origin and some fruits, vegetables and minimally processed foods (Molins, et al., 2001).

2.6.2.2 Machine Sources of X–Rays (Bremsstrahlung) with Electron Energies up to 5 MeV

X-rays were discovered by Roentgen in 1895 and called X – ray because of their unknown nature, one of the characteristic features being its ability to penetrate even solid matter. X-rays are produced in a Coolidge tube, where electrons supplied by an electrically heated filament are accelerated by a high positive potential to a target (anode) metal of high melting point and high atomic number. When the electron interacts with the target nucleus part of the energy is degraded to heat and part goes into producing X-rays. At 100 keV less than 1 % of the energy of the primary electron is converted into radiation, and over 99 % appears as heat (Prasad, 1995).

2.6.2.3 Machine Sources of Electron Beams with Energies up to 10 MeV

Electron accelerators are produced in a variety of forms and can be designed to produce electron beams with electron energies ranging from about 0.15 to 10 MeV for commercial applications (Cooper, et al., 1998). Despite the fact that electrons are less penetrating than gamma radiation, the advantage with electron accelerators is that the electron penetration can be tailored to the application by controlling the energy of the electrons. Characterization of an accelerator irradiator includes (a) measuring the mean energy of the electron beam, (b) beam spot profile and (c) scan width with the last two parameters ensuring that the dose is uniformly delivered on the surface of the process load, while the penetration of the electrons depends on the beam energy, and it is measured by determining the depth-dose distribution along the beam axis in a reference material, usually water or polystyrene (Grosswendt, 1994; IAEA, 2002; ISO/ASTM, 2002).

The Van de Graaff particle accelerator consists of an ion source, an evacuated region in which ions can be accelerated, and a source of high potential to do the acceleration (Prasad, 1995). The charge transfer is accomplished by means of a moving belt placed externally to the insulator column (Fig. 2.6) to supply the large potentials, and accelerators of this type can supply particles of up to a few million electron volts (Miller, 2005; Prasad, 1995). The resulting voltage is determined according to $V = Q/C$, where Q is the net transferred charge, and C is the capacitance between the high voltage terminal and ground.

CHAPTER III

PREDICTION OF ACCUMULATION (GROWTH AND MOBILITY) OF *SALMONELLA ENTERICA* SEROVAR TYPHIMURIUM IN FRESH CUT CANTALOUPE (*CUCUMIS MELO* L.)

3.1 OVERVIEW

Fresh cantaloupe flesh, with a moisture content of 88.52 %, a pH of 6.68 and 11 % Total Soluble Solids is an optimal medium for *S. typhimuriun* to adapt, grow and internalize into the internal mesocarp tissues. Growth of *Salmonella typhimuriun* in fresh cut cantaloupe flesh and mobility into internal mesocarp tissues was investigated. Growth was described by the gompertz growth model, while the internalization (50 mm length and 19.05 mm diameter cylinders) by space was predicted using an excel based power law function. The predicted growth dynamics are an exponential growth rate of 0.1963 Log (CFU/g)/hr, a generation time of 2.7 hours, a lag phase of 7.76 hours and a maximum population density of 7.98 logs (CFU/g) in 30 hours. Internalization of up to 20 mm was observed after 10 hours with a final bacterial load of 2.84 logs CFU/g, and a load of 2.64 logs CFU/g, was observed at 50 mm depth after 15 hours. The study shows that over 10 – 30 hours after invasion of fresh produce, the pathogenic bacteria can grow to infectious dose levels at the site of contamination, and also migrate to surrounding internal mesocarp tissues, rendering conventional surface decontamination processes deficient in ensuring food safety.

3.2 INTRODUCTION

Cantaloupe *(Cucumis melo* L.) has been associated with foodborne outbreaks involving Escherichia coli 0157:H7, Norovirus and numerous serovars of *Salmonella*, including *Salmonella chester, Salmonella poona, Salmonella oranienburg* and *Salmonella saphra* (Parnell, et al., 2005), and several national and international outbreaks of salmonellosis have been epidemiologically linked to consumption of fresh cantaloupes (Richards & Beutchat, 2005b). Contamination of produce such as cantaloupe can occur anywhere along the farm-to-fork pathway, from sources such as irrigation water, runoff water from adjacent livestock farms, manure, wash water, handling by workers, and feces of rodents (Akins, et al., 2008; Richards & Beuchat, 2005b). The mesocarp tissues of cantaloupes are particularly susceptible to contamination when the rind surface integrity is compromised by disease, bruising, cutting, or peeling.

Predictive Microbiology (PM) or the quantitative microbial ecology of foods attempts to provide mathematical rationale for microbial growth under a variety of environmental conditions – e.g temperature, pH, a_w and the effect of preservatives (Bidlas, et al., 2008). *Salmonella* spp. are a leading cause of bacterial foodborne disease all over the world, causing a diversity of illnesses that include typhoid fever, gastroenteritis and septicemia, and although more than 1500 Salmonella serovars exist, the most frequently isolated serotype is *S. typhimurium*, which accounts for about 35% of reported human isolates (Alvarez-Ordonez, et al., 2008). Models now exist that can predict growth of a wide range of pathogenic and spoilage microbes. These models have been derived mainly from growth data obtained in broth, but the growth behavior observed in a wide range of foods is close to that predicted by the models provided

temperature is maintained constant (Baranyi & Roberts, 1995). Comparisons between and within sample differences in Aerobic Plate Counts (APC) of *Salmonella enteritidis* var. *Rochester* in chicken at an abusive temperature of 27^{o}C confirmed that the data fit the Gompertz function, and therefore empirically derived models such as the Gompertz may be used to describe microbial growth in chicken and perhaps other foods (Langston, et al., 1993). Several other researchers, using extensive experimental data also concluded that the Gompertz model chosen from a large number of explicit models either proposed in the literature or newly developed can be regarded as the best model for microbial growth prediction, particularly because it has biologically meaningful parameters such as the maximum specific growth rate μ_m , the lag time λ, and the asymptotic value A (Van Impe, et al., 1992). However, deficiencies exist in modeling microbial growth in structured environments where space and time have to be taken into account. This structure involves two parts, one in which microbial growth is modeled as a function of the local environment over time, and the other involving transfer of biomass between neighboring sites (Dens & Van Impe, 2001). The dimension of time and space considerations in modeling microorganisms in food is based on the hypothesis that there is mobility of microorganisms in food, enabling them to internalize further into the food structure.

Minimal infective dose, which is the dose of the pathogen needed to cause infection is dependant on many factors such as the type of organism and type of host, specifically the age and health status. The lowest dose causing illness of 2 x 10^9 has been reported for *S. typhimurium* (Blaser & Newman, 1982). Blaser and Newman (1982) further cautioned that the notion that large inocula of salmonellae are necessary to induce

illness in humans is based on the results of studies involving volunteers. However, investigations of out- breaks of salmonellosis suggest that the infective dose was often low. Therefore, the actual infective dose for *S. typhimurium* may only be determined case by case, with high variability of the quantitative number of organisms.

Recovery of *S. poona* from tissues at depths of up to 3 – 4 cm below the inoculated wound supports this hypothesis that foodborne pathogens can migrate from the site of inoculation into adjacent mesocarp tissues (Richards & Beuchat, 2005a). Cantaloupes have an average moisture content of 88.52 % wet basis, a pH of 6.68 and 11 % Total Soluble Solids making them an optimal medium for *S. typhimuriun*, and the fact that they are consumed fresh without any cooking makes them a viable human infection vehicle.

Therefore, the objective of this study was to quantify the accumulation (growth and mobility) of *S. typhimurium* in fresh cut cantaloupe.

3.3 MATERIALS AND METHODS

3.3.1 Cantaloupes

A total of 63 ripe cantaloupes (golden/orange in color underneath and within the outer rind) were randomly selected and purchased from the local fresh produce market on the day of the experiment.

3.3.2 Cantaloupe Quality Determination

Quality characteristics were assessed daily to determine if there were notable quality changes on the cantaloupe during the duration of the experiment, seven days. All tests were conducted in triplicates at 23^{o}C.

pH**:** A 100 g mass of fresh cantaloupe flesh was blended in a regular kitchen blender, and the pH of the homogenate determined using a Cole Parmer pH 500 series meter (Cole Parmer, Vernon Hills, IL, USA). Prior to use the pH meter was calibrated to pH 7, 4 and 10 using standard buffer solutions.

Water Activity**:** A Haake C Water Activity meter coupled to a Rotronic Hygrolab Water Activity Sensor (Rotronic Instrument Corp. Huntington, NY, USA) and a water bath (23^{o}C) were used to measure the water activity of the samples.

Total Soluble Solids (degrees brix): A 1 ml volume of juice from the cantaloupe flesh was squeezed using a cheese cloth, and placed into an Automatically Temperature Compensated Hand-Held Refractometer (Sugar-Brix Refractometer, Scottsdale, AZ, USA) for measurement.

Moisture Content: This test was carried out by the Association of Official Analytical Chemists (AOAC) official method number 2.013 (AOAC, 1980), with some modifications. The procedure consisted of drying the cantaloupe flesh in a vacuum oven set at 19.4 ^{o}C and -100 kPa vacuum pressure, using a Welch vacuum pump for approximately 8 hours. All tests were conducted in triplicates. Table 3.1 shows a summary of the fresh cantaloupe quality characteristics.

Table 3.1

Measured Fresh Cantaloupe Quality Characteristics at 23^{o}C (Mean $\pm$SD)

pH	Water Activity (decimal)	^{o}Brix (%)	Moisture Content (% wet basis)
6.68 ± 0.06	0.91 ± 0.01	11 ± 0.31	88.52 ± 1.48

*Values are Means of 3 Replications per Day for 7 Consecutive Days.

3.3.3 Preparation of Salmonella Inoculum

Nalidixic acid and novobiocin resistant *S. typhimirium* was obtained from Dr James Q.A. Bryd (USDA-ARS, College Station, TX), and maintained and grown in tryptic soy broth (TSB) supplemented with 20 μg/ml nalidixic acid (Sigma, St Louis, Mo, USA) and 25 μg/ml novobiocin (Sigma, St Louis, Mo, USA). A minimum of two transfers with a transfer after every instance of incubation of the culture media for 18 - 24 hours and subsequent serial dilutions up to a yield of 3 – 4.11 $\log_{10}$ CFU/g were done to produce the inoculum ready for the challenge test.

3.3.4 Sample Preparation and Bacterial Inoculation

The cantaloupes were peeled and a 19.05 mm diameter aluminum core was used to core out ten (10) samples of 50 mm length and 19.05 mm diameter cantaloupe flesh. Each core sample was wrapped in aluminum foil, placed in a test tube rack with the top end open, and inoculated with 50 μL volume of 3.77 – 4.11 logs CFU/g concentration of *S. typhimirium* inoculum. The cantaloupe samples were inoculated at the top end and allowed 7 – 10 minutes in the undisturbed normal position for the inoculum to soak into it, and then either left in the same position (normal placement), or rotated at a 90^{o} or 180^{o} angle (Fig. 3.1). Samples were then left at room temperature (23^{o}C) for 0.5, 5, 10, 15, 20, 25 and 30 hours, which are the time periods during which bacterial mobility into the sample was evaluated.

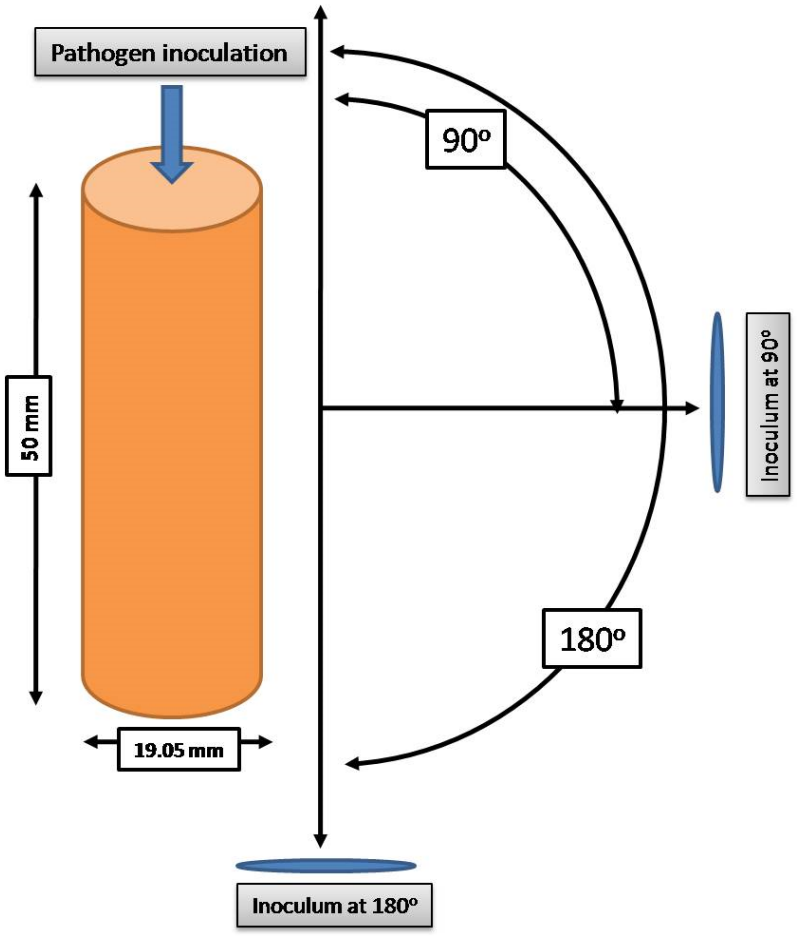

Fig. 3.1 Variable Placement Positions of Cantaloupe Sample after Microbial Inoculation.

3.3.5 Microbiological Analysis

The standard plate count method using Tryptic Soy Agar (TSA) medium supplemented with 1 mL/L nalidixic acid (Sigma, St Louis, Mo, USA) and 1 mL/L novobiocin (Sigma, St Louis, Mo, USA) was used to determine total colony counts.

Ten samples of 2.5 g mass (10 mm length) were cut aseptically from the top 10 mm depth of the 50 mm length cantaloupe flesh (Fig. 3.2) at time intervals of 0.5. 5, 10, 15, 20, 25 and 30 hours and each homogenized in a sterile stomacher bag with 22.5 mL of Buffered Peptone Water (BPW) using a hand meat tenderizer, providing a 1:10 dilution. Subsequent required dilutions were made by transferring 1 mL of the homogenate to 9 mL of sterile BPW. A 0.1 mL volume of each dilution in duplicate was plated onto a sterile TSA plate, and incubated for 24 hours at 37^{o}C. Colonies formed were counted and calculations made by multiplying the total number of colonies by the dilution factor, to get the bacterial growth at the specific growth duration in CFU/g.

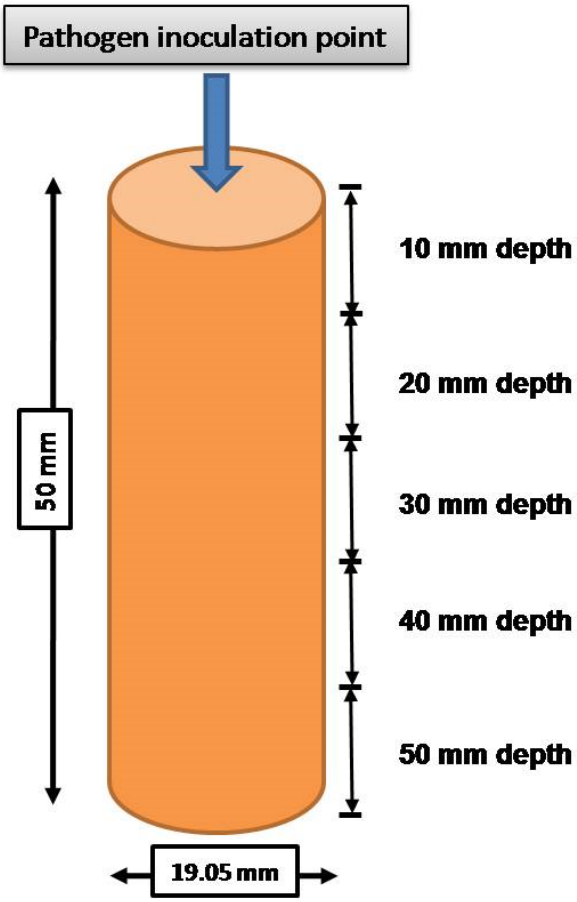

Fig. 3.2 Specific Depth Sample Position along the 50 mm Depth.

Bacterial mobility was determined by cutting five samples of 2.5 g mass (10 mm length) aseptically at every 10 mm depth along the 50 mm length of the cantaloupe flesh (Fig. 3.2) and homogenizing it in a sterile stomacher bag with 22.5 mL of Buffered Peptone Water (BPW) using a hand meat tenderizer, providing a 1:10 dilution. Subsequent required dilutions were made by transferring 1 mL of the homogenate to 9 mL of sterile BPW. A 0.1 mL volume of each dilution in duplicate was plated onto a sterile TSA plate, and incubated for 24 hours at 37^{o}C. Colonies formed were counted and calculations made by multiplying the total number of colonies by the dilution factor, to get the bacterial growth at the specific growth duration, at the particular depth. Mobility was determined by prediction of the bacterial growth by depth for the specific time intervals.

3.3.6 Curve Fitting, Bacterial Growth Modeling and Mobility Prediction

SPSS (SPSS, 2006) was used to generate a logistic curve from the $\log_{10}$ of bacterial population counts as a function of time. The logistic curve was deemed appropriate because it consists of the four stages of microbial growth, namely an initial lag phase where no change occurs, followed by a period of accelerating change, a period of decelerating change and finally a stationary period (Gibson, et al., 1987) and is of the following form:

$$L_t = \frac{1}{\frac{1}{U}+\beta_0\beta_1{}^t} \qquad (3.1)$$

where L_t is the log count of bacteria at time (in hours) t, U is the asymptotic amount of growth that occurs as t increases indefinitely, β_0 is a constant and β_1 is the slope of the log bacteria versus time curve.

Substituting the numerical values of the constants, Eq. 3.2 can be written as:

$$L_t = \frac{1}{0.138+0.219^t} \quad (3.2)$$

The Gompertz model (EQ. 2.5) was fitted to the experimental data and the values of the coefficients are given in Table 3.2. The Gompertz model in EQ. 2.5 is re-written after substitution of the experimentally based constants (Table 3.2) as:

$$L_t = 3.41 + 4.56 * e^{-e^{(-0.12(t-16.31))}} \quad (3.3)$$

Bacterial mobility into the fresh cut cantaloupe sample was predicted using linear regression (Excel, Microsoft, Redmond, WA) spreadsheet. The Log of bacterial population for each specific depth (10, 20, 30, 40 and 50 mm) was plotted against the time intervals of 10, 15, 20, 25 and 30 hours, resulting in a linear function with a distinct gradient for each depth, and a constant of 1.70 logs CFU/g which is the minimum detection limit as shown in Fig. 3.3.

The specific slopes for each depth were plotted against depth to determine the common gradient for all depths (Table 3.3). The trend-line tool of Excel (Microsoft, Redmond, WA) spreadsheet was used to generate a power law function (selected on the basis of the highest R^2) of the gradient against depth, which was reinserted as the slope in the initial prediction of log of bacteria population by time for the various time intervals (Fig. 3.4). The developed prediction is written as:

$$BM = (0.756*d^{-0.575})*t + 1.70 \quad (3.4)$$

where BM is the log count of bacteria population [log(CFU/g)], as it grows and moves over time t (in hours), and d is the bacterial depth within the sample for the specific predicted time (mm).

Table 3.2

Experimentally Derived Constants from the Logistic Curve (EQ. 3.1) and Initial Iteration Constants for the Gompertz Model (EQ. 2.5)

Constant	Definition	Value	Units
β_0	Constant in EQ. 3.1	0.234	
β_1	Slope in EQ. 3.1	0.934	
U	Maximum population density in EQ. 3.1	7.23	$\log_{10}$(CFU/g)
A	Asymptotic log count as time decreases indefinitely (EQ. 3.3)	3.41	$\log_{10}$(CFU/g)
C	Asymptotic log count as time increases indefinitely (EQ. 3.3)	4.56	$\log_{10}$(CFU/g)
M	Time at which the absolute growth rate is maximum (EQ. 3.3)	16.31	hours
B	Relative growth rate at M (EQ. 3.3)	0.12	$\log_{10}$(CFU/g)/h

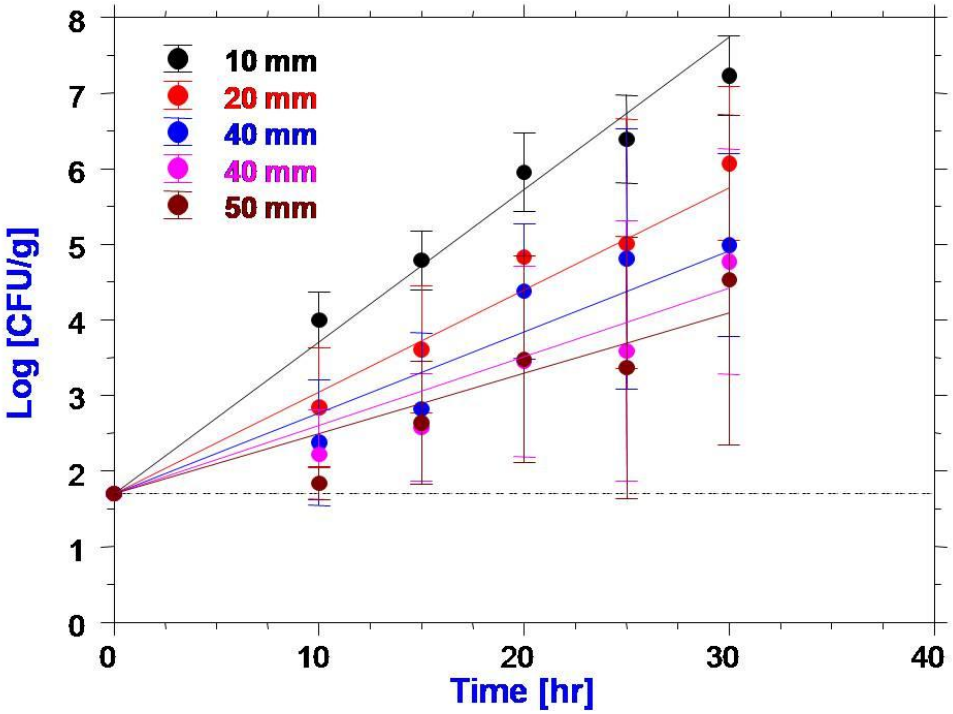

Fig. 3.3 Log of Bacteria Mobility against Time.

Table 3.3

Bacteria Mobility Prediction - Linear Model Constants (Fig. 3.3)

Depth [mm]	Slope [log(CFU/g)/hr]	Intercept [log(CFU/g)]	R^2
10	0.194	1.7	0.979
20	0.140	1.7	0.978
30	0.112	1.7	0.918
40	0.085	1.7	0.903
50	0.079	1.7	0.858

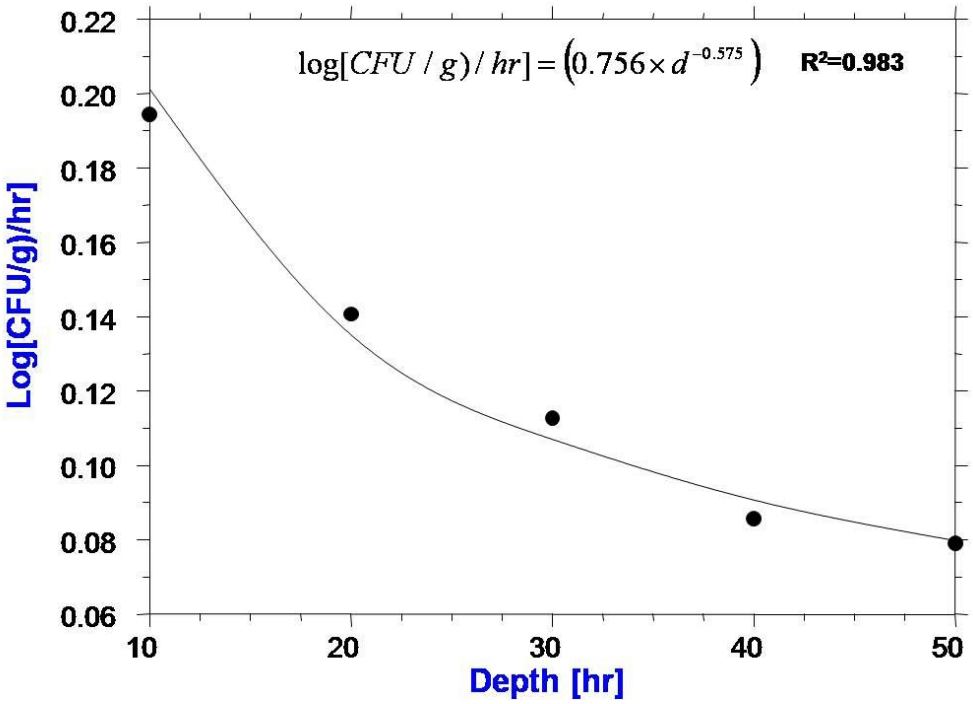

Fig. 3.4 Slope Values (Fig. 3.3) for Specific Depths Plotted against Sample Depth.

3.3.7 Statistical Analysis

SPSS was used to compare means using one way ANOVA, on subsets of data for significant differences ($p \leq 0.05$) due to depth and time, using the Duncan's Multiple Range Test. Coefficient of Determination (R^2), Root Mean Square Error (RMSE) and Mean Bias Error (MBE) were used to evaluate the performance of the gompertz growth model in comparison to the actual measurement of growth in the cantaloupe.

3.4 RESULTS AND DISCUSSION

3.4.1 Fresh Cantaloupe Quality Characteristics

Fresh cantaloupes stored at 23 ^{o}C for up to seven days retained the same quality characteristics for the entire duration of the experiment (Table 3.1). Even though the growth and mobility analysis on the fresh cut samples was done for up to 30 hours, it was critical to determine the stability of the baseline nutritive value of cantaloupe and the environment it offers for survival of bacteria. The results confirm that the fresh cut samples offer a conducive baseline environment for the growth of *S. typhimurium*.

3.4.2 Bacterial Growth Modeling

Sample placement positions of normal (0^{o}), 90^{o} and 180^{o} (Fig. 3.1) had no significant differences ($p<0.05$) in terms of *S. typhimurium* accumulation in the cantaloupe. Further analysis of results was therefore not categorized according to sample placement position, and all samples were placed in the normal placement position.

The growth kinetics of *S. typhimurium* modeled using the Gompertz model (EQ. 3.2) are shown in Table 3.4. The model predicted the bacterial growth kinetics with quantities which are similar to the experimental data (Fig. 3.5), with a coefficient of determination, R^2 of 0.99 and a root mean square error (rmse) of 0.11. The closeness of

the R^2 value to 1, and the rmse to 0 indicates that the model has a high level of accuracy in predicting the bacterial growth. An exponential growth rate of 0.20 log (CFU/g)/hr, a generation time of 2.70 hours, a lag phase of 7.76 hours and a maximum population density of 7.98 log (CFU/g) were predicted. These growth kinetics parameters show the rate at which *S. typhimurium* accumulates in fresh cantaloupe and the levels of population growth that can be attained in a period of 30 hours. The results are further support to the determination that the Gompertz model (EQ. 3.2) can be regarded as the best model for microbial growth prediction (Langston, et al., 1993; Van Impe, et al., 1992). The model can be used to predict bacterial growth in fresh produce with similar quality characteristics as fresh cantaloupe at room temperature.

3.4.3 Bacterial Accumulation (Growth and Mobility) Prediction

The Microsoft excel based power law function developed from experimental data (EQ. 3.4) predicted the accumulation of *S. typhimurium* in fresh cantaloupe sample with R^2 of 0.98. The plot of log of bacterial population against depth for the 30 hour time interval is shown in Fig. 3.6. The standard deviation typically increases with increasing depth because bacterial population decreases with increasing depth, making it more difficult to accurately quantify populations. These results show that *S. typhimurium* has the ability to internalize and invade subsequent internal mesocarp tissues of fresh cantaloupe up to 50 mm within a duration of 30 hours (Richards & Beuchat, 2005a). Bacterial population at the various depths for all the time intervals are shown in Table 3.5.

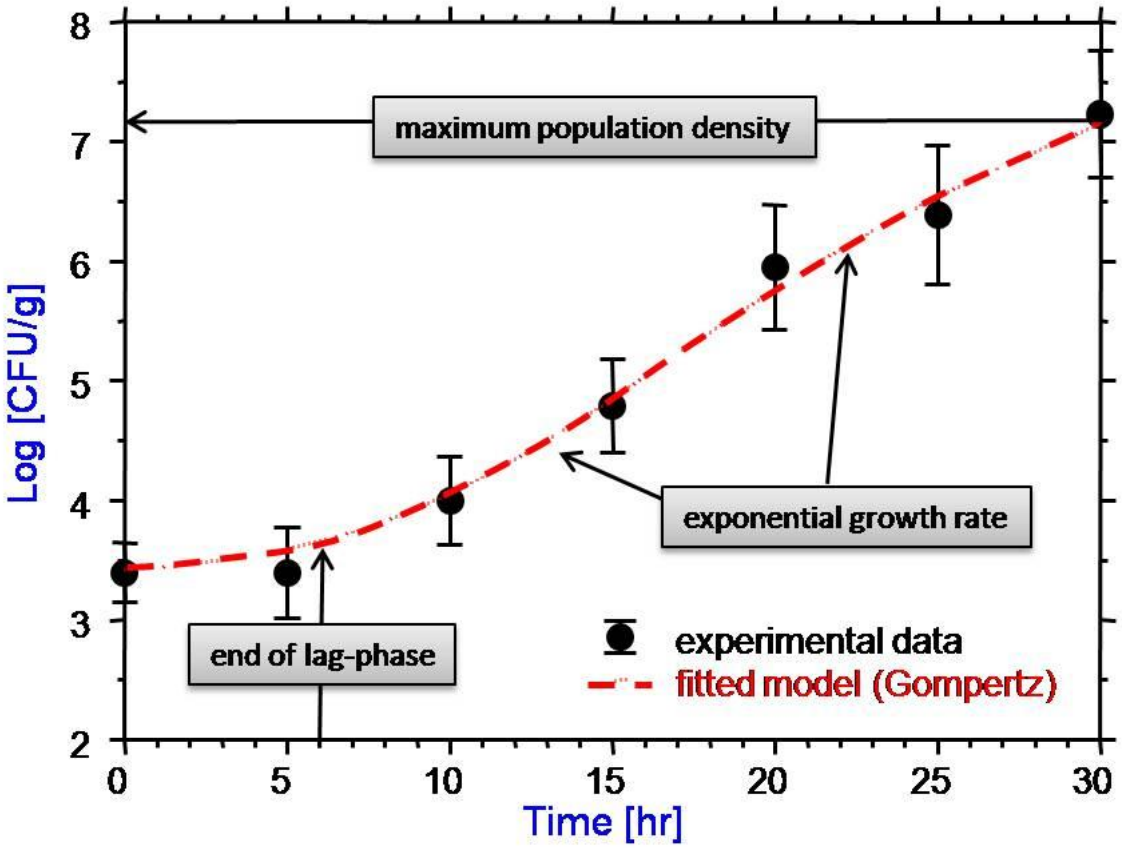

Fig. 3.5 Growth of *S. typhimirium* Modeled in Fresh Cantaloupe by the Gompertz Model (EQ. 3.3) at 23^{o}C.

Table 3.4

Growth Kinetics of *S. typhimurium* in Fresh Cantaloupe at 23°C

Parameter	Gompertz Model (Eq. 3.3)	Units
Exponential growth rate (EGR)	0.20	[log(cfu/g)/h]
Generation time (GT)	2.70	[h]
Lag phase duration (LPD)	7.76	[h]
Maximum population density (MPD)	7.98	[log(cfu/g)]
Coefficient of Determination, R^2	0.99	
Root Mean Square Error, RMSE	0.11	

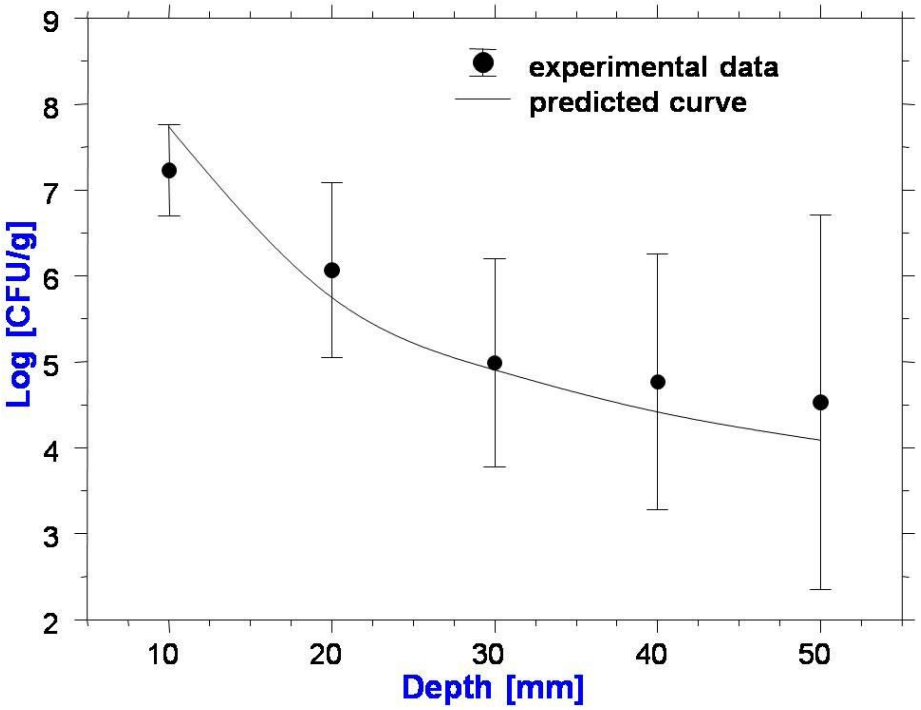

Fig. 3.6 Log of Bacterial Population against Sample Depth for 30 Hour Interval at 23^{o}C.

Table 3.5

S. typhimurium Population (Log CFU/g) in Fresh Cantaloupe at Variable Growth Intervals and Depths at 23°C

Time (hrs)	D.L	Depth (mm)				
		10	20	30	40	50
D.L	1.70 (0.00)	1.70 (0.00)	1.70 (0.00)	1.70 (0.00)	1.70 (0.00)	1.70 (0.00)
10	$_{v}$1.70 (0.00)	$_{y}$4.00 (0.37)	$_{x}$2.84 (0.79)	$_{w,x}$2.38 (0.83)	$_{v,w}$2.22 (0.59)	$_{v}$1.84 (0.22)
15	$_{v}$1.70 (0.00)	$_{y}$4.79 (0.39)	$_{x}$3.61 (0.84)	$_{w}$2.83 (1.00)	$_{w}$2.58 (0.71)	$_{w}$2.64 (0.81)
20	$_{v}$1.70 (0.00)	$_{y}$5.95 (0.52)	$_{x}$4.83 (0.70)	$_{x}$4.38 (0.89)	$_{w}$3.45 (1.26)	$_{w}$3.48 (1.37)
25	$_{v}$1.70 (0.00)	$_{z}$6.39 (0.58)	$_{y}$5.01 (1.65)	$_{x,y}$4.81 (1.72)	$_{w,x}$3.59 (1.72)	$_{w}$3.37 (1.73)
30	$_{v}$1.70 (0.00)	$_{y}$7.23 (0.53)	$_{x}$6.07 (1.02)	$_{w,x}$4.99 (1.21)	$_{w}$4.77 (1.49)	$_{w}$4.53 (2.18)

[1]D.L. refers to Detection Limit

[v-z]Means within a Row, which are not Followed by a Common Superscript Letter, are Significantly Different ($P<0.005$), () Standard Deviation

This capability of *S. typhimurium* to migrate into cantaloupe tissue for up to 50 mm depth makes surface decontamination treatments such as washing and chlorination deficient in controlling bacteria which had infected the fruits and had a minimum duration of 10 hours to internalize into the interior mesocarp tissues. Thus 10 hours would be sufficient for the bacteria to internalize the produce to at least 20 mm, deeming it inappropriate for common surface decontamination interventions. The need for microbial treatment systems which have the ability to penetrate and inactivate the internalized microorganisms such as *S. typhimurium* becomes the only suitable alternative. The accumulation of bacterial load from 2.84 logs at 20 mm depth after 10 hours to 6.07 logs after 30 hours shows that even a low non-infective dose can increase to an infective dose level, particularly because investigations of outbreaks of salmonellosis suggest that the infective dose was often low (Blaser & Newman, 1982).

Accumulation predictions can be used to determine if the contamination has reached the minimum infective dose level and therefore be a useful food safety tool. They also enable prediction of the rate of internalization of *S. typhimurium* into internal mesocarp tissues of fresh produce, and direct food safety intervention treatments such as irradiation, which have the capability to penetrate the fresh produce to the site of the bacterial pathogen.

3.5 CONCLUSION

The Gompertz model (EQ. 3.3) predicted the growth kinetics of *S. typhimurium* in fresh cut cantaloupe flesh at room temperature (23^{o}C) with a coefficient of determination of 0.99. An exponential growth rate of 0.1963 Log (CFU/g)/h, Generation Time (GT) of 2.70 hours, a Lag Phase Duration (LPD) of 7.76 hours as well as a Maximum Population Density (MPD) of 7.98 log CFU/g were determined.

Bacterial internalization into the fresh cut cantaloupe sample was observed after a minimum time interval of 10 hours, and the power law function (EQ. 3.4) predicted the internalization with an R^2 of 0.98. A bacterial population of 4.02 logs (CFU/g) was determined at the 50 mm depth after an interval of 30 hours.

In summary, microbial pathogen inactivation strategies in fresh produce must have the capability to penetrate into the produce and inactivate internalized pathogens at depths of up to 50 mm because surface interventions alone such as chlorination and washes with water will be inadequate for treating the internalized pathogens. Electron beam irradiation has that capability to penetrate into fresh produce and inactivate the internalized pathogenic bacteria.

CHAPTER IV

CORRELATIVE MICROSCOPIC ANALYSIS AND A PLATE ASSAY METHOD AS A BASIS FOR *SALMONELLA ENTERICA* SEROVAR TYPHIMURIUM LT2 INTERNALIZATION IN FRESH CUT CANTALOUPE (*CUCUMIS MELO* L.)

4.1 OVERVIEW

Cylindrical cantaloupe flesh samples (19.05 mm diameter, 50 mm length) of cantaloupe flesh were inoculated with *S. typhimuriun* LT2, and the bacteria observed in internal mesocarp tissues up to 50 mm depth using a Scanning Electron Microscope after 20 – 30 hours at 23^{o}C. Transmission Electron Microscopy (TEM) and Light Microscopy (LM) showed that the cantaloupe structure is made of intercellular spaces which could be the route for the bacterial internalization. Observation and subsequent imaging of a 2 µL volume of a liquid culture of the *S. typhimurium* LT2 inoculum in a JEOL 1200EX TEM revealed that the bacterial cells had flagella. A plate assay to determine whether *S. typhimurium* LT2 was capable of producing extracellular plant cell wall-degrading enzymes such as polygalacturonase showed that *S. typhimurium* LT2 does not possess that ability. It was concluded that *S. typhimurium* LT2 internalization can only be through diffusion or flagella aided mobility through the intercellular spaces.

4.2 INTRODUCTION

Phytobacteriologists generally agree that plant-pathogenic bacteria do not posses penetration structures, such as pegs commonly found in fungi, therefore, plant pathogenic bacteria are unable to exert mechanical or physical forces to penetrate into intact epidermal tissues (Huang, 1986). However, pathogenic gram negative bacteria such as *S. typhimurium* sense and respond to a wide variety of environmental signals during the

transition from a free-living state to infection of a suitable host, whereby oxygen tension, osmolarity, iron availability, pH, nutrient limitation, temperature, and even specific bacterium-host physical interactions regulate expression of virulence genes (Ahmer, et al., 1998). This study used an attenuated laboratory strain *Salmonella typhimurium* LT2 which differs from the virulent *Salmonella typhimurium* strains at the *rpoS* locus. The *rpoS* gene in strain LT2 contains a rare UUG start codon which is responsible for the inability of LT2 to display a sustained log-phase acid tolerance response (Lee, et al., 1995; Wilmes-Riesenberg, et al., 1997). The availability of nonpathogenic bacteria which have similar responses to specific food processes as the pathogenic bacteria, offers the ability to validate a process in-plant, without the use of the actual pathogens, for example such as coliforms were used as process indicators for pasteurization in the dairy industry (Niebuhr, et al., 2008).

Increase in the consumption of fresh produce such as cantaloupe has resulted in an increase in food borne illnesses, with 25 outbreaks associated with consumption of cantaloupes reported to the CDC food borne outbreak surveillance system between 1973 and 2003 (Bowen, et al., 2006). Cantaloupes may become contaminated before harvest, during harvesting, packing, and storage, and during processing or preparation of cut products. Mesocarp tissues of fruits are particularly subject to contamination when rind surface integrity is compromised by disease, bruising, cutting or peeling, and the growth habit of cantaloupes enhances the potential for contamination. Richards and Beutchat (2006) stated that cellulases and pectinases produced by phytopathogens cause softening and release of cell fluids from plant tissues, which results in the breakdown of the structural integrity of tissues which favors movement of foodborne pathogens from

wounded and decaying tissues to otherwise sound tissue on the same fruit or adjacent fruit. The extracellular virulence factors such as plant cell wall-degrading enzymes, toxins, DNA, hormones, siderophores, and signaling molecules have roles in bacterial survival within, or ingression of, the host plant (Salmond, 1994).

Pectins are the major matrix components of plant cell walls and consist of a heterogeneous class of cell wall polymers important for growth and development of higher plants, control of wall porosity, adhesion of adjoining cells and regulation of the ionic environment of the cell wall (Eder & Utz-Meindl, 2008). Homogalacturonan and rhamnogalacturonans are the main constituents of pectins in higher plants. Plants being multicellular organisms have adhesion molecules in their extracellular matrices (ECMs) that serve to maintain the integrity of the organism and to provide a scaffold for cell to cell communication. The plant cell wall or ECM contains many polymers, the most abundant and best known being cellulose, but this well known polymer is embedded in a matrix of molecules called hemicelluloses and pectins. Pectins are likely to be implicated in adhesion because they occur in the middle lamella, the site of cell adhesion, and they are secreted from epidermal walls when carpel fusion occurs in formation of the transmitting tract (Lord & Mollet, 2002). Pectin consists of D-galacturonic acid units with very small quantities of neutral sugars (Monsoor, et al., 2001).

A large volume of the plant body is occupied by an intercellular space system which is developed by separation of contiguous primary walls through the middle lamella (Esau, 1977). Plant cells such as the legume epidermal root hair cell have specialized anatomical modifications of the normal intercellular space in that they have an intracellular tunnel, sheathed by plant cell membrane and plant cell wall materials,

referred to as the infection thread and the tunnel is the first stage in the process of internalization of bacteria, such as rhizobia by plant cells (Vandenbosch, et al., 1989).

Hollowing in watermelons and tomatoes is a physiological disorder which decreases their market value, and is physiologically linked to intercellular space development. Watermelon fruitlets grow mostly by cell division for 4 days after pollination before and shortly after anthesis (period during which a flower is fully open and functional), and subsequently growth is mostly attributed to cell enlargement which is concurrent with intercellular air space development (Kano, 1993). According to Woolley (1983) air-filled intercellular spaces in higher plants are necessary for the respiration of all massive plant tissues, such as potato tubers and large fruits, at least during growth and development. In addition to their function as pathways for diffusion of CO_2 for photosynthesis, air-filled intercellular spaces (with adjacent cells) in the leaf provide refractive index discontinuities which cause the leaf to scatter much of the incoming radiation. Flotation of aquatic plants or plant parts is possible because of air-filed intercellular spaces.

Woolley (1983) further reported that plants maintain an air spaces in a matrix consisting primarily of water because a wettable intercellular space with a diameter of 2 μm would have a capillary potential of about $-1.5 * 10^5$ N/ m^2, while typical nutrient solutions have osmotic potentials in the range of $-5 * 10^4$ N/m^2, so that as a cell approaches equilibrium with the nutrient solution the cell water potential exceeds the capillary potential of the intercellular space, such that (given sufficient time) the water should flow into that space.

The intercellular space serves as a container for various secreted materials. This network of intercellular spaces in the plant anatomy is possibly the route through which bacteria internalize into the internal mesocarp tissues of injured fruits such as cantaloupe. The injury results in an imbalance of the osmolarity and osmotic potential which is maintained by a healthy plant such that it can retain air spaces in a predominantly water medium. The invading pathogenic bacterium possibly exploits this imbalance and internalizes into the plant structure.

The objective of this study was to develop a correlative basis for internalization of *S. typhimurium* LT2 into the internal mesocarp tissues of fresh and intact cantaloupe flesh.

4.3 FUNDAMENTALS OF CORRELATIVE MICROSCOPY

Correlative microscopy enables the study of the same tissue or cell with the light microscope (LM), scanning electron microscope (SEM) and transmission electron microscope (TEM), giving variable cell details consistent with the desirable level of resolution (Hayat, 2002). Correlatively, the different microscopes complement each other in imaging the cantaloupe structure resulting in visualization of the desired detail of information. The light microscope (LM) employs visible light to detect small objects, and objects as small as bacteria can be observed and cell shape recognized at a mere 100x magnification. The transmission electron microscope (TEM) operates on the same basic principles as the light microscope but uses electrons instead of light. Visualization with a light microscope is limited by the wavelength of light, while the TEMs use electrons as "light source" and their much lower wavelength makes it possible to get a resolution a thousand times better than with a light microscope. The variable visualization capability

of the LM and the scanning and transmission electron microscopes enable the visualization of the overall structure of the cantaloupe flesh cells (LM), the detail of individualized cantaloupe cell with intercellular spaces (TEM), and localization of the *S. typhimurium* LT2 in the cantaloupe flesh (SEM).

4.4 MATERIALS AND METHODS

4.4.1 Correlative Microscopy Study

4.4.1.1 Sample Procurement and Inoculation with S. typhimurium LT2

Three ripe cantaloupes (*Cucumis melo)* were procured from the local retail market and the flesh samples were cored out (cylindrical 19 mm diameter and 50 mm length) using a stainless steel core attached to a wooden handle (Fig. 4.1A). At least 4 flesh samples were cored out per cantaloupe. Ripeness was assessed by ensuring that the cantaloupe is slightly soft at the blossom end, and the skin is beige with grey toned netting, while the flesh is pale orange. Owing to biological safety concerns and the requirement that only avirulent strains are allowed in the Texas A&M University Microscopy and Imaging Center laboratory, an avirulent surrogate of the real pathogen was used. The inoculum was prepared by maintaining and growing nalidixic resistant *S. typhimurium* LT2 (ATCC 700720) acquired from the laboratory of Dr Alejandro Castillo of Texas A&M University in tryptic soy broth supplemented with 20 μg/ml nalidixic acid (Sigma, St. Louis, MO, USA). A minimum of two transfers with a transfer after incubation of the culture medium for 18-24 hrs was done to produce the inoculum. Samples were placed vertically in a test tube rack (Fig. 4.1B) and inoculated with 50 μl (8 logs) of *S. typhimurium* LT2 inoculum.

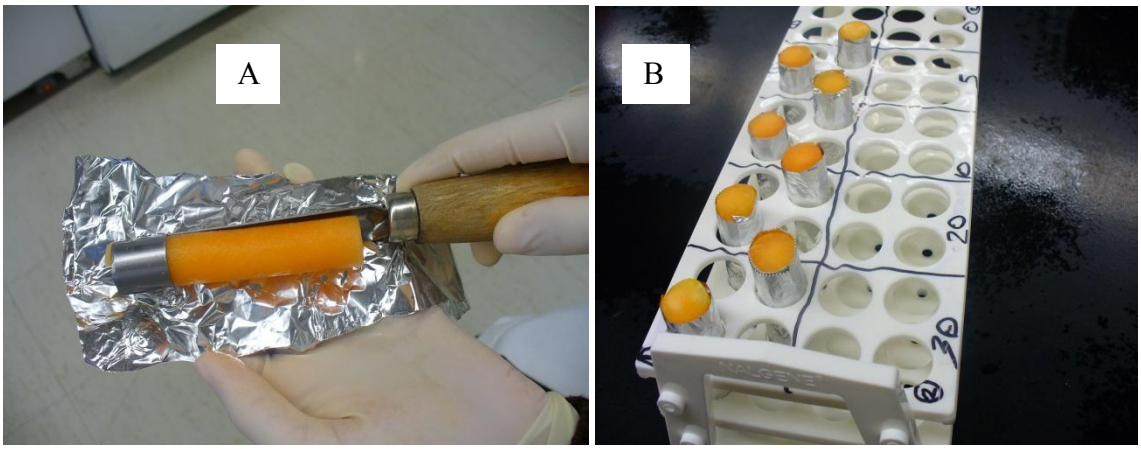

Fig. 4.1 Cantaloupe Flesh Samples (A) Cored Out and (B) Placed in a Test Tube Rack.

4.4.1.2 Sample Preparation for Transmission Electron Microscope (TEM), Scanning Electron Microscope (SEM) and Light Microscope (LM)

Small portions (cylindrical,1 mm thick, 8 mm diameter) of cantaloupe flesh were cored from the center of the 1 mm thick slice and cut at a depth of not less than 15 mm (15 – 40 mm) into the sample (Fig 4.2) using a brass cylindrical core. The 1 mm thick and 8 m diameter sample was the optimal size for the subsequent fixation and preparation for visualization in the LM, SEM and TEM. Primary fixation was done in 6% (vol/vol) glutaraldehyde in 0.05 M HEPES buffer, pH 7.3) at room temperature for 20 minutes followed by treatment with intermittent vacuum (5 min On, 5 min Off at 15 in. Hg) for 30 min. Final fixation was done in a Biowave® laboratory microwave (Ted Pella, Inc., Redding, CA, USA) for a 6 min cycle (2 min On, 2 min Off, 2min On) at 200 watts with intermittent vacuum (30 sec On and 30 sec Off) during the 6 min cycle (Hopwood, 1967, 1972; Llewellyn-Smith & Minson, 1992). Specimens were then rinsed 3X1 min at 200 watts with 0.05 M HEPES, pH 7.3 followed by post fixation overnight at 4 °C in 1% (wt/vol) osmium tetroxide in 0.05 M HEPES, pH 7.3 plus 1.5% (wt/vol) potassium ferricyanide. Post fixation was completed with a 6 min cycle (2 min On, 2 min Off, 2min On) at 100 watts with intermittent vacuum (30 sec cycles). Specimens were washed with 0.05 M HEPES buffer, pH 7.3 for 1 min in the microwave at 200 watts. Specimens were then dehydrated in methanol in 5% steps (5%-100%) at 1 min/step in the microwave at 200 watts and intermittent (30 sec/cycle) vacuum. The 25, 50, 75 and 100% methanol steps were microwaved using a 6 min cycle (2 min On, 2 min Off, 2min On) at 200 watts and intermittent (30 sec/cycle) vacuum. Dehydration was finished with acidified 2,2-dimethoxypropane (Electron Microscopy Sciences, Hatfield, PA, USA) (Lin, et al.,

1977) followed by propylene oxide as the transitional solvent. Specimens were then infiltrated and embedded in a Quetol 651 modified Spurr epoxy resin formulation (Table 4.1). Thick sections (>2 μm) were stained with 1% (wt/vol) toluidine blue in 1% (wt/vol) sodium boratebuffer and imaged with a Zeiss Axiophot light microscope (Neurodigitech, LLC. San Diego, CA, USA). Ultrathin sections (< 2 μm) were poststained with 2% (wt/vol) aqueous uranyl acetate followed by Reynolds lead citrate (Reynolds, 1963) and then imaged in a JEOL 1200EX TEM (JEOL USA, Inc. Peabody, MA, USA) at an accelerating voltage of 100 kV (0.2 nm resolution and x50 to 1,000,000 magnification).

Light microscopy (LM) samples were prepared by cutting 2 – 4 micron slices from the polymerized epoxy resin infiltrated sample and placing them on a slide for drying on a hot plate and subsequently dying them with toluidine blue. An oil droplet was placed on the sample which was then covered with a cover slip and viewed with 5x lens of the Zeiss Axiophot microscope.

Four specimens for SEM were transferred from 100% methanol and critical point dried with hexamethyldisilizane (HMDS) (Electron Microscopy Sciences, Hatfield, PA, USA) for three changes with the last change going overnight (Nation, 1983). After the last change of HMDS was allowed to volatilize off in the fume hood, specimens were fractured with a clean razor blade to expose the interior parts of the specimen (Shapter, et al., 2008). Specimens then were mounted on stubs with carbon sticky tape with the exposed interior surfaces positioned for optimal imaging. Specimens were sputter coated with gold:palladium (60:40) and imaged in a JEOL 6400 SEM (Capovani Brothers Inc. Scotia, NY, USA) at an accelerating voltage of 15 kV, with a magnification of 300 000x.

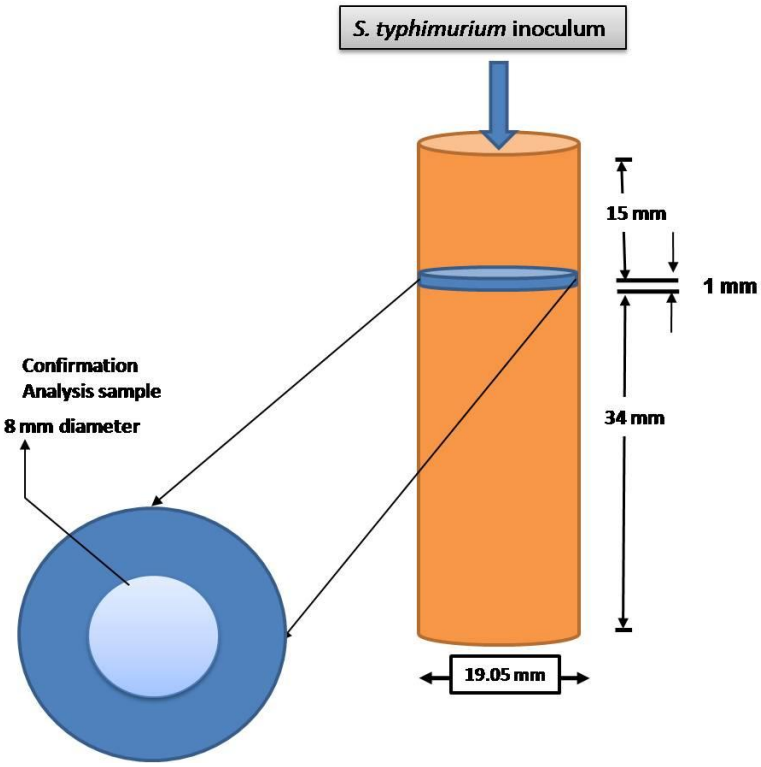

Fig 4.2 Extraction of an Internalized Portion of Cantaloupe Sample for Microbiological Analysis.

Table 4.1

QUETOL 651:ERL 4221 Formulation in Grams

Grams	Quetol 651	ERL 4221	DER 736	NSA	BDMA
10	1.40	2.22	1.43	6.38	0.20 mL

Source: Ellis, E. A. (2006).

4.4.1.3 Negative Staining of Bacteria

A small volume (2 μl) of cells grown in liquid culture were deposited on carbon stabilized formvar coated 400 mesh grids which were glow discharged immediately before staining with a 2% (wt/vol) solution of ammonium molybdate, pH 7.0. The specimen was then imaged in a JEOL 1200EX TEM at an accelerating voltage of 100 kV.

4.4.2 Polygalacturonase Activity Determination

4.4.2.1 Growth Medium

The growth medium was prepared according to the method described by McKay (1988). A 2.5 Polygaracturonic acid (VWR International, West Chester, PA, USA) was prepared as a 2.5 % stock solution and adjusted to pH 5.5 with potassium hydroxide and autoclaved at 10 psi for 15 minutes. The prepared growth medium (VWR International, West Chester, PA, USA) contained 1.25 % polygalacturonic acid, 50 mM potassium phosphate, Difco yeast nitrogen base (6.7 g per liter) and was solidified by agarose (0.5 % final concentration), and supplemented with 0.2 % glucose (McKay, 1988).

4.4.2.2 Polygalacturonase Activity Screening Procedure

Ten (10) μL volume of challenge study ready inoculum of *S.typhimurium* was point inoculated on the polygalacturonase agarose medium (VWR International, West Chester, PA, USA) in petri dishes using a sterile pipette. The plates were incubated at 37^{o}C for 1, 2 and 3 days in a conventional incubation chamber. During days 2 and 3 excessive drying out of agar during incubation was minimized by placing a stack of 3 experimental plates on top of a petri dish containing cotton balls moistened with distilled water. Subsequent to incubation the plates were stained for 5 minutes by flooding with a

filter sterilized 0.1 % solution of ruthenium red (VWR International, West Chester, PA, USA) dissolved in distilled water, and destained by flooding with sterile distilled water. The destaining removes the ruthenium red polygalacturonate complex on the surface layers of the plate. Polygalaturinate degradation around a bacterial colony shall be observed by the ability of the ruthenium red to penetrate deeply into the agarose medium, resulting in the colony being surrounded by a deep purple halo contrasted against the clear background of the washed plate (McKay, 1988). A negative control was run by also staining polygalacturonase agarose medium in petri dishes which were not inoculated with any bacteria. Photographs of both the negative control and sample plates were taken for comparison.

4.5 RESULTS AND DISCUSSION

The studies illustrate how *S. typhimurium* LT2 internalizes into cantaloupe tissues beyond the entry point which usually is an injury wound or stem scar. Correlative microscopic analysis studies confirmed that indeed the bacteria internalized into the cantaloupe which evidently has intercellular air spaces. *S. typhimurium* LT2 also has mobility enhancement organelles such as flagella, and the combination of the cantaloupe anatomic structure and the mobility enhancing features of the bacteria make the basis for the mode of internalization. Internalization can therefore be suggested to be only possible through the intercellular spaces, and not through the cell wall as the *S. typhimurium* was confirmed not to be capable of producing cell wall degrading enzymes.

4.5.1 SEM Images

High-resolution SEM (300 000x magnification) provided surface detail about *S. typhimurium* LT2, located on samples acquired from internal portions of the cantaloupe

(Fig. 4.3), despite the fact that the images could not explicitly show whether the bacteria was in the intercellular space or inside the cell. This confirms that the bacteria does internalize into the interior mesocarp tissues subsequent to invasion through means such as an injury or stem scar.

4.5.2 TEM and LM Images

The TEM images provided details of how individual cantaloupe cells are spatially organized, specifically showing intercellular spaces which can be the passage through which invading bacterial cells can travel to the internal mesocarp tissues (Fig. 4.4). The imaged *S. typhimurium* LT2 sample was measured and determined to be having an average size of 2.55 µm length and 0.8 µm width while the intercellular spaces were determined to be having variable shapes and sizes of approximately 5 µm length and 1 µm width. The LM images also showed intercellular spaces (Fig. 4.5). *S. typhimurium* LT2 also has flagella which can be functional as organelles of motility, as well as virulence factors (Carsiotis, et al., 1984). The flagella were observed on the *S. typhimurium* LT2 using the TEM (Fig. 4.6).

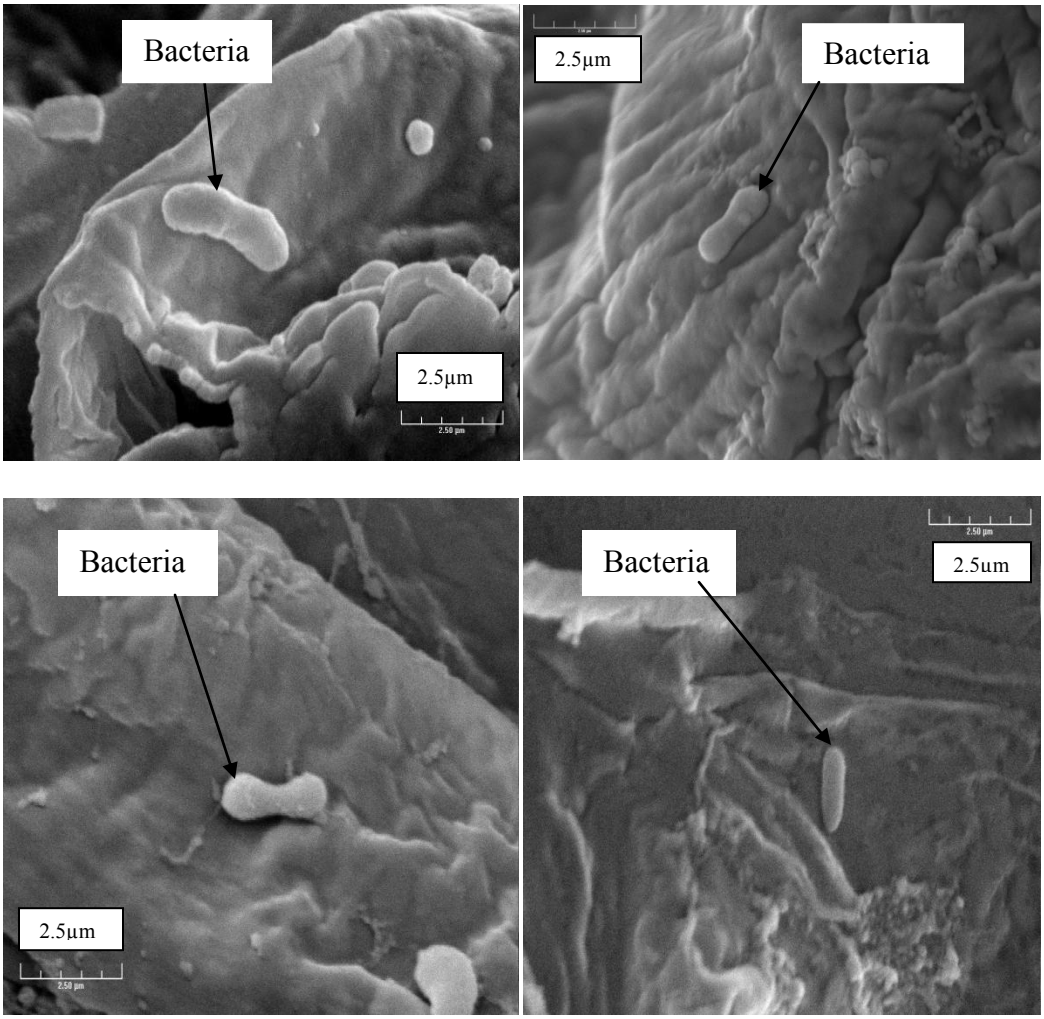

Fig. 4.3 Scanning Electron Microscope (SEM) Picture of Cantaloupe Cells Showing Bacteria in the Cell Structure (Magnification 300 000x).

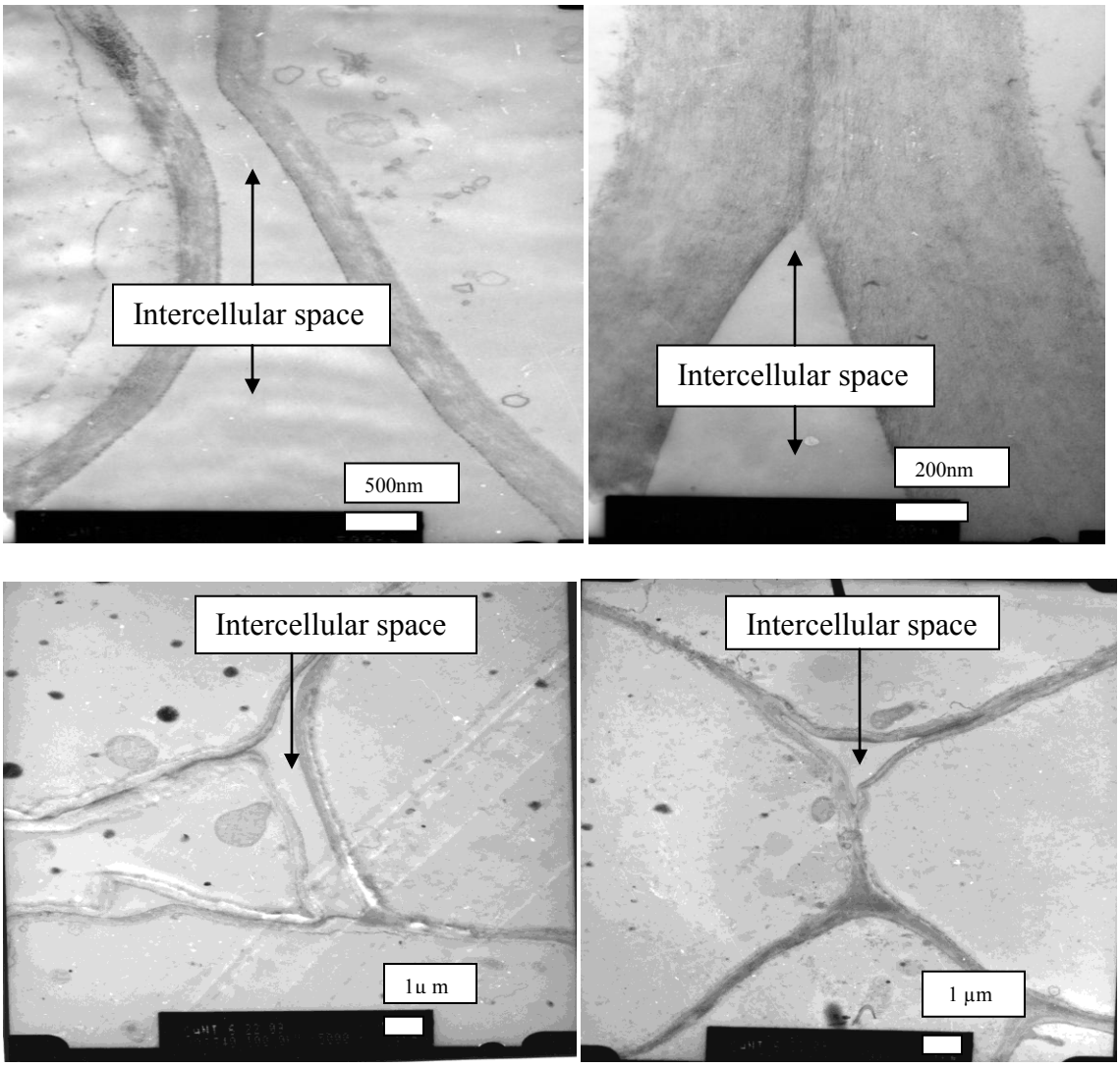

Fig. 4.4 TEM Images of Cantaloupe Cells Showing Intercellular Spaces

(Magnification 1 000 000x).

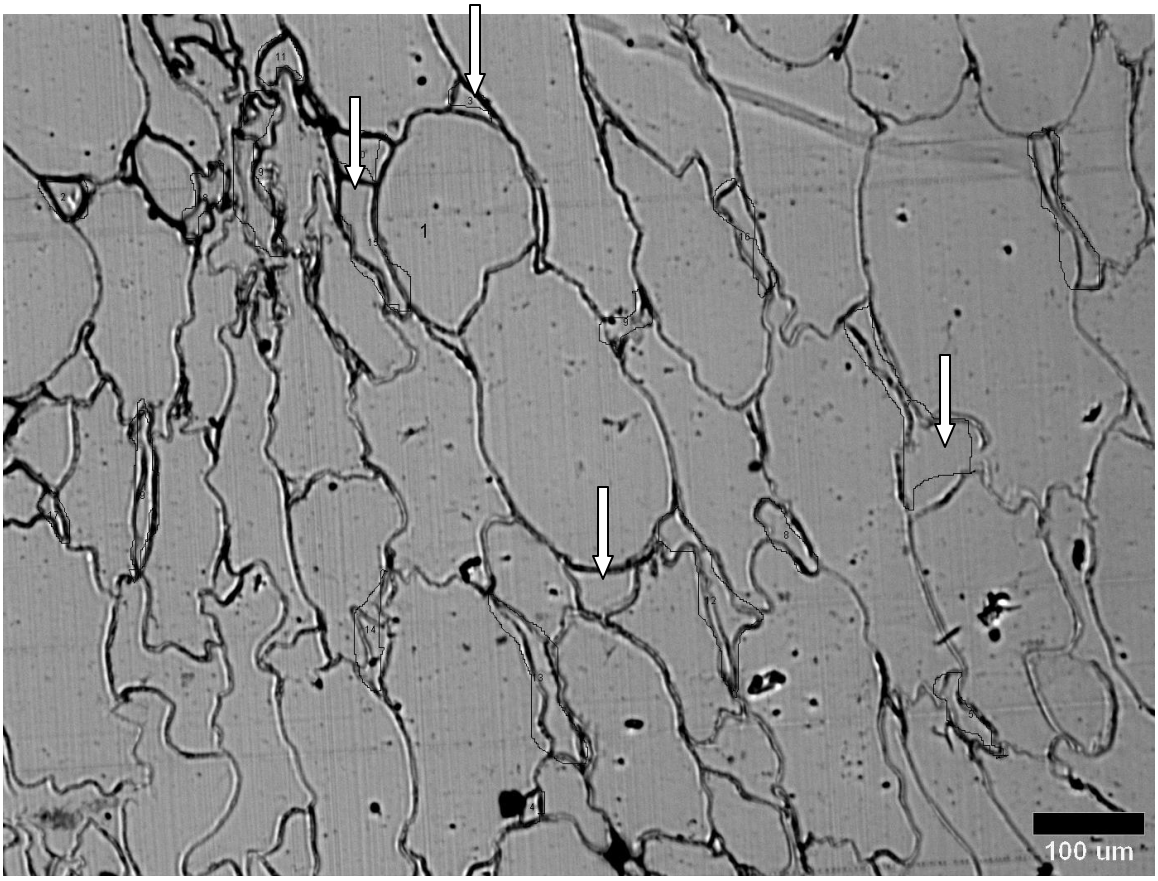

Fig. 4.5 Light Microscope Image of Cantaloupe Cells with Intercellular Spaces Marked Out (Magnification 40x).

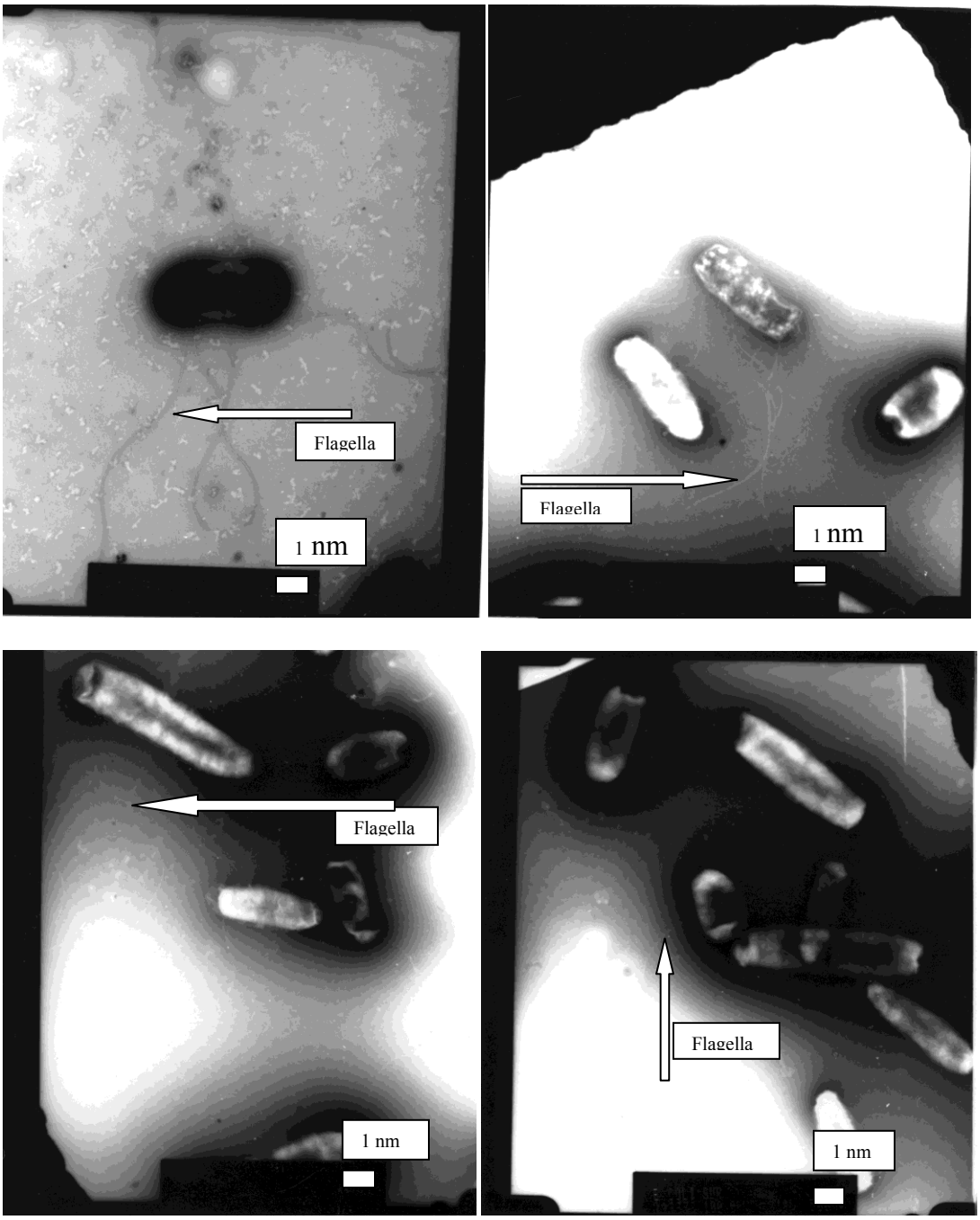

Fig. 4.6 TEM Images of *S. typhimurium* Showing Flagella (Magnification 1 000 000x).

4.5.3 Assessment of *S. typhimurium* LT2 for Polygalacturonase Activity

The ability to produce extracellular plant cell wall-degrading enzymes such as polygalacturonase would enable *S. typhimurium* LT2 to break up the adhesion bonds binding the cellulose membranes and thereby allow it to internalize the host cell through the cell wall. However, it is evident that *S. typhimurium* LT2 does not possess that ability. There is a lack of polygalacturonic acid hydrolysis as there is no purple red color which should have been observed subsequent to breakdown of polygalacturonic acid and penetration of the ruthenium red into the polygalacturonate agarose medium (Fig. 4.7), and this is confirmed by the control which is the same as the treatment (Fig. 4.8).

4.6 CONCLUSIONS

Cantaloupe like many other fruits has extensive intercellular spaces through which bacteria can internalize into the interior mesocarp tissues. *S. typhimurium* does not produce enzymes which break down cell wall structures such as cellulose and pectin. However, internalization of *S. typhimurium* into fresh cut cantaloupe flesh for 15 – 40 mm depth in 20 – 30 hours at 23^{o}C was measured. It is concluded that this internalization occurred through mobility primarily through the intercellular spaces, the pathogenic bacteria being aided by extracellular virulence enabling factors such as the flagella which enable bacterial mobility. Extracellular virulence factors being molecules such as flagella presented on the bacterial cell surface or translocated to the extracellular environment and capable of influencing growth of the pathogen on the plant (Salmond, 1994). Furthermore, an injured plant cell loses the ability to regulate osmotic potential and control transport of substances through its intercellular space network, giving rise to an unhindered access of the invading pathogenic organism into the plant.

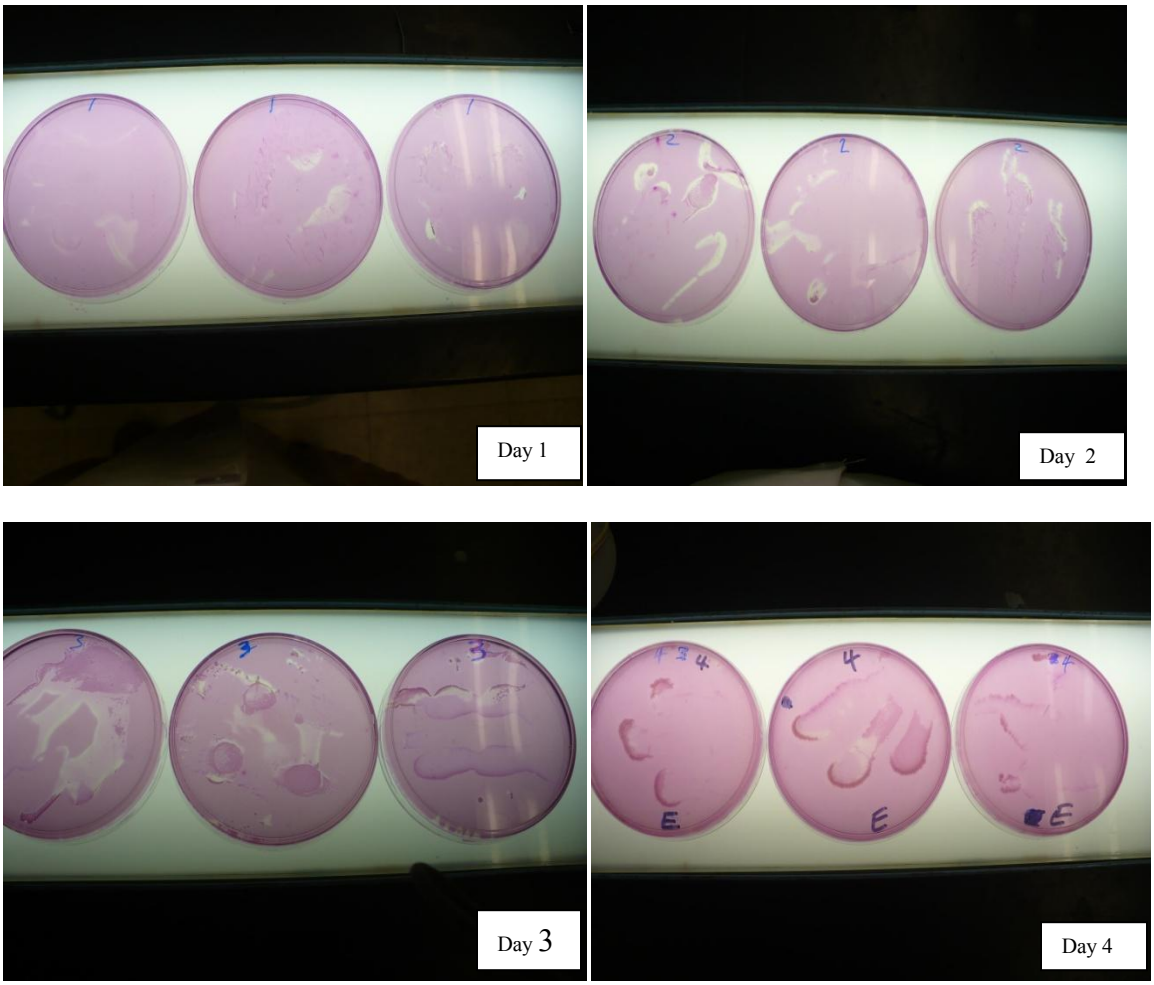

Fig. 4.7 Polygalacturonate Agarose Medium Inoculated with 40 µL of *S. typhimurium* LT2, Stained with Ruthenium Red and Destained with Distilled Water.

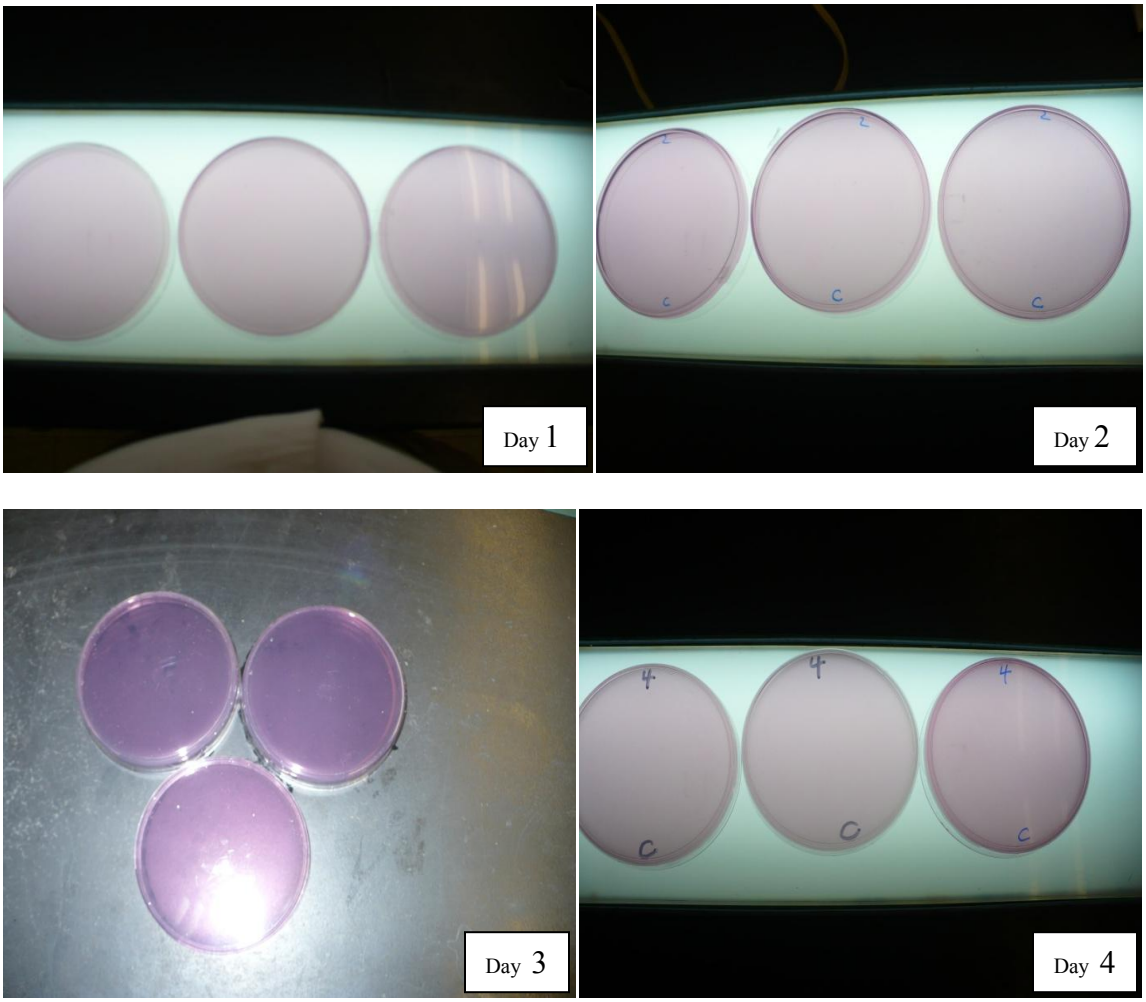

Fig. 4.8 Polygalacturonate Agarose Medium Stained with Ruthenium Red and Destained with Distilled Water (Control).

CHAPTER V

PREDICTION OF TARGETED *SALMONELLA ENTERICA* SEROVAR TYPHIMURIUM INACTIVATION IN FRESH CUT CANTALOUPE (*CUCUMIS MELO* L.) USING ELECTRON BEAM IRRADIATION

5.1 OVERVIEW

The radiation sensitivity of *S. typhimurium* LT2 inoculated into fresh cut cantaloupe flesh was determined by inoculating 8.01 logs CFU/g of bacteria in the exponential growth phase into the sample and irradiating with 0.2, 0.4, 0.5, 0.6 and 0.8 kGy electron beam irradiation doses using a 1.35 MeV Van de Graaff accelerator. The D_{10}-value (~0.18 kGy) for the bacteria was computed by taking the inverse of the slope of the difference of the log of initial population and the surviving population against dose.

Growth duration dependent *S. typhimurium* LT2 inactivation was determined by inoculating 21 fresh cantaloupe flesh samples (cylindrical, 50 mm long and 19.05 mm diameter) with 3.47 logs CFU/g of *S. typhimurium* LT2 inoculum and allowing variable time intervals of 0.5 – 30 hours for growth, and subsequently irradiating with a 1.0 kGy electron beam irradiation dose using the 1.35 MeV Van de Graaff accelerator (High Voltage Engineering Corp., Cambridge, MA). Microbiological analysis was done on the top 5 mm depth of the sample by plating the sample dilutions on Tryptic Soy Agar (TSA) medium supplemented with 1 mL/L nalidixic acid (Sigma, St Louis, Mo, USA) to determine the surviving population. The study determined that the 1.0 kGy dose was suitable for inactivation of the bacteria after 0.5 – 15 hours of growth, because it achieved log reductions of 1.62 for 0.5 hours, 1.82 for 5 hours, 1.98 for 10 hours and 2.53 for 15 hours, resulting in the surviving population for all those time intervals being not

significantly different from the detection limit of 1.70 logs CFU/g. However, in case of growth durations of 20 - 25 hours the 1.0 kGy dose resulted in log reductions of 2.72 for 20 hours, 2.71 for 25 hours and 2.65 for 30 hours, with the surviving population still being significantly ($p < 0.05$) greater than the detection limit. Therefore a dose higher than 1.0 kGy, is required for inactivation of the bacteria after growth intervals of more than 15 hours to levels equivalent statistically to the detection limit. Based on the D_{10}-value (0.18 kGy) of the *S. typhimurium* LT2, a dose of 0.9 kGy would yield a 5-log reduction, however, this was not achieved with the 1.0 kGy treatment. This variation may be due to variability of biological materials and systems which evolve and acclimatize to effects such as recovery after irradiation, where response to irradiation can only be estimated with expectation of possible variation.

Microbial load (growth and mobility) was predicted for cantaloupe flesh inoculated with the pathogenic *S. typhimurium* for 0.5 to 30 hours using the Gompertz model (EQ. 3.3) and the power law function (EQ. 3.4). The optimal electron beam irradiation dose based on the closeness of the predicted dose to the target dose was predicted with the objective of targeting the bacterial load in terms of time and depth within the cantaloupe. The required electron beam irradiation dose (D_x) for bacterial inactivation was predicted using a 10 MeV linear accelerator on the basis of the D_{10}-value, the bacterial population for a 30 hour period of bacterial internalization into the sample and an inactivation assurance level (N), set at 1.70 logs.

Variable attenuation thicknesses using Lucite® were evaluated and the best predictive equation was selected on the basis of the highest R^2 of the dose estimation, further optimized to ensure mimimum MSEP, and ensuring that the selected dose is at

least equal to or greater than the target dose at all depths. Prediction was based on the depth–dose curve of a 10 MeV electron beam into fresh cantaloupe. Sensitivity analysis on D_{10}-value, initial bacterial population (No) and the inactivation asurance level (N) suggests that dose was most sensitive to the initial bacterial load, followed by the D_{10}-value and least to the inactivation assurance level.

5.2 INTRODUCTION

Irradiation of foods for microbial inactivation requires quantification of both the microbial load and the desired optimal dose to ensure safety while maintaining product quality. The mobility of plant pathogenic bacteria within the host (the fresh produce) needs to be fully understood and quantified as a function of time and space so that fresh produce inactivation interventions can be properly guided and targeted. Maintaining organoleptic and nutritional quality and keeping costs down are important factors, making it desirable to use the lowest possible doses necessary to achieve desired levels of microbiological and parasite control on a commercial scale. This requires establishment of the efficacy of the radiation treatment and threshold doses for quality changes (Farkas, 1998).

Increased microbial resistance has been observed in food-borne pathogens such as enterohemorrhagic *E. coli* O157:H7 inoculated in ground beef and repeatedly subjected to electron beam irradiation, resulting in a significant increase ($P < 0.05$) of the D_{10}-value from 0.24 ± 0.03 to 0.63 ± 0.02 kGy for ATCC strain 35150 and isolate L3, following four cycles of e-beam processing with the microorganism being able to resist doses as high as 3.0 kGy (Levanduski & Jaczynski, 2008). The practical implications of this increased microbial resistance to e-beam processing for the food industry and general

public health is that the minimum level of radiation for several relevant foods may need to be revised.

Fan and Sokorai (2008) reported that the appearance, texture, and aroma of most of the fresh-cut vegetables (iceberg, romaine, green and red leaf lettuce, spinach, tomato, cilantro, parsley, green onion, carrot, broccoli, red cabbage, and celery) were not negatively affected by 1.0 kGy gamma irradiation when stored in air or MAP (Modified Atmospheric Packaging). The authors further observed that the appearance and aroma of many irradiated vegetables were better than that of the corresponding controls after 14 day storage at 4^{o}C, probably due to the reduction of decay and browning. However, vitamin C content was reduced by irradiation in some vegetables, particularly green and red leaf lettuce.

Gomes and others (2008) observed that broccoli heads irradiated up to a dose of 3.0 kGy using electron beam showed same quality attributes as the non – irradiated samples. High irradiation doses may have undesirable effects on quality and sensorial attributes of the produce, therefore it is crucial to minimize the dose. Sensory quality of fresh cut lettuce was preserved by an irradiation dose of 1.0 kGy for 8 days at a storage temperature of 4^{o}C, while a 1.5 kGy dose resulted in a decrease in sensory quality, possibly due to damage to tissue caused by the high dose (Zhang, et al., 2006). Rodriguez and others (2006) assessed the radiation sensitivity of pathogenic bacteria such as *Listeria monocytogenes*, and *E. coli* K-12 MG1655 by comparing their D_{10}-value in cantaloupe with that in model foods, and it was observed that *E. coli* K-12 MG1655 had higher D_{10}-values in cantaloupe (~0.45 kGy) than in the model food (gelatin system) (~0.18 kGy) while *Listeria monocytogenes* had similar D_{10}-values in both cantaloupe (~0.15 kGy) and

the gelatin system (~0.15 kGy). The research findings show that irradiation sensitivity is food product specific, therefore it should not be generalized for all fresh produce.

Research on targeted irradiation inactivation of bacteria in terms of the level of bacterial contamination and location of the pathogens (space dimension) is deficient, resulting in either an under-dose or over-dose of some parts of the produce. The need for targeted irradiation is even more relevant due to the ability of pathogens such as *S. typhimurium* to internalize in fresh produce to depths up to 50 mm (Chimbombi, et al.; Gomes, et al., 2009).

The objective of this study was to determine the dose required for targeted inactivation of *S. typhimurium* internalized in fresh cantaloupe flesh using electron beam irradiation.

5.3 FUNDAMENTALS OF DOSE PREDICTION FOR BACTERIAL INACTIVATION

In the processing of foodstuffs by radiation, the absorbed dose (sometimes referred to as 'dose'), D is the amount of energy absorbed per mass of irradiated matter at a point of interest, and is defined as the mean energy, $d\bar{\varepsilon}$, imparted by ionizing radiation to the matter in a volume element divided by the mass, dm of that element (IAEA, 2002). Dose is important because it has practical and economic consequences in the sense that the higher the dose, the more energy is used and consequently the higher the cost of irradiation. The SI derived unit of absorbed dose is the gray (Gy), which is 1 J/kg (ANS, 2009).

Radiation energy limits exist for the sources suitable for food irradiation and they range approximately from a minimum of 0.1 MeV up to a maximum of 10 MeV (IAEA,

2002). The approximate range of absorbed dose used in food processing is from 0.01 to 100 kGy, and the specifics of the quantity are subject to the type of food and reason for irradiating. An example is that a maximum dose of 1.0 kGy is allowed for growth and maturity inhibition in fresh foods, while a maximum dose of 4.0 kGy is allowed for control of foodborne pathogens and extension of shelf life in fresh iceberg lettuce and fresh spinach (Table 5.1). This study predicts the targeted inactivation of *S. typhimurium* using electron beams from a 10 MeV linear accelerator because it can achieve the 50-mm range in penetration sought in fresh cut cantaloupe flesh by this study, and Texas A&M University where the experiment is undertaken has a 10 MeV linear accelerator available for commercial and research purposes.

According to Turner (2007), the dose in radiobiological experiments can be determined by measuring the current from a thin walled ionization chamber placed at different depths in a water target exposed to the beam (Fig 5.1).

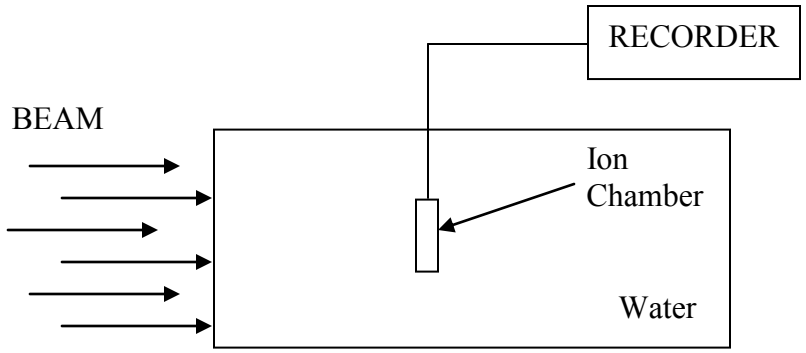

Fig. 5.1 Measurement of Dose or Dose Rate as a Function of Depth in Water Exposed to a Beam of Charged Particles. Adapted from Turner (2007).

Table 5.1

Foods Permitted to be Irradiated under Federal Drug Administration (FDA) Regulations

Food	Purpose	Dose
Fresh foods	Growth and maturation inhibition	1 kGy max.
Fresh or frozen, uncooked poultry products	Pathogen control	3 kGy max.
Frozen packaged meats (solely NASA)	Sterilization	44 kGy min.
Refrigerated, uncooked meat products	Pathogen control	4.5 kGy max.
Frozen uncooked meat products	Pathogen control	7 kGy max.
Fresh shell eggs	Control of *Salmonella*	3.0 kGy max.
Seeds for sprouting	Control of microbial pathogens	8.0 kGy max.
Fresh or frozen molluscan shellfish	Control of *Vibrio* species and other foodborne pathogens	5.5 kGy max.
Fresh iceberg lettuce and fresh spinach	Control of food-borne pathogens, and extension of shelf-life	4.0 kGy max.

Adapted from FDA (2009).

The D value (D_{10}-value for irradiation) in thermal processing of foods is the decimal reduction time, or the time required to destroy 90 % of the organisms. It is numerically equal to the number of minutes required for the survivor curve to traverse one log cycle, and mathematically it is equal to the reciprocal of the slope of the survivor curve and it is a measure of the death rate of an organism (Jay, 1978). Similarly, D_{10}-value in irradiation (death rate) multiplied by the desired log reduction gives the required dose .

$$D_x = D_{10} * (Log_{10}No - Log_{10}N) = D_{10} * Log_{10}(\frac{No}{N}) \quad (5.1)$$

where No is the initial bacterial population (CFU/g) and N is the surviving bacterial population after irradiation (CFU/g).

The use of ionizing radiation for the sterilization of disposable medical products has increased during the last 20 years, and the choice of radiation dose is dependent on three parameters, namely the initial microbiological contamination, the radio sensitivity of microorganisms and the assurance of sterility required (Gazso, et al., 1990). While a lot of countries prescribe a minimum dose of 25 kGy for sterilizing disposable medical products, Gazso et. al. (1990) and Darbord et. al. (1987) determined a theoretical basis for radiation sterilization dose (kGy) from experimental calculations of the initial bacterial count (N_0), the D_{10}-value (EQ. 5.1) and the surviving bacterial population after irradiation, N defined as the desired sterility assurance level. The sterility assurance level for this study is 1.70 logs, determined computationally as the minimum population possible when 100 µL volume of inoculums is plated on two microbial plates.

5.4 MATERIALS AND METHODS

5.4.1 D_{10}-Value Determination for *S. typhimurium* LT2 in Fresh Cut Cantaloupe Flesh

Fifteen (15) cylindrical fresh cantaloupe samples (50 mm long and 19.05 mm diameter) were placed in a test tube rack and point inoculated with 8.01 logs CFU/g (50 μL) of nalidixic acid resistant *S. typhimurium* LT2 inoculum at the top end. The non-pathogenic surrogate bacteria *S. typhimurium* LT2 was used because of the practical limitations of using the pathogenic bacteria in the Van de Graaff Irradiation Facility. The inoculum was prepared by maintaining and growing nalidixic resistant *S. typhimurium* LT2 (ATCC 700720) acquired from the laboratory of Dr Alejandro Castillo of Texas A&M University in tryptic soy broth supplemented with 20 μg/ml nalidixic acid (Sigma, St. Louis, MO, USA).

Three samples each were then irradiated with electron beam doses of 0.2, 0.4, 0.5, 0.6, and 0.8 kGy respectively using a 1.35 MeV Van de Graaff accelerator (High Voltage Engineering Corp., Cambridge, MA) at room temperature (23^{o}C), with the beam targeted at the point of bacterial inoculation. The radiation set up is as shown in Fig. 5.2. The delivered dose by the Van de Graaff accelerator was measured using an ion chamber, which measures the charge C resulting from electrons passing through it. Microbiological analysis was done on the 5-mm thick top end by the standard plate count method using Tryptic Soy Agar (TSA) medium supplemented with 1 mL/L nalidixic acid (Sigma, St Louis, Mo, USA) to determine total colony counts. The samples were cut 50 mm-long for ease of handling, placement and bacterial inoculation despite that the analysis was done on the top 5-mm length. The D_{10}-value was calculated according to the method

described byGomes and others (2008) by computing the slope of the survivors against the dose. Each dose treatment was replicated at least 3 times.

5.4.2 Growth Duration Dependent *S. typhimurium* Inactivation in Fresh Cut Cantaloupe Flesh

A total of seven (7) fresh and ripe cantaloupes were purchased from the local fresh produce market on the day of the experiment, and after peeling, twenty one (21) 50-mm long cantaloupe flesh samples were cored out using a 19.05 mm diameter aluminum core. The samples were wrapped in an aluminum foil, placed in a test tube rack with the top end open and inoculated with 3.47 logs cfu/g of *Salmonella typhimurium* LT2 inoculum, and allowed variable time intervals of 0.5, 5, 10, 15, 20, 25 and 30 hours for growth. The inoculum was prepared by maintaining and growing nalidixic resistant *S. typhimurium* LT2 (ATCC 700720) acquired from the laboratory of Dr Alejandro Castillo of Texas A&M University in tryptic soy broth supplemented with 20 μg/ml nalidixic acid (Sigma, St. Louis, MO, USA).

The samples were then irradiated with a dose of 1.0 kGy using a 1.35 MeV Van de Graaff accelerator (High Voltage Engineering Corp., Cambridge, MA) at room temperature (23^{o}C). The dose delivered by the Van de Graaff accelerator was measured using an ion chamber, which measures the charge C resulting from electrons passing through it. Subsequent to irradiation, survivors (N) were obtained using standard plate count method on the top 5-mm depth of the cylindrical sample by plating the sample dilutions on Tryptic Soy Agar (TSA) medium supplemented with 1.0 mL/L nalidixic acid (Sigma, St Louis, Mo, USA).

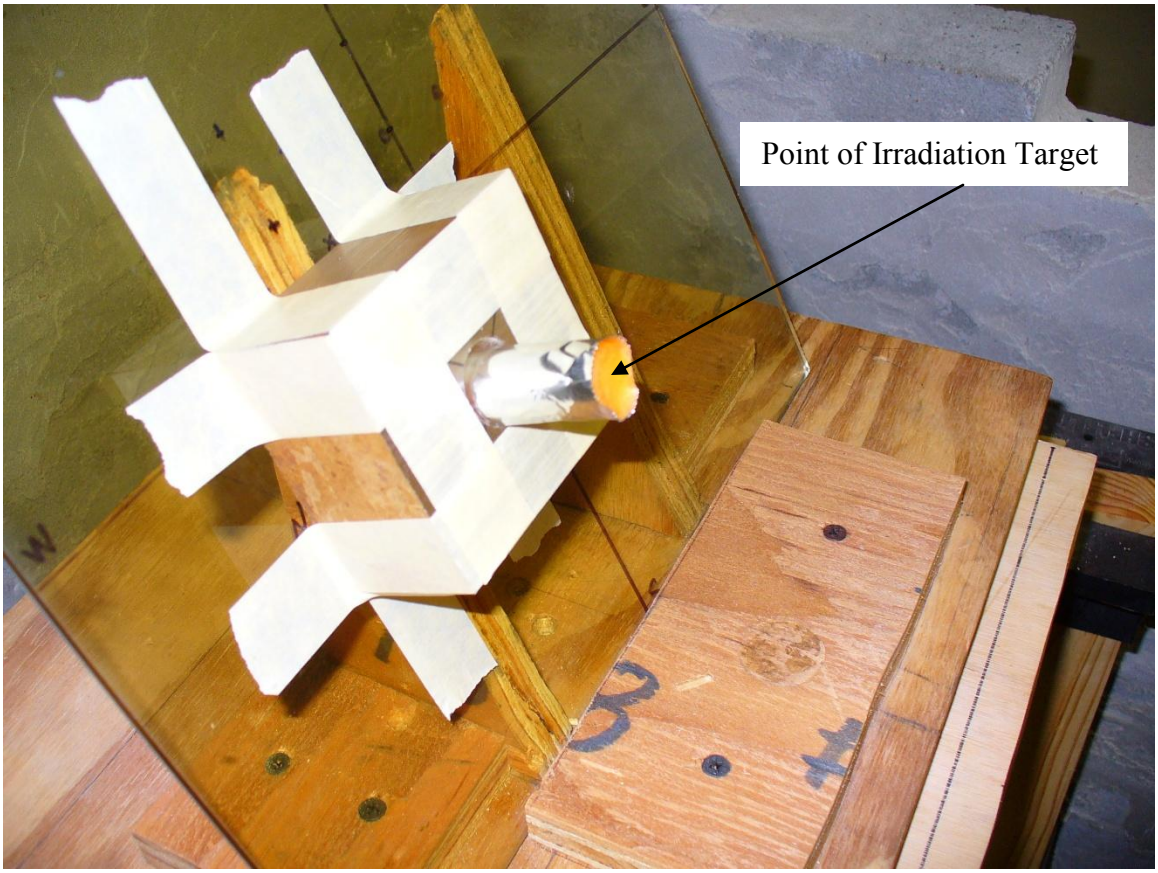

Fig 5.2 Sample Placement for Irradiation using the 1.35 MeV Van de Graaff Accelerator.

5.4.3 Depth – Dose Curve for 10 MeV Electron Beam in Fresh Cut Cantaloupe Samples

The depth–dose curve describes the energy transport of electrons through matter based on the spectral and angular fluence distribution of the primary electrons subject to the geometrical and chemical characteristics of the irradiated material (Grosswendt, 1994). A depth-dose curve for 10 MeV electron beam irradiation was simulated for the single and double beam (Fig. 5.3) modes using MCNP-5 software (Monte Carlo N-Particle-Version 5), which is a general purpose code for the transport of neutrons, photons, and electrons (Kim, et al., 2009; MCNP, 2005).

The National Institute of Standards and Technology (NIST) program called ESTAR calculates stopping power, density effect parameters, range, and radiation yield tables for electrons in various materials (ESTAR, 2009). Elemental composition of the fresh cantaloupe as shown in Table 5.2 was determined from the USDA National Nutrient Database for Standard Reference (USDA, 2009), and used as input for the ESTAR program. The $Z_{effective}$ for cantaloupe was computed by:

$$Z_{effective} = \sum_i \frac{\left(\frac{W}{A}\right)_i * {Z_i}^2}{\left(\frac{W}{A}\right)_i * Z_i} \tag{5.2}$$

where A is the atomic mass, z is the number of protons and W is a computational product of elemental proportion in the constituent material and the atomic mass, while i is the numeric count of the constituent elements. The units for A and z are grams for molar considerations, but can be any unit of mass used.

Lucite® is the trademark name of polymethyl methacrylate, a synthetic organic compound of high molecular weight made by combination of many simple molecules of the ester methyl methacrylate (monomer) into long chains (polymer). The polymerization

process may be effected by light or heat, although chemical catalysts are usually employed in manufacture of the commercial product (Brittanica, 2009). For the purpose of this study, Lucite® was chosen for attenuation because it has properties similar to those of cantaloupe, and the MCNP simulation was done with the assumption that both fresh cantaloupe and Lucite® have an identical density of 1.00 g/cm^3. Lucite® composition derived from the ESTAR (2009) database is that it has a density of 1.19 g/cm^3 and a mean excitation of 74 eV as well as a fraction by weight as shown in Table 5.3. The information was used to develop subsequent elemental composition of Lucite®.

Attenuation is done fundamentally to dampen or increase the delivered dose based on the behavior of the electron beam, so that it can be reduced or increased through the attenuation material (such as Lucite®) in order for delivery of an accurate desired dose in the target material, which in this case is the cantaloupe flesh. A depth-dose curve for both the target material (cantaloupe) and the attenuating material is necessary for irradiation planning. However, based on the assumption in this study that both the cantaloupe and Lucite® have a density of 1.00 g/cm^3, a single depth-dose curve (Fig. 5.3) was used for both materials.

Table 5.2

Calculation of $Z_{effective}$ for Cantaloupe. Adapted from USDA (2009)

Element	Z	A (u)	Weight Fraction	$\left(\frac{W_i}{A_i}\right) * (Z_i)^2$	$\left(\frac{W_i}{A_i}\right) * Z_i$
C	6	12.01	0.041767	0.125197	0.020866
H	1	1.008	0.104714	0.103883	0.103883
O	8	16	0.847675	3.390700	0.423838
N	7	14.01	0.001408	0.004924	0.000703
Ca	20	40.08	0.000140	0.001397	0.000070
Fe	26	55.85	0.000003	0.000036	0.000001
Mg	12	24.3	0.000140	0.000830	0.000069
P	15	30.97	0.000217	0.001577	0.000105
K	19	39.1	0.003935	0.036331	0.001912
Mn	25	54.94	0.000001	0.000011	0.000000
Total			1.000000	3.664886	0.551448
				$Z_{effective}$	6.646

u is the Atomic Mass Unit

Table 5.3

Calculation of $Z_{effective}$ for Lucite®. Adapted from ESTAR (2009)

Element	Z	A (u)	Weight Fraction	$\left(\frac{W_i}{A_i}\right) * (Z_i)^2$	$\left(\frac{W_i}{A_i}\right) * Z_i$
C	6	12.01	0.599848	1.800000	0.30000
H	1	1.008	0.080538	0.080000	0.080000
O	8	16.00	0.319614	1.280000	0.160000
		Total	1.0000	3.160000	0.5430000
				$Z_{effective}$	5.852

u is the Atomic Mass Unit

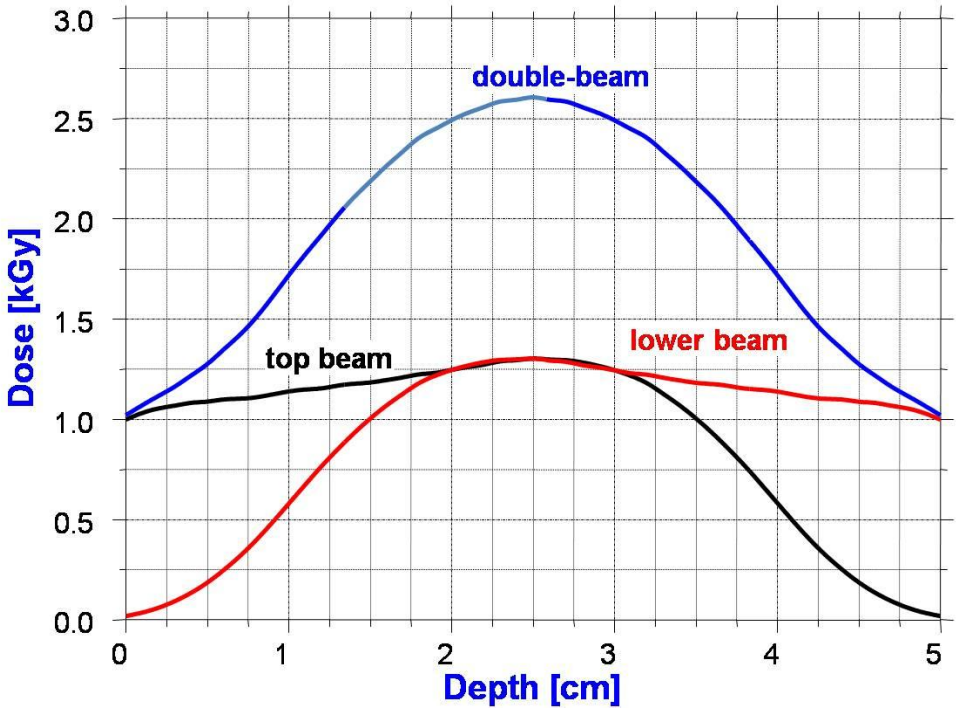

Fig. 5.3 Depth – Dose Curve of Electrons in Fresh Cantaloupe Sample Using a 10 MeV Linear Accelerator (LINAC).

The ESTAR program outputs a continuous stopping distance approximation (CSDA) range (kg/m^2) which is divided by the density of the cantaloupe (or Lucite®) to give the penetration distance for the 10 MeV electron beam in the sample:

$$R_p = \frac{CSDA}{\rho} \tag{5.3}$$

where R_p is the practical range (cm), or total distance the electrons travel in the specific material, CSDA is the continuous stopping distance approximation range (g/cm^2) and ρ is the material density (g/cm^3). Dose predictions for the various cantaloupe flesh depths (up to 50 mm) were derived based on the depth-dose curve (Fig. 5.3).

A typical example of deriving the dose from the depth-dose curve for the 10MeV LINAC (Fig. 5.3) is that a single beam, denoted top beam with no attenuation will deliver an average dose of 1.08 kGy within the top 0 - 10 mm depth, an average dose of 1.19 kGy within the 10 - 20 mm depth of cantaloupe, 1.28 kGy within the 20 – 30 mm depth, 0.97 kGy within the 30 – 40 mm depth and a dose of 0.23 kGy within the 40 – 50 mm depth (Table 5.4). The MCNP simulation outputs the dose per depth at 10 mm intervals, therefore the predicted delivered dose was obtained by averaging the dose for the 10 locations within the 10.0 mm depth of the sample. A singe beam denoted lower beam with no attenuation, on the contrary will deliver an average dose of 0.23 kGy within the top 0 – 10 mm depth of the sample, an average dose of 0.97 kGy within the 10 – 20 mm depth, 1.28 kGy within the 20 – 30 mm depth, 1.19 kGy within the 30 – 40 mm depth and 1.08 kGy within the 40 – 50 mm depth (Table 5.5). The double beam is the sum of the top and lower beams at the specified depths. At the 0 – 10 mm depth the double beam with no attenuation on either side will delivers a total dose of 1.31 kGy, which consists of 1.08 kGy from the top beam and 0.23 kGy from the bottom beam (Table 5.5). The double

beam will subsequently deliver an average dose of 2.16 kGy at the 10 – 20 mm depth, 2.56 kGy at the 20 – 30 mm depth, 2.16 kGy at the 30 – 40 Kgy and 1.31 kGy at the 40 – 50 mm depth (Table 5.5). The various attenuation schemes and subsequent delivered doses are computed in Appendix A.

An example of attenuation based on Fig. 5.3 is that when not attenuated, the top beam can deliver an average dose of 1.08 kGy within the 0 – 10 mm depth, but if attenuated with 1.0 cm of lucite® the delivered dose at the 0 – 10 mm depth of the target material (cantaloupe) by the top beam shall be 1.19 kGy, while in case of the lower beam, if un-attenuated, it will deliver a dose of 0.23 kGy within the 0 – 10 mm depth (Appendix A3), while if attenuated with a 1.0 cm thick Lucite® the lower beam will deliver an average dose of 0.00 kGy within the 0 – 10 mm depth.

5.4.4 Bacterial Inactivation Dose (D_x) Prediction

The target dose is determined from the experimentally derived bacterial population within the depth of the cantaloupe sample of 50-mm length. The initial bacterial load (No) for the 30 hour growth period was determined as described in Section 3.3.5. The target dose (EQ. 5.1) for the 30 hour time interval was computed by multiplying the D_{10}-value with the required log reduction from the initial bacterial population (No) to the inactivation assurance level of 1.70 logs (N) for all the depths of the 50-mm long sample (Table 5.6).

Table 5.4

Typical Single Beam Irradiation Doses (kGy) Estimated Based on the Depth-Dose Curve for 10 MeV Electrons in Cantaloupe for Inactivation of *S. typhimurium* after 30 Hours of Internalization at 23^{o}C

Depth	Lucite® Attenuation Thickness (cm)			
(mm)	0	1.0	2.0	3.0
0 - 10	1.08	1.19	1.28	0.97
10 - 20	1.19	1.28	0.97	0.23
20 - 30	1.28	0.97	0.23	0.00
30 - 40	0.97	0.23	0.00	0.00
40 - 50	0.23	0.00	0.00	0.00

Table 5.5

Typical Double Beam Irradiation Doses (kGy) Estimated Based on the Depth-Dose Curve for 10 MeV Electrons in Cantaloupe for Inactivation of *S. typhimurium* after 30 Hours of Internalization at 23^{o}C

Depth	Lucite® Attenuation Thickness (cm) for Top and Bottom Beam					
(mm)	Top - 0	Bottom - 0	Total	Top – 2	Bottom – 3	Total
0 - 10	1.08	0.23	1.31	1.28	0.00	1.28
10 - 20	1.19	0.97	2.16	0.97	0.00	0.97
20 - 30	1.28	1.28	2.56	0.23	0.00	0.23
30 - 40	0.97	1.19	2.16	0.00	0.23	0.23
40 - 50	0.23	1.08	1.31	0.00	0.97	0.97

The predicted dose was determined by extracting the delivered dose at the various depths of the sample from an entry dose of 1.0 kGy electron beam into cantaloupe (Fig. 5.3). Subsequently, different predicted doses (Tables 5.4 and 5.5) were computed by varying multiple options of single and double beam with attenuation and non-attenuation with the objective of obtaining a dose for all the depths of the sample which is closest to the target dose in Table 5.6. The different possibilities of irradiation schemes plotted for comparison of matching with the target dose are as shown in Fig. 5.4.

A specific predicted dose was determined for the various single beam attenuation options of 0.0, 1.0, 2.0 and 3.0 cm with Lucite®. Table 5.4 shows that with no attenuation, the 1.0 kGy entry dose will deliver an average dose of 1.08 kGy within the 0 – 10 mm depth of the sample, and a dose of 1.19 kGy within the 10 – 20 mm depth of the sample, and 1.28 kGy dose within the 20 - 30 mm depth. The dose is increasing up to the 30 mm depth because of the phenomenon of diffuse max (Attix, 1986). A diffuse max occurs due to the fact that the small mass of electrons makes them scatter easily, and as a result they do not give rise to a Bragg peak near the end of their projected range as heavy particles do, instead, a diffuse maximum is reached at roughly half of the maximum penetration depth. A dose of 0.97 kGy is delivered at the 30 - 40 mm depth, and 0.23 kGy at the 40 - 50 mm depth. An attenuation of 1.0 cm Lucite® for a single beam will result in the delivery of an average dose of 1.19 kGy within the 0 - 10 mm depth of the cantaloupe sample, 1.28 kGy within the 10 - 20 mm depth, 0.97 kGy within the 20 - 30 mm depth, 0.23 kGy within the 30 - 40 mm depth and 0.00 kGy within the 40 - 50 mm depth of the cantaloupe sample (Table 5.4). This is because an average dose of 1.08 kGy would have been dissipated in the 0 – 10 mm depth of the Lucite attenuation.

An optimum single beam and double beam attenuation scheme was determined by comparing the predicted doses with the target dose by means of the coefficient of determination (R^2), the highest value R^2 deemed the optimal scheme (Fig. 5.4). Further optimization on the initial optimal scheme chosen was done by varying the attenuation schemes to yield a predicted dose which is equal to or greater than the target dose at all depths, and has the lowest mean squared error of prediction (MSEP) for all values of the unknown parameters (Allen, 1971). The MSEP is calculated as:

$$MSEP = \sum(\hat{Y} - Y)^2 \tag{5.6}$$

The established irradiation set up entails a cantaloupe flesh sample of cylindrical dimensions of 50-mm length and 19.05-mm diameter (Figs. 5.5 and 5.6) inserted in the holes drilled in the Lucite® block. Variable attenuation schemes for either or both at the top and bottom (Fig. 5.4) with Lucite® blocks were evaluated. An electron beam is targeted at the block with the cantaloupe flesh sample incorporated as part of the block. An irradiation dose is subsequently estimated on the basis of the atomic constituent properties of cantaloupe and the Lucite® block.

Table 5.6

Target Irradiation Doses (kGy) by Depth for *S. typhimurium* Inactivation in Fresh Cut Cantaloupe Sample after 30 Hours of Internalization at 23^{o}C (EQ. 5.1)

Depth (mm)	Target dose (kGy)
0 - 10	0.98
10 - 20	0.78
20 - 30	0.58
30 - 40	0.55
40 - 50	0.50

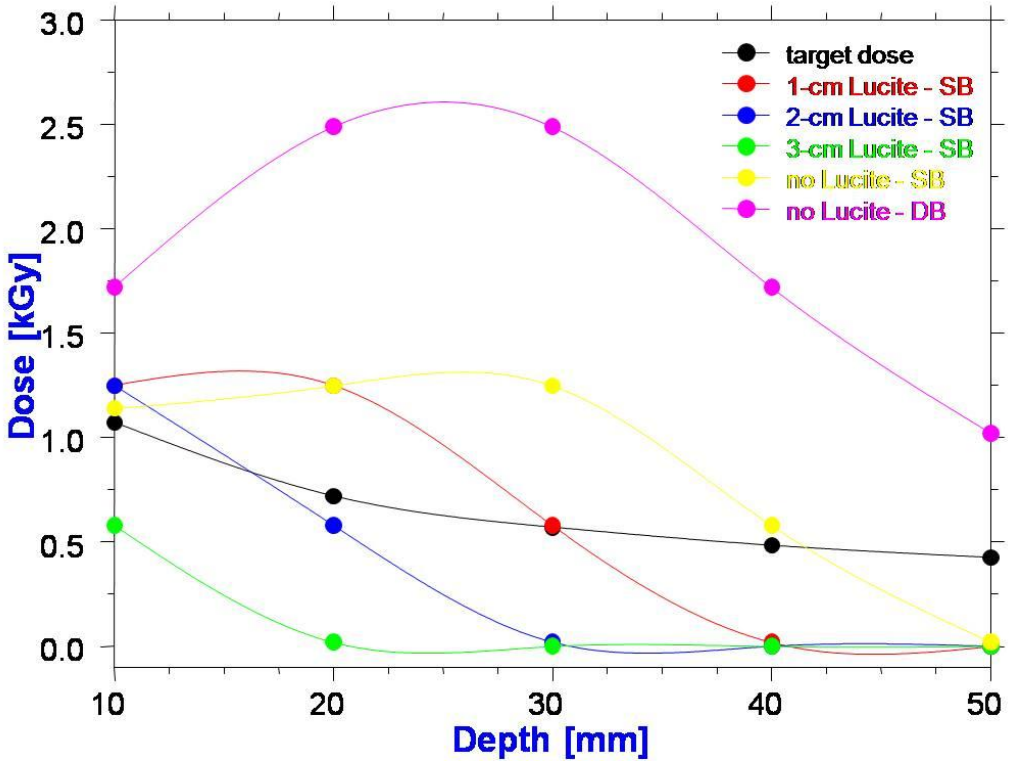

Fig. 5.4 Target and Predicted Doses Plotted against Depth for Various Single and Double Beam Irradiation Schemes.

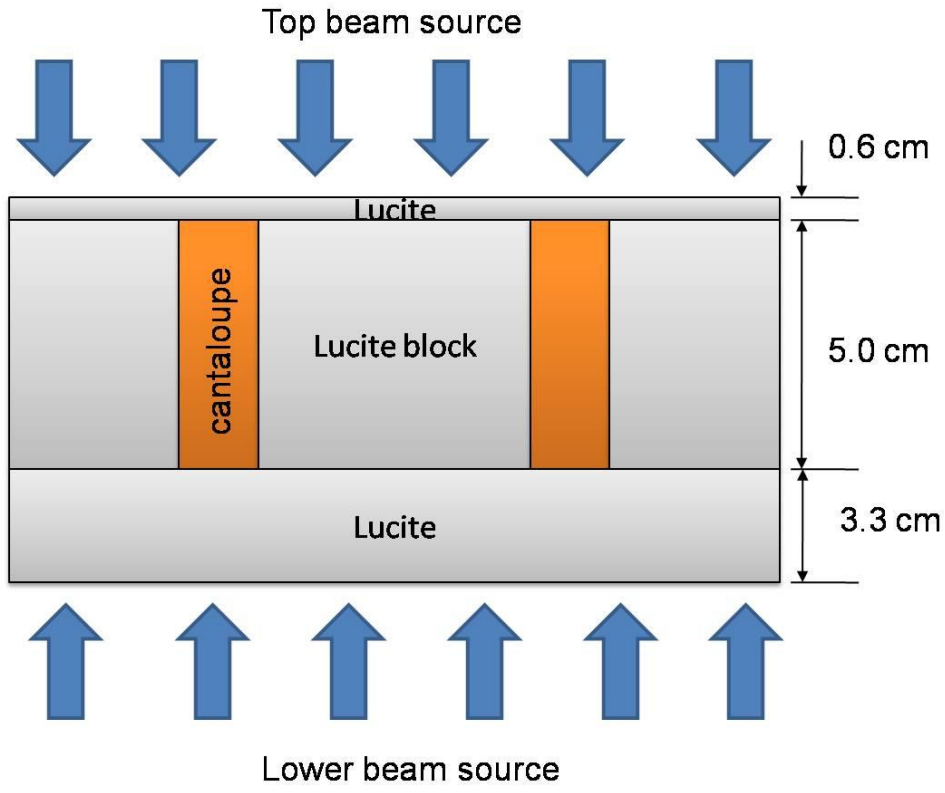

Fig. 5.5 Schematic of an Optimal Irradiation Set Up Using a 10 MeV Electron Beam Accelerator for Cantaloupe Flesh in Lucite® Block with 0.6 cm Lucite® Attenuation at the Top and 3.3 cm at the Bottom.

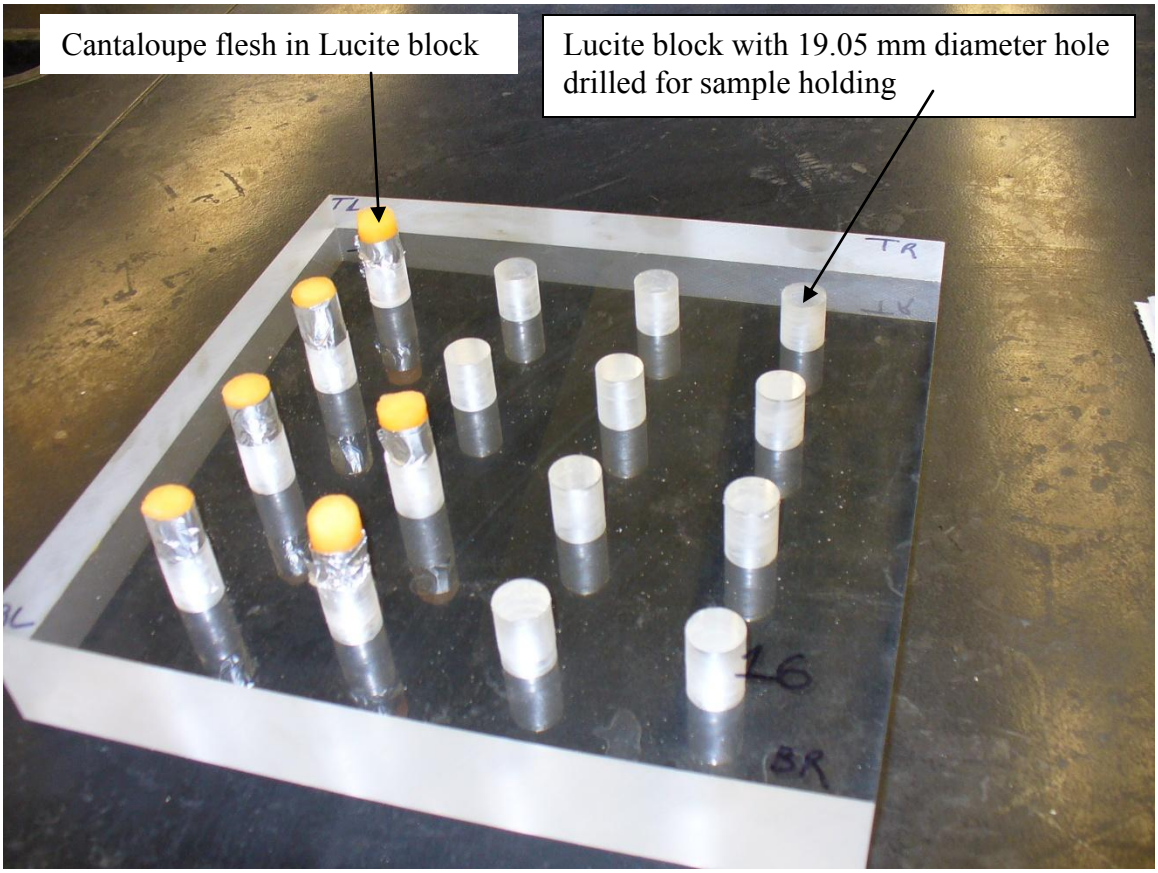

Fig. 5.6 Lucite Block (50 mm thick) with Cantaloupe Flesh Samples.

5.4.5 Sensitivity Analysis

Sensitivity analysis is a powerful and systematic way to determine quantitatively the relationship between the solution to a model and the various parameters that appear in the model's definition (Lutz, et al., 1997). With one-way sensitivity analysis each component of the equation is varied individually while the others retain their base-case specifications in order to establish the separate effect of each component on the results of the analysis (Briggs, et al., 1994). A one way sensitivity analysis was performed on the entry dose (D_x) computed as in EQ. 5.1 by varying each of the three parameters, D_{10} value, initial bacterial load (No) and the inactivation assurance level (N) across a plausible range of 10 – 50 % at increments of 10 % and tabulating the quantitative effect on the output (D_x).

5.5 RESULTS AND DISCUSSION

5.5.1 D_{10}-Value Determination

The radiation sensitivity (D_{10}-value) of *S. typhimurium* LT2 inoculated into fresh cut cantaloupe flesh was found to be 0.18 kGy (Fig. 5.7), which is comparable with the D_{10}-value reported by Niemira (2003) who found an average D_{10}-value of 0.26 kGy for *Salmonella* internalized in different varieties of lettuce. The D_{10}-value is critical in dose calculation and it is assumed in this study that the D_{10} is the same at all depths of the sample. The other assumption made is that the D_{10}-value of the surrogate bacteria *S. typhimurium* LT2 is the same as that one for the pathogenic bacteria strain *S. typhimurium*.

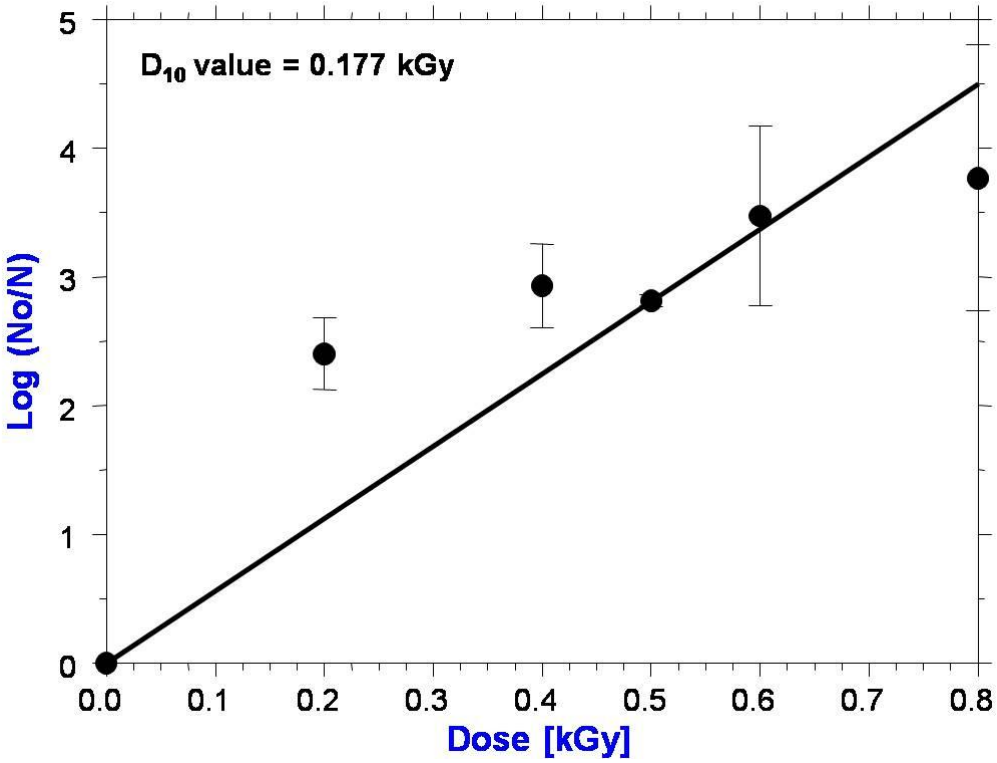

Fig. 5.7 Survival Curve of *S. typhimurium* LT2 in Irradiated Fresh Cut Cantaloupe Flesh Using a 1.35 MeV Van de Graaff Accelerator at 23^{o}C.

5.5.2 Growth Duration Dependent *S. typhimurium* LT2 Inactivation

Exposure to 1.0 kGy electron beam irradiation dose decreased the bacterial population of *S. typhimurium* LT2 in fresh cut cantaloupe at 23^{o}C, for all durations of growth (Fig. 5.8). The log reductions ranged from 1.62 after 0.5 hours of growth, 1.82 logs for 5 hours, 1.98 logs for 10 hours and 2.53 for 15 hours of growth. Since the initial population (No) was only 4.84 logs at 15 hours of growth, the 1.0 kGy dose reduced it to the equivalence of the detection limit for all time intervals up to 15 hours. These results indicate that the 1.0 kGy dose was adequate to inactivate the bacterial populations accumulated due to growth up to 15 hours (Table 5.7).

At the maximum growth duration of 30 hours a log reduction of 2.65 was obtained. Despite the fact that the log reduction achieved at 30 hours was less than that at 20 hours, the surviving bacterial population at 30 hours was 4.49 logs, which was the highest ($p<0.05$) than all the surviving bacterial populations (Table 5.7).

Log reductions of 2.72, 2.71 and 2.65 were achieved for the growth intervals of 20, 25 and 30 hours respectively, and despite these log reductions the surviving population was still significantly ($p<0.05$) higher than the detection limit. The implication of this is that the 1.0 kGy dose was inadequate to inactivate the bacteria accumulated due to growth from 20 – 30 hours. Adequacy of dose is determined by the surviving population not being significantly different from the detection limit, which is the level of assurance of sterility.

The desirable log reductions for the 20, 25 and 30 hours growth durations would have had to be 4.09, 4.89 and 5.44 logs respectively. A 5.0-log reduction should require a dose of 0.90 kGy based on the D_{10}-value of 0.18 kGy determined for *S. typhimurium* LT2

in fresh cantaloupe at 23^{o}C. However, a 5.0-log reduction was not achieved with the 1.0 kGy dose. The inability to achieve a 5.0-log reduction may be due to potential errors in the experimental determination of the D_{10}-value.

5.5.3 Bacterial Inactivation Dose Prediction

The MCNP simulation (Fig. 5.9) from a 10 MeV linear accelerator shows the 1.0 kGy dose distribution after entry at the 0.0 mm depth position. The simulation also shows that the dose decreases to 0.0 kGy at the 50 mm depth. This implies that since there are bacteria at the 50 mm depth after 30 hours, a double beam will be the adequate choice for targeting the bacteria in that region.

The optimum dose (D_x) for a 1.0 kGy dose targeted at inactivating *S. typhimurium* after 30 hours of internalization is attained using a 0.5 cm Lucite® attenuation at the top and 3.3 cm attenuation at the bottom (Fig. 5.10). The predicted dose scheme at variable depths shown in Table 5.8 is in agreement with the simulation scheme in Fig. 5.9 where an irradiation beam from the bottom must be used to reach the 50 mm depth where the distribution from the top beam has almost reached 0.0 kGy.

The MSEP for this optimal dose scheme is 0.6969 and the comparison of the target to the predicted dose is shown in Fig. 5.8. The key element to this dose scheme is to minimize overdosage, and also to target the minimum tolerable overdose to the top part of the sample where there are more bacteria (7.23 logs) in contrast to the lower part of the sample where there are only 4.53 logs (Table 3.3). The optimal scheme shown in Fig. 5.10 shows that at the 40 mm depth the predicted and the target dose are almost equal.

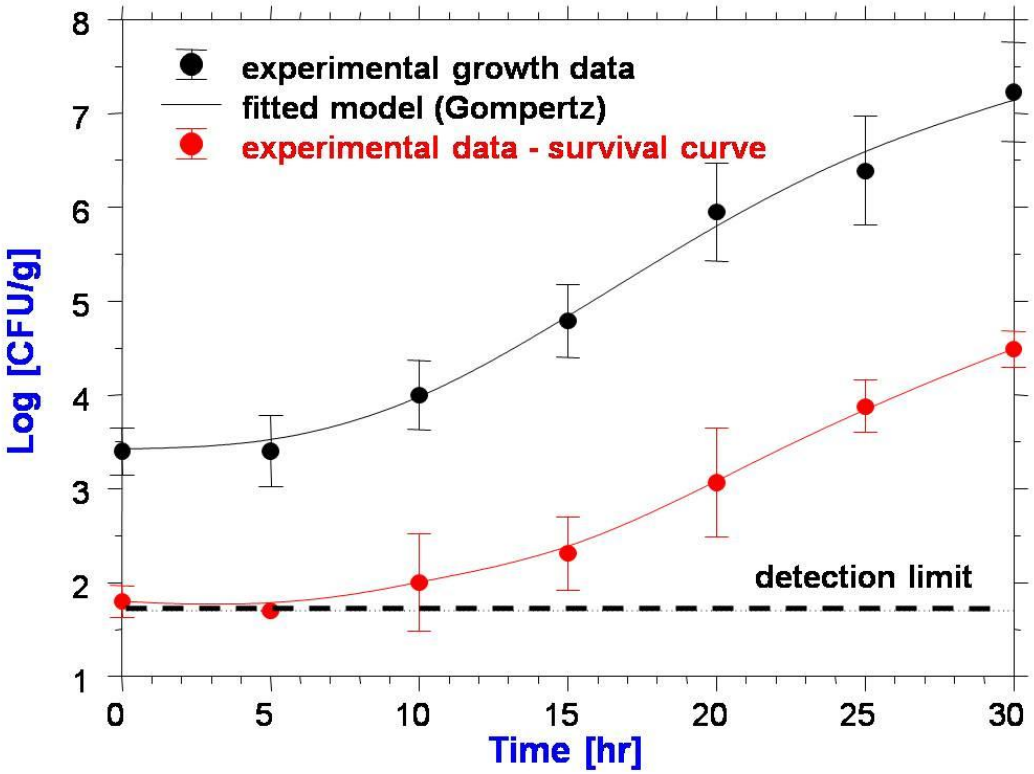

Fig. 5.8 Growth and Inactivation of *S. typhimurium* LT2 in Fresh Cantaloupe Flesh Samples at 23^{o}C Using a 1.0 kGy Dose from a 1.35 MeV Van de Graaff Accelerator.

Table 5.7

Surviving Population (Log CFU/g) of *S. typhimurium* LT2 in Fresh Cantaloupe after 1.0 kGy at 23^{o}C at Variable Growth Durations Using a 1.35 MeV Electron Van de Graaff Accelerator.

Time (hrs)	N(Log CFU/g)	Log Reduction
D.L	1.70[a] (0.00)	n/a
0.5	1.80[a] (0.17)	1.62
5	1.70[a] (0.00)	1.82
10	2.00[a] (0.52)	1.98
15	2.31[a] (0.39)	2.53
20	3.07[b] (0.58)	2.72
25	3.88[c] (0.28)	2.71
30	4.49[d] (0.19)	2.65

[a-d]Means within a Column, which are not Followed by a Common Superscript Letter, are Significantly Different (P<0.005)

() Standard Deviation & n/a Refers to Not Applicable.

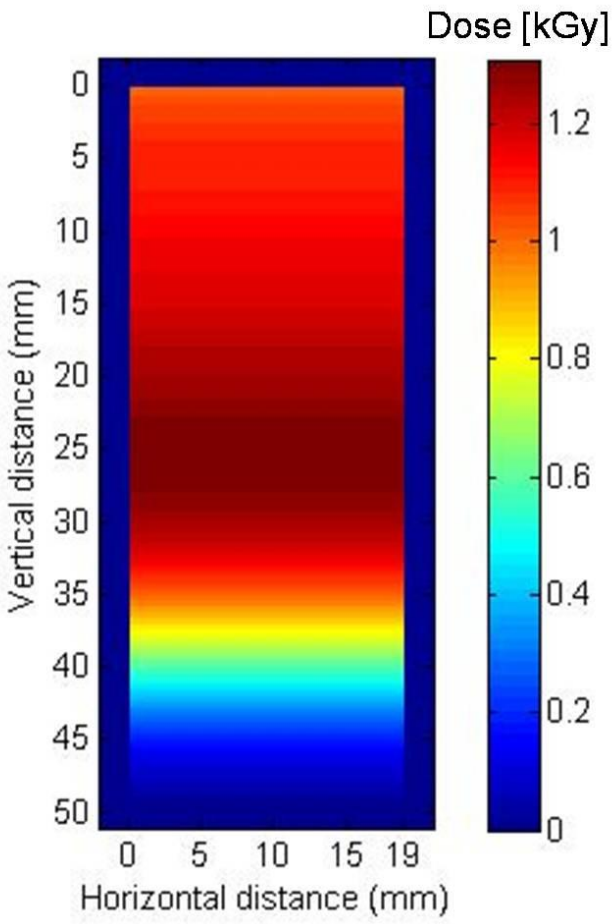

Fig. 5.9 MCNP Simulation of 1.0 kGy Dose Distribution in a Cylindrical Cantaloupe Flesh Sample with 19.05 mm Diameter and 50 mm Height.

Table 5.8

Optimal Estimated Double Beam Irradiation Doses (kGy) Based on the Depth-Dose Curve for 10 MeV Electrons in Cantaloupe for Inactivation of *S. typhimurium* after 30 Hours of Internalization at 23^{o}C

Depth	Lucite® attenuation thickness (cm) for top and bottom beam		
(mm)	Top – 0.5	Bottom – 3.3	Total
10	1.13	0.00	1.13
20	1.25	0.00	1.25
30	1.21	0.00	1.21
40	0.59	0.10	0.68
50	0.05	0.75	0.79

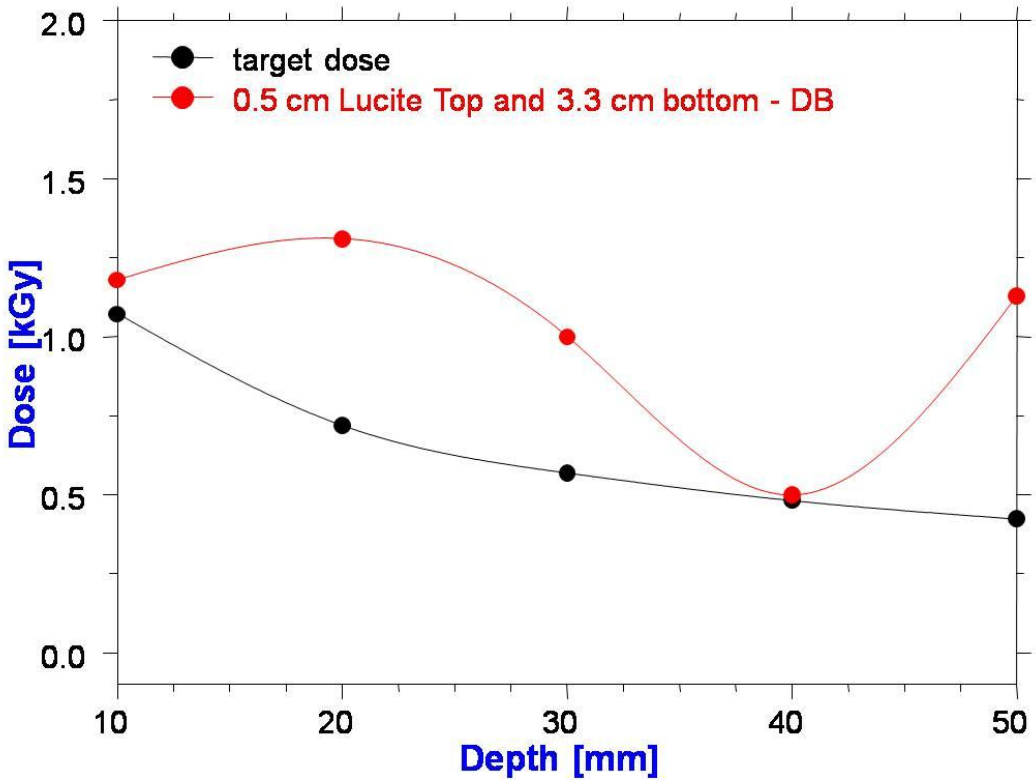

Fig. 5.10 Target and Predicted Dose (Double Beam Set-Up)

Plotted against Depth for 30 Hours.

Table 5.9

Percent Variation of Dose with 10 – 50 % Variation of Model Parameters, D_{10}-Value, Initial Bacterial Population (No) and the Inactivation Assurance Level (N) for the 30 Hour Time Interval

% Adjustment	% Dose Variation After Adjustment of		
	D_{10}-Value (kGy)	No $(Logs\ \frac{CFU}{g})$	N $(Logs\ \frac{CFU}{g})$
10	49.82	54.07	31.94
20	63.44	71.94	27.69
30	77.06	89.82	23.43
40	90.67	107.69	19.18
50	104.29	125.57	14.93

5.5.4 Sensitivity Analysis

One way sensitivity analysis done on the dose estimated using EQ. 5.1 on a plausible variation range of 10 – 50 % shows that the dose (D_x) is most sensitive to the bacterial population (No), which is the level of contamination, followed by the D_{10} value and least by the inactivation assurance level (N) as shown in (Table 5.9). The plausible range of 10 – 50 % is based on the possibility of change of the prediction parameters. The sensitivity is consistent for all the percentages of variation (10, 20, 30, 40 and 50). The implication of this analysis is that it is crucial for the level of contamination to be accurately determined or predicted, because it has the highest impact on the dose level to be required for irradiation treatment. An overdose or an under dose both have detrimental effects, therefore dose has to be accurate.

The percentages of variation show that even though the D_x is not as sensitive to the D_{10}-value as it is to the initial bacterial level (No), the D_{10}-value is also important in impacting on the D_x. The D_{10}-value is important in irradiation because it quantifies the sensitivity of the bacterial organism to radiation (dose) and it is crucial in determining the magnitude of the D_x. At the 10 mm depth the D_{10}-value causes a D_x variation by 49.82 % while the initial bacterial level (No) impacts a variation of 54.07 % at after a 10 % adjustment. Despite impacting least sensitive on the variation of dose, the inactivation assurance level as well impacts a 31.94 % change on the dose after a 10 % variation. The lowest dose variation is impacted by N at 50 % adjustment, resulting in a 14.93 % variation of dose.

The overall implication of the results on Table 5.9 is that all the dose prediction parameters impact a non-negligible change on the dose. All these parameters have to be

accurately determined for optimal dose prediction. A change in any of the dose prediction parameters warrants a re-assessment of dose and the irradiation scheme.

5.6 CONCLUSIONS

The D_{10}-value of *S. typhimurium* LT2 was found to be 0.18 kGy. This is consistent with findings by Niemira (2003) who found D_{10}-values ranging from 0.23 – 0.31 for *Salmonella* in different varieties of lettuce. The D_{10}-value is a determination of the sensitivity of the bacteria to electron beam irradiation treatment.

A 1.0 kGy electron beam irradiation treatment reduced the population of *S. typhimurium* LT2 to levels statistically ($p<0.05$) equivalent to the detection limit for up to growth intervals of 15 hours at 23^{o}C, beyond which the bacterial population could not be effectively controlled by the treatment. Longer growth durations (20 - 30 hours) resulted in even less effectiveness of the 1.0 kGy electron beam irradiation treatment, but the bacterial population was still reduced (Fig. 5.7) to 3.07, 3.88 and 4.49 logs for 20, 25 and 30 hours, respectively. Bacterial infestation and subsequent internalization into cantaloupe would require electron beam irradiation doses higher than 1.0 kGy after 15 hours of infestation. The implication of the need for more than 1.0 kGy dose requirement beyond 15 hours of growth is that subsequent to injury of the cantaloupe skin and rind, *S. typhimurium* LT2 can grow on the injury location, multiply and internalize into the entire internal mesocarp tissues.

The dose required for inactivation of *S. typhimurium* LT2 internalized in fresh cantaloupe can be predicted using an experimentally determined D_{10}-value, the log of initial bacterial population and the inactivation assurance level. It was determined that an optimal irradiation scheme for *S. typhimurium* internalized in fresh cantaloupe for 30

hours at 23^{o}C can be achieved from a 1.0 kGy dose by using 0.5 cm Lucite® attenuation at the top and 3.3 cm at the bottom (Fig. 5.4). The dose is most sensitive to the initial bacterial load, followed by the D_{10}-value and least to the inactivation assurance level.

The results of this study cannot be applied holistically to other foods because different foods have different nutritional composition, pH regimes and other quality determinant factors which are critical for microbial growth and survival. Comparatively as an example, cantaloupe has an average pH of 6.68 and 88.52 % moisture content while fresh pineapple has an average ph of 3.86 and a moisture content of 86 %. The low pH in pineapple may hinder the growth and mobility of microorganisms such as *Salmonella* while acid tolerant bacteria may grow well in pineapple.

Different microorganisms have different desired optimal temperatures, therefore the application of this research is only relevant to the temperature of 23^{o}C at which the tests were done. Irradiation sources can also not be generalized in this kind of study because different sources have different penetration potential and interactions with the product. For example, irradiation with a heavy particle such as a neutron may not penetrate to the 50 mm depth at which we have observed bacteria, while x-rays or gamma rays may have the penetration which is better than the one for electron beams. The size of food product should be considered specifically in applications of these findings because if infestation is confirmed to be at an identified location, it may take more than 30 hours for bacterial mobility to reach the other parts of the product which may be further than 50 mm.

CHAPTER VI

CONCLUSIONS

- The Gompertz model (R^2 of 0.99) predicted well the growth of *S. typhimurium* in fresh cut cantaloupe flesh at room temperature (23^{o}C), and the power law function predicted the accumulation (growth and mobility) with an R^2 of 0.98.
- Mobility of the pathogens starts after a time interval in excess of the lag phase duration of 7.76 hours, and can be up to as much as 50 mm within a time interval of 30 hours.
- The ability of *S. typhimurium* to migrate into cantaloupe tissue for up to 50 mm depth makes surface decontamination treatments such as washing and chlorination deficient in controlling bacteria that had at least 10 hours to internalize into the interior mesocarp tissues.
- The need for microbial inactivation treatments such as irradiation which have the ability to penetrate and inactivate the internalized microorganisms becomes the only suitable alternative.
- Correlative microscopic analysis using the Scanning Electron Microscope, Transmission Electron Microscope and Light Microscopy showed that cantaloupe fruit has a vast network of intercellular spaces which may be the route for internalization of gram negative bacteria such as *S. typhimuriun* LT2.
- The bacterium *S. typhimurium* LT2 has no capability of producing extracellular plant cell wall-degrading enzymes such as polygalacturonase, but it does have flagella which may be used as a virulence factor in aiding the mobility within the intracellular spaces. The inability to produce cell wall degrading enzymes

suggests that *S. typhimuriun* LT2 may not gain entry into an intact cantaloupe cell.

- The D_{10}-value of *S. typhimuriun* LT2 in fresh cantaloupe at 23^{o}C was determined to be 0.18 kGy using a 1.35 MeV Van der Graaf accelerator..
- Irradiation treatment must be targeted at the predicted bacterial accumulation on the basis of the bacterial load and location within the produce (depth) since mobility of bacteria was observed within the fresh cut cantaloupe.
- Initial bacterial load which is the degree of contamination is the most sensitive to the dose, followed by the D_{10} value, while the inactivation assurance level has the least sensitivity. The implication of a high sensitivity of dose to the initial bacterial load is that it is critical to determine accurately the degree of contamination for produce of interest prior to developing the irradiation dosimetry.
- Prediction of the irradiation treatment of fresh cantaloupe samples using single and double beam modes showed that for growth interval of 30 hours a double beam irradiation scheme with 0.5 cm Lucite® attenuation at the top and 3.3 cm at the bottom was optimal.

CHAPTER VII

RECOMMENDATIONS FOR FURTHER RESEARCH

The suggested recommendations for further research are the following:

1. An experimental validation of the proposed dose estimation model is necessary to fine tune the prediction tool. This could not be carried out during this study because of problems with the 10 MeV Linear Accelerator (LINAC).
2. Bacterial growth and mobility prediction must be conducted for different fresh produce types which are prone to bacterial contamination, causing foodborne illnesses.
3. This study must be extended to different bacterial strains.
4. The effect of produce quality must be incorporated into the model.
5. The prediction model should be expanded to 3-D whole produce configurations.
6. Further investigate the variability of D_{10}-values for a variety of food products.

REFERENCES

Ahmer, B. M., van Reeuwijk, J., Timmers, C. D., Valentine, P. J., & Heffron, F. (1998). *Salmonella typhimurium* encodes an SdiA homolog, a putative quorum sensor of the LuxR family, that regulates genes on the virulence plasmid. *Journal of Bacteriology*, 180(5), 1185-1193.

Akins, E. D., Harrison, M. A., & Hurst, W. (2008). Washing practices on the microflora on Georgia-grown cantaloupes. *Journal of Food Protection,* 71(1), 46-51.

Allen, D. M. (1971). Mean square error of prediction as a criterion for selecting variables. *Technometrics,* 13(3), 469 - 475.

Alvarez-Ordonez, A., Fernandez, A., Lopez, M., Arenas, R., & Bernardo, A. (2008). Modifications in membrane fatty acid composition of *Salmonella typhimurium* in response to growth conditions and their effect on heat resistance. *International Journal of Food Microbiology,* 123(3), 212-219.

Annous, B. A., Burke, A., & Sites, J. E. (2004). Surface pasteurization of whole fresh cantaloupes inoculated with *Salmonella poona* or *Escherichia coli*. *Journal of Food Protection,* 67(9), 1876-1885.

ANS (2009). Food: Benefits/Effects of Food Irradiation. In A. N. Society (Ed.). La Grange Park, IL. American Nuclear Society.

AOAC (1980). Official Methods of Analysis of the Association of Official Analytical Chemists. Washington, DC: Association of Official Analytical Chemists.

Attix, F. H. (1986). *Introduction to Radiological Physics and Radiation Dosimetry*. New York, John Wiley and Sons.

Bai, J. H., Saftner, R. A., Watada, A. E., & Lee, Y. S. (2001). Modified atmosphere maintains quality of fresh-cut cantaloupe (Cucumis melo L.). *Journal of Food Science,* 66(8), 1207-1211.

Baranyi, J., & Roberts, T. A. (1994). A dynamic approach to predicting bacterial growth in food. *International Journal of Food Microbiology,* 23(3-4), 277-294.

Baranyi, J., & Roberts, T. A. (1995). Mathematics of predictive food microbiology. *International Journal of Food Microbiology,* 26(2), 199-218.

Bidlas, E., Du, T. T., & Lambert, R. J. W. (2008). An explanation for the effect of inoculum size on MIC and the growth/no growth interface. *International Journal of Food Microbiology,* 126(1-2), 140-152.

Blaser, M. J. (1996). How safe is our food? - Lessons from an outbreak of salmonellosis. *The New England Journal of Medicine,* 334(20), 1324 - 1325.

Blaser, M. J., & Newman, L. S. (1982). A review of human salmonellosis: I. Infective dose. *Revisions in Infectious Diseases,* 4(6), 1096-1106.

Bowen, A., Fry, A., Richards, G., & Beuchat, L. (2006). Infections associated with cantaloupe consumption: a public health concern. *Epidemiology and Infection,* 134(4), 675-685.

Briggs, A., Sculpher, M., & Buxton, M. (1994). Uncertainty in the economic evaluation of health care technologies: the role of sensitivity analysis. *Health Economics,* 3(2), 95-104.

Brittanica Encyclopedia, 2009. Last Accessed 11/23/2009. http://www.britannica.com /EBchecked/topic/350622/Lucite-153 Edinburgh: Scotland.

Buchanan, R. L., & Phillips, J. G. (1990). Response-surface model for predicting the effects of temperature ph, sodium-chloride content, sodium-nitrite concentration and atmosphere on the growth of *listeria-monocytogenes*. *Journal of Food Protection,* 53(5), 370-376.

Buchanan, R. L., & Whiting, R. C. (1997). *Concepts in Predictive Microbiology.* Paper presented at the 50th Annual Reciprocal Meat Conference, Champaign, IL.

Carsiotis, M., Weinstein, D. L., Karch, H., Holder, I. A., & O'Brien, A. O. D. (1984). Flagella of *Salmonella typhimurium* are a virulence factor in infected C57BL/6J Mice. *Infection and Immunity,* 46, 814 - 818.

Castillo, A., Mercado, I., Lucia, L. M., Martinez-Ruiz, Y., Ponce de Leon, J., Murano, E. A., (2004). Salmonella contamination during production of cantaloupe: a binational study. *Journal of Food Protection,* 67(4), 713-720.

CDC (2009). *Foodborne Illness*. Retrieved 10/09/2009. http://www.cdc.gov/.

Chimbombi, E., Castell-Perez, E., Moreira, R., & Sanchez-Plata, M. X. (2009). *Prediction of accumulation (growth and mobility) of Salmonella enterica serovar Typhimurium in freshly cut cantaloupe (Cucumis melo L.).* Paper presented at the Institute of Food Technology Conference, Anaheim, CA.

Cooper, W. J., Curry, R. D., & O'Shea, K. E. (Eds.). (1998). *Environmental Applications of Ionizing Radiation*. New York: John Wiley & Sons.

Darbord, J. C., & Laizier, J. (1987). A theoretical basis for choosing the dose in radiation sterilization of medical supplies. *International Journal of Pharmaceutics,* 37(1-2), 1-10.

Dens, E. J., & Van Impe, J. F. (2001). On the need for another type of predictive model in structured foods. *International Journal of Food Microbiology,* 64, 247 - 260.

Eder, M., & Utz-Meindl, U. L. (2008). Pectin-like carbohydrates in the green alga micrasterias characterized by cytochemical analysis and energy filtering TEM. *Journal of Microscopy*, 231(2), 201–214.

Ellis, E. A. (2006). Corrected formulation for spurr low viscosity embedding medium using the replacement epoxide ERL 4221. *Microscopy and Microanalysis* 12 (2), 288 - 289.

Esau, K. (1977). *Anatomy of Seed Plants* (2nd ed.). New York: John Wiley & Sons.

ESTAR (2009). Estar Database Program (Publication no. http://physics.nist.gov/PhysRef Data/Star/Text/ESTAR.html). Retrieved 09/20/2009.

Fan, X., & Sokorai, K. J. B. (2008). Retention of quality and nutritional value of 13 fresh-cut vegetables treated with low dose radiation. *Journal of Food Science,* 73(7), S367 - S372.

FAO (1983). Codex General Standard for Irradiated Foods. Geneva, Switzerland: FAO

Farkas, J. (1998). Irradiation as a method for decontaminating food - A review. *International Journal of Food Microbiology,* 44(3), 189-204.

FDA (2009). *Foods Permitted to be Irradiated Under FDA Regulations (21 CFR 179.26)*. Retrieved 11/06/2009. http://www.fda.gov/.

Gazso, L. G., Dam, A., Molnar, A., & Daroczy, E. (1990). Determination of radiation sterilization dose of disposable needles based on D_{10} values and aami recommendation. *Radiation Physics and Chemistry,* 35(1-3), 404-407.

Gibson, A. M., Bratchell, N., & Roberts, T. A. (1987). The effect of sodium-chloride and temperature on the rate and extent of growth of clostridium-botulinum type-a in pasteurized pork slurry. *Journal of Applied Bacteriology,* 62(6), 479-490.

Golden, D. A., Rhodehamel, E. J., & Kautter, D. A. (1993). Growth of salmonella spp in cantaloupe, watermelon, and honeydew melons. *Journal of Food Protection,* 56(3), 194-196.

Gomes, C., Da Silva, P., Chimbombi, E., Kim, J., Castell-Perez, E., & Moreira, R. G. (2008). Electron-beam irradiation of fresh broccoli heads (*Brassica oleracea L. italica*). *Lwt-Food Science and Technology,* 41(10), 1828-1833.

Gomes, C., Da Silva, P., Moreira, R. G., Castell-Perez, E., Ellis, E. A., & Pendleton, M. (2009). Understanding E. coli internalization in lettuce leaves for optimization of irradiation treatment. *International Journal of Food Microbiology,* 135(3), 238-247.

Gomes, C., Moreira, R. G., Castell-Perez, M. E., Kim, J., Da Silva, P., & Castillo, A. (2008). E-beam irradiation of bagged, ready-to-eat spinach leaves (*Spinacea oleracea*): An engineering approach. *Journal of Food Science,* 73(2), E95-E102.

Grosswendt, B. (1994). Determination of electron depth-dose curves for water, icru tissue, and pmma and their application to radiation protection dosimetry. *Radiation Protection Dosimetry,* 54(2), 85-97.

Hayat, M. A. (2002). *Microscopy, Immunohistochemistry, and Antigen Retreival Methods for Light and Electron Microscopy*. New York: Kluwer Academic Publishers

Hillers, V. N., Medeiros, L., Kendall, P., Chen, G., & DiMascola, S. (2003). Consumer food-handling behaviors associated with prevention of 13 foodborne illnesses. *Journal of Food Protection,* 66(10), 1893-1899.

Hopwood, D. (1967). Some aspects of fixation with glutaraldehyde. A biochemical and histochemical comparison of the effects of formaldehyde and glutaraldehyde fixation on various enzymes and glycogen, with a note on penetration of glutaraldehyde into liver. *Journal of Anatomy,* 101(1), 83-92.

Hopwood, D. (1972). Theoretical and practical aspects of glutaraldehyde fixation. *Histochemical Journal,* 4, 267-303.

Huang, J. (1986). Ultrastructure of bacterial penetration in plants. *Annual Review of Phytopathology,* 24, 141-157.

Huang, L. (2008). Growth kinetics of *listeria monocytogenes* in broth and beef frankfurters - determination of lag phase duration and exponential growth rate under isothermal conditions. *Journal of Food Science,* 73(5), E235-E242.

IAEA (Ed.). (2002). *Dosimetry for Food Irradiation*. Vienna: International Atomic Energy Agency.

ISO/ASTM (2002). Standard Practice for Dosimetry in an Electron Beam Facility for Radiation Processing at Energies Between 300 keV and 25 MeV. Geneva, Switzerland. International Atomic Energy Association.

Jay, J. (1978). *Modern Food Microbiology* (2 ed.). New York: D. Van Nostrand Company.

Josephson, E. S., Thomas, M. H., & Calhoun, W. K. (1978). Nutritional aspects of food irradiation: an overview. *Journal of Food Processing and Preservation,* 2, 299 - 313.

Kano, Y. (1993). The relationship between the occurence of hollowing in watermelon and the size and the number of fruit cells and intercellular air spaces. *Japanese Journal of the Society of Horticultural Science,* 62(1), 103 - 112.

Kim, J., Moreira, R., & Castell-Perez, E. (2009). Simulation of pathogen inactivation in whole and fresh-cut cantaloupe (*Cucumis melo*) using electron beam treatment. *Journal of Food Engineering,* doi:10.1016/j.jfoodeng.2009.10.038.

Kunstadt, P., Steeves, C., & Beaulieu, D. (1993). Economics of food irradiation. *Radiation Physics and Chemistry,* 42(1-3), 259-268.

Lamikanra, O., Chen, J. C., Banks, D., & Hunter, P. A. (2000). Biochemical and microbial changes during the storage of minimally processed cantaloupe. *Journal of Agricultural Food Chemistry,* 48(12), 5955-5961.

Lamikanra, O., Richard, O. A., & Parker, A. (2002). Ultraviolet induced stress response in fresh cut cantaloupe. *Phytochemistry,* 60(1), 27-32.

Langston, S. W., Altman, N. S., & Hotchkiss, J. H. (1993). Within and between sample comparisons of Gompertz parameters for *salmonella-enteritidis* and aerobic plate counts in chicken stored in air and modified atmosphere. *International Journal of Food Microbiology,* 18(1), 43-52.

Lee, I. S., Lin, J., Hall, H. K., Bearson, B., & Foster, J. W. (1995). The stationary-phase sigma factor sigma S (RpoS) is required for a sustained acid tolerance response in virulent Salmonella typhimurium. *Molecular Microbiology,* 17(1), 155-167.

Lester, G. E., & Bruton, B. D. (1986). Relationship of netted muskmelon fruit water-loss to postharvest storage life. *Journal of the American Society for Horticultural Science,* 111(5), 727-731.

Levanduski, L., & Jaczynski, J. (2008). Increased resistance of *Escherichia coli* O157:H7 to electron beam following repetitive irradiation at sub-lethal doses. *International Journal of Food Microbiology,* 121(3), 328-334.

Lin, C. H., Falk, R. H., & Stocking, C. R. (1977). Rapid chemical dehydration of plant material for light and electron-microscopy with 2,2-dimethoxypropane and 2,2-diethoxypropane. *American Journal of Botany,* 64(5), 602-605.

Llewellyn-Smith, I. J., & Minson, J. B. (1992). Complete penetration of antibodies into vibratome sections after glutaraldehyde fixation and ethanol treatment: light and electron microscopy for neuropeptides. *Journal of Histochemistry and Cytochemistry,* 40(11), 1741-1749.

Lobry, J. R., Flandrois, J. P., Carret, G., & Pave, A. (1992). Monods bacterial-growth model revisited. *Bulletin of Mathematical Biology,* 54(1), 117-122.

Lord, E. M., & Mollet, J. C. (2002). Plant cell adhesion: a bioassay facilitates discovery of the first pectin biosynthetic gene. In *Proceedings of the National Academy of Science, U S A,* 99(25), 15843-15845.

Lu, Z. X., Lu, F. X., Zhang, L. K., Bie, X. M., & Zou, X. K. (2007). Predictive modeling and growth models of aerobic mesophilic bacteria on fresh-cut lettuce by hypochlorite-washing. *Journal of Food Safety,* 27(2), 157-168.

Lutz, A. E., Kee, R. J., & Miller, J. A. (1997). *SENKIN: A fortran program for predicting homogenous gas phase chemical kinetics with sensitivity analysis*. Livermore, CA: Sandia National Laboratories.

McKay, A. M. (1988). A plate assay method for the detection of fungal polygalacturonase secretion. *Fems Microbiology Letters,* 56, 355 - 358.

MCNP (2005). MCNP-A General Monte Carlo N-Particle Transport Code, Version 5. Los Alamos National Laboratory: Los Alamos, NM.

Miller, R. B. (2005). *Electronic Irradiation of Foods. An Introduction to the Technology*. New York: Springer.

Molins, R. A., Motarjemi, Y., & Kaferstein, F. K. (2001). Irradiation: a critical control point in ensuring the microbiological safety of raw foods. *Food Control,* 12(6), 347-356.

Monsoor, M. A., Kalapathy, U., & Proctor, A. (2001). Determination of polygalacturonic acid content in pectin extracts by diffuse reflectance Fourier transform infrared spectroscopy. *Food Chemistry,* 74, 233 - 238.

Nagy, Z., Hernadi, F., Kovacs, P., & Valyi-Nagy, T. (1968). Correlation between the physiological state of bacteria and the radioprotective effectiveness of cysteine. *Archives of Microbiology,* 61(4), 327-334.

Nation, J. L. (1983). A new method using hexamethyldisilizane for preparation of soft insect tissue for scanning electron microscopy. *Stain Technology,* 58, 347 - 351.

Niebuhr, S. E., Laury, A., Acuff, G. R., & Dickson, J. S. (2008). Evaluation of nonpathogenic surrogate bacteria as process validation indicators for Salmonella

enterica for selected antimicrobial treatments, cold storage, and fermentation in meat. *Journal of Food Protection,* 71(4), 714-718.

Niemira, B. A. (2003). Radiation sensitivity and recoverability of *Listeria monocytogenes* and *Salmonella* on 4 lettuce types. *Journal of Food Science,* 68(9), 2784 - 2787.

O'Connor, R. E., Roberts, R., Ford, A. L., & Nottingham, S. M. (1994). Shelf life of minimally processed honeydew, kiwifruit, papaya, pineapple and cantaloupe. *Journal of Food Science,* 59(6), 1202 - 1206.

Parnell, T. L., Harris, L. J., & Suslow, T. V. (2005). Reducing *salmonella* on cantaloupes and honeydew melons using wash practices applicable to postharvest handling, foodservice, and consumer preparation. *International Journal of Food Microbiology,* 99(1), 59-70.

Prasad, K. N. (1995). *Handbook of Radiobiology* (2 ed.). Boca Raton, FL: CRC Press.

Radomyski, T., Murano, E. A., Olson, D. G., & Murano, P. S. (1994). Elimination of pathogens of significance in food by low-dose irradiation - a review. *Journal of Food Protection,* 57(1), 73-86.

Reynolds, E. S. (1963). Use of lead citrate at high ph as an electron-opaque stain in electron microscopy. *Journal of Cell Biology,* 17(1), 208-212.

Richards, G. M., & Beuchat, L. R. (2005a). Infection of cantaloupe rind with *Cladosporium cladosporiodes* and *Penicillium expansum*, and associated migration of *Salmonella poona* into edible tissues. *International Journal for Food Microbiology,* 103, 1 - 10.

Richards, G. M., & Beutchat, L. (2005b). Metabiotic associations of molds and *Salmonella Poona* on intact and wounded cantaloupe rind. *International Journal of Food Microbiology,* 97, 327 - 339.

Rodgers, S. L., Cash, J. N., Siddiq, M., & Ryser, E. T. (2004). A comparison of different chemical sanitizers for inactivating *Escherichia coli* 0157:H7 and *Listeria monocytogenes* in solution and on apples, lettuce, strawberries, and cantaloupe. *Journal of Food Protection,* 67(4), 721-731.

Rodriguez, O., Castell-Perez, M. E., Ekpanyaskun, N., Moreira, R., & Castillo, A. (2006). Surrogates for validation of electron beam irradiation of foods. *International Journal of Food Microbiology,* 110, 117-122.

Salmond, G. P. C. (1994). Secretion of extracellular virulence factors by plant pathogenic bacteria. *Annual Review of Phytopathology,* 32, 181-200.

Shapter, F. M., Henry, R. J., & Lee, L. S. (2008). Endosperm and starch granule morphology in wild cereal relatives. *Plant Genetic Resources: Characterization and Utilization,* 6, 85 - 97.

Sivapalasingam, S., Friedman, C. R., Cohen, L., & Tauxe, R. V. (2004). Fresh produce: a growing cause of outbreaks of foodborne illness in the United States, 1973 through 1997. *Journal of Food Protection,* 67(10), 2342-2353.

SPSS (2006). SPSS Base 15.0 User's Guide. Chicago, IL 60606-6412: SPSS Inc.

Tauxe, R. V. (1997). Emerging foodborne diseases: an evolving public health challenge. *Emerg Infect Dis,* 3(4), 425-434.

Tauxe, R. V. (2002). Emerging foodborne pathogens. *International Journal of Food Microbiology,* 78, 31 - 41.

Turner, J. E. (2007). *Atoms, Radiation, and Radiation Protection* (3 ed.). New York, John Wiley and Sons.

Ukuku, D. O. (2004). Effect of hydrogen peroxide treatment on microbial quality and appearnace of whole and fresh-melons contaminated with *Salmonella* spp. *International Journal of Food Microbiology,* 95, 137 - 146.

Ukuku, D. O., Fan, X. T., & Kozempel, M. F. (2006). Effect of vacuum-steam-vacuum treatment on microbial quality of whole and fresh-cut cantaloupe. *Journal of Food Protection,* 69(7), 1623-1629.

Ukuku, D. O., & Fett, W. F. (2002). Relationship of cell surface charge and hydrophobicity to strength of attachment of bacteria to cantaloupe rind. *Journal of Food Protection,* 65(7), 1093-1099.

Ukuku, D. O., & Fett, W. F. (2004). Effect of nisin in combination with EDTA, sodium lactate, and potassium sorbate for reducing Salmonella on whole and fresh-cut cantaloupet. *Journal of Food Protection,* 67(10), 2143-2150.

Ukuku, D. O., Pilizota, V., & Sapers, G. M. (2001). Influence of washing treatment on native microflora and *Escherichia coli* population of inoculated cantaloupes. *Journal of Food Safety,* 21(1), 31-47.

Ukuku, D. O., Pilizota, V., & Sapers, G. M. (2004). Effect of hot water and hydrogen peroxide treatments on survival of salmonella and microbial quality of whole and fresh-cut cantaloupe. *Journal of Food Protection,* 67(3), 432-437.

Ukuku, D. O., & Sapers, G. M. (2001). Effect of sanitizer treatments on Salmonella Stanley attached to the surface of cantaloupe and cell transfer to fresh-cut tissues during cutting practices. *Journal of Food Protection,* 64(9), 1286-1291.

USDA (2009). *National Nutrient Database for Standard Reference.* Accessed 12/09/2009. *http://www.nal.usda.gov/fnic/foodcomp/cgi-bin/measure.pl*

Van Impe, J. F., Nicolai, B. M., Martens, T., Debaerdemaeker, J., & Vandewalle, J. (1992). Dynamic mathematical-model to predict microbial-growth and inactivation during food-processing. *Applied and Environmental Microbiology,* 58(9), 2901-2909.

Vandenbosch, K. A., Bradley, D. J., Knox, J. P., Perotto, S., Butcher, G. W., & Brewin, N. J. (1989). Common components of the infection thread matrix and the intercellular space identified by immunocytochemical analysis of pea nodules and uninfected roots. *EMBO Journal,* 8(2), 335-341.

Whiting, R. C., & Buchanan, R. L. (1993). A classification of models in predictive microbiology - reply. *Food Microbiology,* 10(2), 175-177.

Wilmes-Riesenberg, M. R., Foster, J. W., & Curtiss, R. (1997). An altered rpoS allele contributes to the avirulence of *Salmonella typhimurium* LT2. *Infection and Immunity,* 65(1), 203-210.

Woolley, J. T. (1983). Maintenance of air in intercellular spaces of plants. *Plant Physiology,* 72(4), 989-991.

Zhang, L. K., Lu, Z. X., & Wang, H. (2006). Effect of gamma irradiation on micorbial growth and sensory quality of fresh-cut lettuce. *International Journal of Food Microbiology,* 106, 348-351.

APPENDIX A

A1

Estimated Double Beam Irradiation Doses (kGy) Based on the Depth-Dose Curve (Fig. 5.5) of 10 MeV Electrons in Cantaloupe for Inactivation of *S. typhimurium* after 30 Hours of Internalization at 23°C, Starting with 0 cm at the Top and 0 cm at the Bottom Attenuation.

Depth	Lucite® Attenuation Thickness (cm) for Top and Bottom Beam					
(mm)	Top – 0	Bottom - 0	Total	Top - 1	Bottom - 0	Total
10	1.08	0.23	1.31	1.28	0.23	1.51
20	1.19	0.97	2.16	0.97	0.97	1.94
30	1.28	1.28	2.56	0.23	1.28	1.51
40	0.97	1.19	2.16	0.00	1.19	1.19
50	0.23	1.08	1.31	0.00	1.08	1.08

A2

Estimated Double Beam Irradiation Doses (kGy) Based on the Depth-Dose Curve (Fig. 5.5) of 10 MeV Electrons in Cantaloupe for Inactivation of *S. typhimurium* after 30 Hours of Internalization at 23°C, Starting with 2 cm at the Top and 0 cm at the Bottom Attenuation.

Depth	Lucite® Attenuation Thickness (cm) for Top and Bottom Beam					
(mm)	Top - 2	Bottom - 0	Total	Top - 3	Bottom - 0	Total
10	1.28	0.23	1.51	0.97	0.23	1.20
20	0.97	0.97	1.94	0.23	0.97	1.20
30	0.23	1.28	1.51	0.00	1.28	1.28
40	0.00	1.19	1.19	0.00	1.19	1.19
50	0.00	1.08	1.08	0.00	1.08	1.08

A3

Estimated Double Beam Irradiation Doses (kGy) Based on the Depth-Dose Curve (Fig. 5.5) of 10 MeV Electrons in Cantaloupe for Inactivation of *S. typhimurium* after 30 Hours of Internalization at 23^{o}C, Starting with 4 cm at the Top and 0 cm at the Bottom Attenuation.

Depth	Lucite® Attenuation Thickness (cm) for Top and Bottom Beam					
(mm)	Top - 4	Bottom - 0	Total	Top - 0	Bottom - 1	Total
10	0.23	0.23	0.46	1.08	0.00	1.08
20	0.00	0.97	0.97	1.19	0.23	1.42
30	0.00	1.28	1.28	1.28	0.97	2.25
40	0.00	1.19	1.19	0.97	1.28	2.25
50	0.00	1.08	1.08	0.23	1.19	1.42

A4

Estimated Double Beam Irradiation Doses (kGy) Based on the Depth-Dose Curve (Fig. 5.5) of 10 MeV Electrons in Cantaloupe for Inactivation of *S. typhimurium* after 30 Hours of Internalization at 23°C, Starting with 1 cm at the Top and 1 cm at the Bottom Attenuation.

Depth	Lucite® Attenuation Thickness (cm) for Top and Bottom Beam					
(mm)	Top - 1	Bottom - 1	Total	Top - 2	Bottom - 1	Total
10	1.19	0.00	1.19	1.28	0.00	1.28
20	1.28	0.23	1.51	0.97	0.23	1.20
30	0.97	0.97	1.94	0.23	0.97	1.20
40	0.23	1.28	1.51	0.00	1.28	1.28
50	0.00	1.19	1.19	0.00	1.19	1.19

A5

Estimated Double Beam Irradiation Doses (kGy) Based on the Depth-Dose Curve (Fig. 5.5) of 10 MeV Electrons in Cantaloupe for Inactivation of *S. typhimurium* after 30 Hours of Internalization at 23°C, Starting with 3 cm at the Top and 1 cm at the Bottom Attenuation.

Depth	Lucite® Attenuation Thickness (cm) for Top and Bottom Beam					
(mm)	Top - 3	Bottom - 1	Total	Top - 4	Bottom - 1	Total
10	0.97	0.00	0.97	0.23	0.00	0.23
20	0.23	0.23	0.46	0.00	0.23	0.23
30	0.00	0.97	0.97	0.00	0.97	0.97
40	0.00	1.28	1.28	0.00	1.28	1.28
50	0.00	1.19	1.19	0.00	1.19	1.19

A6

Estimated Double Beam Irradiation Doses (kGy) Based on the Depth-Dose Curve (Fig. 5.5) of 10 MeV Electrons in Cantaloupe for Inactivation of *S. typhimurium* after 30 Hours of Internalization at 23°C, Starting with 0 cm at the Top and 2 cm at the Bottom Attenuation.

Depth	Lucite® Attenuation Thickness (cm) for Top and Bottom Beam					
(mm)	Top - 0	Bottom - 2	Total	Top - 1	Bottom - 2	Total
10	1.08	0.00	1.08	1.19	0.00	1.19
20	1.19	0.00	1.19	1.28	0.00	1.28
30	1.28	0.23	1.51	0.97	0.23	1.20
40	0.97	0.97	1.94	0.23	0.97	1.20
50	0.23	1.28	1.51	0.00	1.28	1.28

A7

Estimated Double Beam Irradiation Doses (kGy) Based on the Depth-Dose Curve (Fig. 5.5) of 10 MeV Electrons in Cantaloupe for Inactivation of *S. typhimurium* after 30 Hours of Internalization at 23°C, Starting with 2 cm at the Top and 2 cm at the Bottom Attenuation.

Depth	Lucite® Attenuation Thickness (cm) for Top and Bottom Beam					
(mm)	Top - 2	Bottom - 2	Total	Top - 3	Bottom - 2	Total
10	1.28	0.00	1.28	0.97	0.00	0.97
20	0.97	0.00	0.97	0.23	0.00	0.23
30	0.23	0.23	0.46	0.00	0.23	0.23
40	0.00	0.97	0.97	0.00	0.97	0.97
50	0.00	1.28	1.28	0.00	1.28	1.28

A8

Estimated Double Beam Irradiation Doses (kGy) Based on the Depth-Dose Curve (Fig. 5.5) of 10 MeV Electrons in Cantaloupe for Inactivation of *S. typhimurium* after 30 Hours of Internalization at 23°C, Starting with 4 cm at the Top and 2 cm at the Bottom Attenuation.

Depth	Lucite® Attenuation Thickness (cm) for Top and Bottom Beam					
(mm)	Top - 4	Bottom - 2	Total	Top - 0	Bottom - 3	Total
10	0.23	0.00	0.23	1.08	0.00	1.08
20	0.00	0.00	0.00	1.19	0.00	1.19
30	0.00	0.23	0.23	1.28	0.00	1.28
40	0.00	0.97	0.97	0.97	0.23	1.20
50	0.00	1.28	1.28	0.23	0.97	1.20

A9

Estimated Double Beam Irradiation Doses (kGy) Based on the Depth-Dose Curve (Fig. 5.5) of 10 MeV Electrons in Cantaloupe for Inactivation of *S. typhimurium* after 30 Hours of Internalization at 23°C, Starting with 1 cm at the Top and 3 cm at the Bottom Attenuation.

Depth	Lucite® Attenuation Thickness (cm) for Top and Bottom Beam					
(mm)	Top - 1	Bottom - 3	Total	Top - 2	Bottom - 3	Total
10	1.19	0.00	1.19	1.28	0.00	1.28
20	1.28	0.00	1.28	0.97	0.00	0.97
30	0.97	0.00	0.97	0.23	0.00	0.23
40	0.23	0.23	0.46	0.00	0.23	0.23
50	0.00	0.97	0.97	0.00	0.97	0.97

A10

Estimated Double Beam Irradiation Doses (kGy) Based on the Depth-Dose Curve (Fig. 5.5) of 10 MeV Electrons in Cantaloupe for Inactivation of *S. typhimurium* after 30 Hours of Internalization at 23°C, Starting with 3 cm at the Top and 3 cm at the Bottom Attenuation.

Depth	Lucite® Attenuation Thickness (cm) for Top and Bottom Beam					
(mm)	Top - 3	Bottom - 3	Total	Top - 4	Bottom - 3	Total
10	0.97	0.00	0.97	0.23	0.00	0.23
20	0.23	0.00	0.23	0.00	0.00	0.00
30	0.00	0.00	0.00	0.00	0.00	0.00
40	0.00	0.23	0.23	0.00	0.23	0.23
50	0.00	0.97	0.97	0.00	0.97	0.97

VITA

Ezekiel Maswe Chimbombi received his Bachelor of Science degree in agriculture from the University of Botswana in 1992, and a Master of Science in agricultural engineering from Texas A&M University in 1998, as well as a Master of Business Administration (MBA) from the University of Botswana in 2003. He received a Fulbright scholarship (2005 – 2007) with a complementary scholarship from the Botswana College of Agriculture (2007 – 2009) to pursue a doctoral degree in biological and agricultural engineering, with a focus on food engineering. Ezekiel Chimbombi is a lecturer at the Botswana College of Agriculture and his contact is:

Postal Address:

Botswana College of Agriculture

Private Bag 0027,

Gaborone, Botswana.

Email address is echimbom@bca.temo.bw or echimbombi@gmail.com